Diffusion, Cascade, and Consensus Dynamics on Optimized Networks

防衛大学校理工学研究科後期課程

電子情報工学系専攻・情報知能メディア学教育研究分野

小松　孝紀

平成２５年３月

CONTENTS

Chapter 1

Introduction

1.1 Background and motivation

Network consists of elements, which are called nodes or vertices, with links (or edges) connecting them (Figure 1.1). The network is suitable to model systems where there are interactions among system elements. Examples include the Internet [1], World Wide Web [2], transportation systems [3, 4], electric power grid [5, 6], diffusion of innovation [7-13], citation network [14, 15], ecosystems [16, 17], and food webs [18, 19]. There are optional parameters that introduce more realistic features of the systems into networks. For example, multi-types of nodes, different weights or capacity of each link, directed link, delay time of processing. However, this dissertation is primarily concerned with how network topology (structure) affects three typical dynamical processes on networks: i) probabilistic diffusion such as virus spreading [20], ii) cascade dynamics such as cascade failure [21], and iii) consensus dynamics such as synchronization [22]. This dissertation also aims to design the optimal networks to control those dynamics.

The study of networks began from the problem of Königsberg Bridge by Euler in 1735. There were seven bridges that spanned various sections of the river. The challenge was, could a person walk across each of the seven bridges only once, and

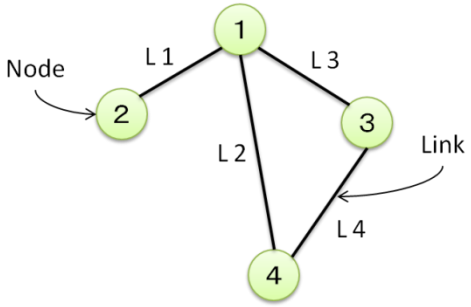

Figure 1.1 A small network with 4 nodes and 4 links.

return home? Euler presented the first mathematical demonstrations of this in 1735 [23], and published his work in 1741 [24]. After that, the understanding of network topology was developed in mathematics as graph theory. For example Kirchhoff developed the theory of trees in 1847 as a tool in the study of electrical networks [25], and Arthur Cayley used tree formed graph to enumerate structural isomers of hydrocarbons in 1875 [26]. Networks are also studied in social science. The form of interaction between people is recognized as a key role to understanding the function of human society. These studies try to find out for example, the most important people for epidemic spreading (super spreader) and the individual who mostly contributes to the connectivity of the social network.

However, in the last ten years the study of networks has been changing significantly from focusing on local functions, which are the centrality of individual nodes and links and the contribution of them to network connectivity, to the more macroscopic and statistical properties of networks. This shift has been driven mainly by the emergence of large-scale networks, which come from big data thanks to the advancement of information communication technology. In large-scale networks it is basically impossible to understand and deal with the exact properties of each node and link, even if there are sufficient data about them. Therefore, statistical data has more meaningful information to understand network properties. For example, Figure 1.2 shows the network of the Top-500 US airports. Counting up the hop distance between all pairs of nodes (airports) has less meaning than the statistical information including the average hop-distance ($= 2.99$) or the diameter ($= 7$) to explain the properties of the network. There is growing emphasis on the statistical data when dealing with large-scale networks, which are called “complex network”.

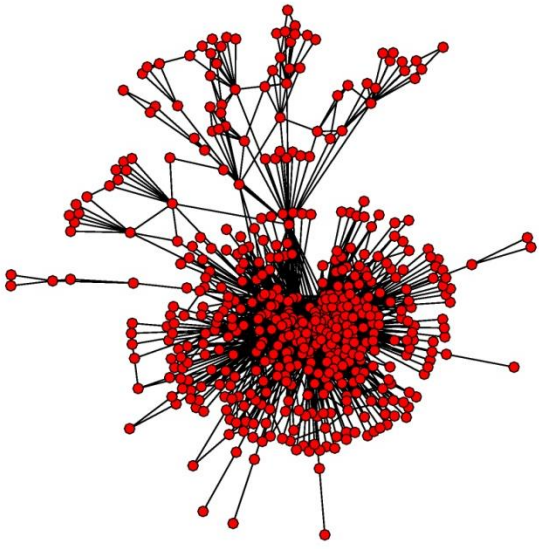

Figure 1.2 Top-500 US Airports (500 nodes, 2980 links): the network consists of the 500 busiest commercial airports, which are represented by nodes, in the United States. A link exists between two airports if a flight was scheduled between them in 2002 [27].

The main scopes of recent studies about complex network are roughly classified into three regions: i) Discovering statistical properties of networks shared commonly in many kinds of systems, which include for example, average hop-distance, clustering coefficients, maximum degree, degree correlation, and degree distribution [28, 29]. ii) Creation of network models (sets of procedures for creation of networks) that is useful for understanding the mechanisms and studying them mathematically [30-32]. iii) Studies on how network topologies affect dynamical processes taking place on networks for controlling or predicting the behavior of them [33-38].

From the beginning of the studies of complex networks, many research focused on the first two regions: i) characterizing networks in the real world and ii) modeling the networks. This led to the groundbreaking discovery of fundamental principles of real networks; the power law and small-world effects (6 degrees of separation). Many models to replicate those networks have been created.

Recently, the studies on the third region have attracted great interests. Physicists and biologists study efficient methods of vaccine supplies to prevent disease outbreaks [39-41]. Economists try to understand the mechanism of financial crisis [42, 43]. Social scientists study when opinion formation or diffusion of innovation can be achieved in society [13, 21]. The development of the studies on them is based on the statistical point of view and the mathematical tools, which are developed by the study on the first and second region (characterizing and modeling complex networks).

One common question about any dynamical processes taking place on network is, "What kind of network is optimal to promote or prevent such dynamics?" and "How do we design optimal networks?"

In this dissertation, I show optimal network topologies on probabilistic diffusion, cascade dynamics and consensus dynamics. Although these dynamics have been studied intensively and have a wide range of applications, little is known about optimal networks.

Probabilistic diffusion is usually used to consider spreading of viruses in networked systems. The infected nodes spread with infection rate β and curing rate δ. However, the applications are not limited into only virus spreading. The diffusion of rumors in social networks or word of mouth effects in viral marketing is another example of applications.

Cascade dynamics is a coordination process where each agent (node) decides to adopt innovation based on the numbers or the fraction of neighboring agents who already have adopted it. The process is also called opinion formation. In addition, cascade failure is another example of cascade dynamics. The failure of one of the nodes can lead to global failure due to cascade dynamics such as chain bankruptcy.

Consensus dynamics is a process to attain coordinated states or synchronized states among agents. Each agent initially has different states (ex. velocity, frequency, geographical position), which represent observed data in sensor networks, internal phase of equipment in phase synchronization, and positions of mobile agents in flocking behavior. In consensus dynamics, all agents need to be in an agreement.

Especially, when the final state is the average of the initial state of agents, it is called an average consensus. Note that there are, of course, other important dynamical processes, which should be studied. Examples include the congestion problem (ex. a traffic jam on a highway and cyber-attack by mass packets on the Internet (distributed denial of service attack) [44-49]), the network tolerance against attacks or failures by removing nodes or links [50-57], and systemic risks [58, 59], however, they will not be discussed in this dissertation.

1.2 **Research objectives**

Understanding the relationship of network topology and dynamical processes is one of the ultimate goals of the study on complex networks [29]. The objective of this dissertation is to show what kind of networks is optimal to promote or prevent dynamical processes. Another objective is to propose efficient methods which can design very large-scale optimal networks.

The dynamics considered in this dissertation are i) probabilistic diffusion, ii) cascade dynamics, and iii) consensus dynamics. These dynamical processes are studied intensively in many papers and they have wide applications.

Scientists, sometimes mimic mechanisms of nature to find solutions to improve our lives: the wings of birds to fly, the lung in the human to remove carbon dioxide efficiently, the infrared sensor of melanophila acuminata to detect wild fire. Nature is a survival-of-the-fittest world, which means current morphology is formed through continual processes of trial and error, and this seems to be an optimal or better solution. For example, networks in our lives including human blood vessels, neural network, and metabolic network are acquired from the accumulation of small improvements over a long time. People study the essence of how these networks function very well. Lately, scientists need to shift from copying existing networks to the creation of entirely new networks to address various problems.

In this dissertation, several kinds of optimal networks are designed using genetic algorithm (GA). The main benefit of GA is that it can work without the knowledge for how to design optimal networks. The GA requires only a proper objective function.

The statistical indexes of networks, which are average-hop distance, clustering coefficient, degree correlation and others, are used to explain properties of networks. However, in this dissertation, the eigenvalue of the adjacency matrix and the Laplacian matrix is used as an index of a network. For example, the maximum eigenvalue of the adjacency matrix is used as an objective function of the evolutionary optimization for probabilistic diffusion, which corresponds to the existence of hub nodes having many links and the interconnectivity between those hub nodes [60]. In other words, the maximum eigenvalue shows whether there are “rich-club phenomena” in the network, which is usually observed in the Internet [61]. Hub nodes have dominant influence in probabilistic diffusion and cascade dynamics on networks, because they represent, for example, super spreader in pandemic and opinion leader in information cascades. The

index can represent the size of hub nodes and the clustering of them simultaneously that will be useful for catching the dominant properties of network topology. Furthermore, the eigenvalue ratio of the second minimum eigenvalue to the largest eigenvalue of the Laplacian matrix defines the time to attain a convergent state mathematically under consensus dynamics among networked agents [22, 62, 63].

The large time complexity of the evolutionary optimization by GA is the side effect of it, which means computation time is large to propose a solution. It is not small problem when we create large-scale networks by the method. Then a two-step approach is used to create an optimal network: First, an optimized network with the suitable size of nodes is designed by the evolutionary optimization. Second, the heuristic network designing model is proposed to scale up them to large-scale networks. The model is not only useful for making large-scale networks but also understanding the topology mathematically. The success of the network models to replicate the properties of optimal networks shows what kind of topology in evolutionary optimized networks is essential to make them optimal.

Complex networks were mainly modeled and analyzed on single networks in previous studies. However, the global optimization of network topology becomes unrealistic or impossible as the number of nodes increase in the network. Furthermore, in general, if a networked system has a very large number of nodes, the system consists of many networks which are interconnected. Therefore, I also propose a network design method that forms a very large-scale network by connecting modular networks recursively. The proposed method can reconstruct the same structure of modular network as the inter-module structure.

1.3 **Outlines**

This dissertation is organized into 8 chapters, including this one, and additionally the bibliography, and the list of the author's publications at the end.

Throughout this dissertation, three types of optimization methods are proposed for designing optimal networks of dynamical processes (Figure 1.3). Each proposed optimization method has suitable application range defined by the number of nodes in the network. If the network size is small, the evolutionary optimization of network topology by genetic algorithm can be applied, but if the network is large, it is better to use heuristic optimization where network models form networks efficiently. However, if the network becomes very large, the global optimization is not realistic. It is very natural the optimization is done locally. Therefore, a very large-scale networked system is assumed to consist of multiple optimal-networks. Each network is optimized by evolutionary optimization or heuristic optimization. A sophisticated method is also proposed to interconnect those networks as modular networks. The details of each chapter are given below.

Chapter 2 presents a brief review of fundamental concepts and results of the study about the dynamical processes considered in this dissertation.

Chapter 3 proposes a new framework for network design consisting of three types of network design methods. It begins with an introduction to the concept of optimization of networks. I propose evolutionary network optimization and explain its properties. I also introduce the concept of the heuristic network model. The model can form required networks efficiently in terms of time and space complexity. Finally, the method using modular networks is proposed to design a very large-scale network.

Chapter 4 deals with probabilistic diffusion processes on networks and show optimal network topologies to maximize (enhance) or minimize (prevent) the diffusion processes. These networks are created by the evolutionary network optimization. I also propose the network model for the maximization of probabilistic diffusion. This network model can produce the same topological properties of evolutionary optimized networks efficiently. Furthermore, numerical simulations validate the performance of optimal networks. Finally, i) the time evolution of the diffusion processes and ii) the relationship between maximum eigenvalue of the adjacency matrix and the properties of networks on diffusion processes are discussed.

Chapter 5 deals with cascade dynamics and show optimal network topologies to maximize the dynamics by evolutionary network optimization. I propose a network model that replicates it. It is shown how the global cascade is driven easily on the optimal network. It is also shown the optimal network minimizing global cascade is the optimal network maximizing probabilistic diffusion. Furthermore, I explore the average cascade size and the frequency of global cascade. It is shown that the probability of a global cascade will be underestimated due to the very small average cascade size.

Chapter 6 deals with consensus dynamics among networked agents and shows evolutionary optimized networks to minimize or maximize the convergence time of consensus dynamics. The network models replicating them with specified average degree are also proposed.

Chapter 7 proposes the method to form very large-scale network efficiently by modular networks with recursive structure of optimal networks. Numerical simulations and spectrum analysis, which is a set of eigenvalues, are done on the modular networks to demonstrate the performance.

Chapter 8 summarizes the results of our work, and provides ideas for future research.

There is a list of the author’s publications at the end.

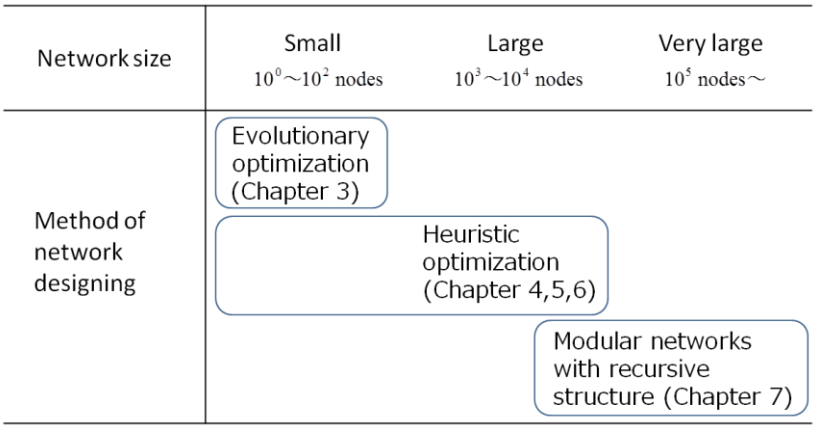

Figure 1.3 Proposed network design methods depending on the network size. Each method has feasible network size to create it. The chapter number after the name of each optimization method represents where the method is proposed and discussed.

1.4 A short glossary of terms

For the convenience of understanding, the definitions of some technical terms used in this dissertation are given as follows.

- **Node or Vertex**: The fundamental unit of a network, which represents, for example, router (in computer network), individual (in social network), and agent (in multi-agent systems).
- **Link or Edge**: The line connecting two nodes, which represents, for example, logical connection (in computer network), some kind of relationship (in social network), interaction (in multi-agent systems).
- **Network or Graph**: A set of nodes (vertex) and links (edges).
- **Undirected link**: A link that has no direction of flow or interaction between two nodes.
- **Degree**: The number of links connected to a node.
- **Average degree**: The average degree $\langle k \rangle$ is an average number of degrees over all nodes, which is defined by $\langle k \rangle = 2L/N$ where L is the number of links and N is the number of nodes. It is also denoted by z in this dissertation.
- **Cluster**: It is a set of vertices, which usually share common attributes. Nodes in a same cluster can be reached from each other by paths running along the links of a network.
- **Hop-distance**: The minimum number of links on the path, which goes from a starting node to a destination node.
- **Adjacency matrix**: The adjacency matrix is defined by the network topology. The element of the matrix $\mathbf{A}$ in the i th row and j th column is expressed as $a_{i,j}$. The elements $a_{i,j} = a_{j,i} = 1$ when node i and node j are connected by an undirected link, and the elements $a_{i,j} = a_{j,i} = 0$ when node i and node j are not connected.

Chapter 2

Dynamical processes on networks

Dynamical processes on networks (ex. virus spreading, diffusion of innovation, opinion formation, collective behavior, cascade failure and synchronization), where the concerned state or quantity of node changes over time, attract the most attention of scientists. They are critical issues in our society. They are also complex; it is difficult to control and complicated to predict their behavior. There are several approaches to study dynamical processes taking place in the system, which are for example, simple differential equation-based-model and complex agent-based-model. In many cases, however, the network-based approach is used, which considers pathways of dynamical processes. This chapter aims to briefly summarize the key points of dynamical processes studied in this dissertation (probabilistic diffusion dynamics, cascade dynamics, and consensus dynamics) and to introduce frameworks for the study on dynamical processes.

2.1 Dynamical processes on networks

Dynamical processes on networks are classified into roughly three types of dynamics: i) probabilistic diffusion such as epidemical diffusion, ii) cascade dynamics on threshold model, and iii) consensus dynamics (or synchronization). They have been well studied because of the importance of the problems. This dissertation aims to design optimal networks focusing on these three types of dynamics.

Probabilistic diffusion is a prototype example of dynamical processes on networks [64, 65]. Epidemiologists, computer scientists and social scientists share a common interest in studying the diffusion phenomena. Of course, they are actually interested in different phenomena in each discipline, but the phenomena can be modeled by a similar model. A classic version of the model is the susceptible infected susceptible (SIS) model. In this model, an infected individual can infect a susceptible individual with probability β, and an infected individual can be in the susceptible state again with probability δ (Figure 2.1). The infection ratio β/δ decides whether a computer virus

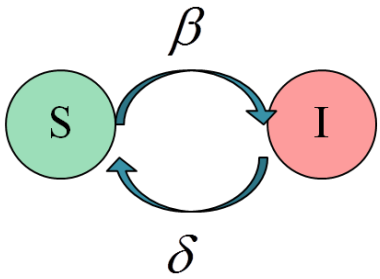

Figure 2.1 SIS model: (β: infection rate, δ: curing rate).

or a rumor survives or not. These epidemiological contact processes are analogical processes in other fields including spread of computer virus on the Internet and diffusion of a rumor or information by the word of mouth in a social network.

The main concern of probabilistic diffusion (SIS model) is the tipping point for the diffusion to take off. For example, the tipping point means the minimum infection ratio where a virus can survive at a steady state. The pioneering work by Pastor-Satorras and Vespignani found that there is no intrinsic epidemic threshold on scale-free networks [66]. Many numerical simulations and mathematical analysis succeeded to show the tipping points of other networks, but the optimal network to promote or prevent the diffusion dynamics is not clear yet.

Our focus here is to find the kind of network topology that is optimal under fixed network resources. A key node characterizing a network for diffusion dynamics is a hub node. Intuitively, one would expect the diffusion dynamics to occur and survive more easily with the increase in the size of the hub node. However, this dissertation will show that the tipping point will be minimized when a network has a cluster of hub nodes of medium size. The cluster structure of hub nodes of medium size maximizes efficiently the number of contact processes between nodes under fixed network resources than few hub nodes of a larger size.

Cascade dynamics on networks can be classified into two types of models: overload model and locally dependent model (threshold model) [42, 56, 67]. The first overload model is used to study failures due to an overload when there is network flow of physical quantity, for example, in power transmission systems, transportation networks or Internet traffic [35, 56, 68, 69]. In this model, the failure of nodes or links will change the direction and the amount of flows and it makes new congestion or overload causing another failure of nodes or links. Due to the iteration of this process, the failure of even one node could sweep out all nodes in the entire network.

The second threshold model is used to study the decision making of interacting agents, diffusion of innovation, and cascade failures due to risk diffusion [21, 58, 70]. In this model, a node has a binary state, for example, 0 or 1, good or bad, or normal or failure. The state of each node depends on the state of its neighboring nodes, and this model has locality with positive externality, that means they try to do the same action with their neighbors. The conditional region in which the states of all nodes are attuned

to the change is defined by the average degree of networks and the resistance (threshold) of nodes, which is called the “cascade window”.

The networks that maximize or minimize the size of a cascade window are not well known in previous studies. Previous studies show a network with a degree distribution that obeys exponential distribution maximizes cascade window, because it has a relatively large number of nodes, called the vulnerable nodes that conforms easily with neighboring nodes. However, this dissertation shows the coexistence of a cluster of vulnerable nodes and a cluster of hub nodes that makes those vulnerable nodes more sensitive to neighboring nodes plays a crucial role in maximizing a cascade. The accumulation of change in a cluster of vulnerable nodes changes the state of hub nodes when the amount of accumulation exceeds a critical mass. In addition, this dissertation shows that a cluster of hub nodes works to minimize a cascade when a network does not have a cluster of vulnerable nodes. The cluster of hub nodes is very stable even if the state of a few hub nodes in the cluster is changed, because their neighboring hub nodes are not affected by the changed nodes.

Consensus dynamics has a long history in computer science and form the foundation of the field of distributed computing [62, 71]. Formal study of consensus dynamics conducted by groups of experts originated in statistics [72]. The original idea was in aggregation of information with uncertainty obtained from multiple sensors or experts. Distributed computation over networks has a tradition in systems and control theory on agreement problem for distributed decision-making systems [73].

In networked agents, consensus means to reach an agreement regarding a certain quantity of interest that depends on the internal state of all agents. A consensus algorithm is an interaction rule that specifies the information exchanged between an agent and all of its neighbors on the network [74]. The theoretical framework for posing and solving consensus problems for networked systems is well surveyed by Olfati-Saber and Murray in [22].

The consensus problem is also related to the problem of synchronization [74]. In recent studies, the reason for the occurrence of synchronized networks becomes clear and the underlying network topology is important [75]. However, synchronization often occurs unexpectedly and little is known what the best network topology for synchronization is. The small network distance does not mean a network is suitable for fast consensus.

It is confirmed in this dissertation that heterogeneous degree distributions typically seen in scale-free networks inhibit the synchronizability [76]. Earlier works suggest the specific regular network called “Ramanujan network” is optimal for fast consensus [75]. However, this dissertation shows the regular network is not always optimal for fast consensus especially for sparse networks.

2.2 **Frameworks for the study on dynamical processes**

Dynamical processes had been studied at first under homogeneous mixing of population where all agents interact directly (Figure 2.2 (a)) and a short time later the new concept of network-based approach is introduced, which studied the dynamical processes on a random graph.

A groundbreaking 1998 paper by Watts and Strgatz [5] showed that the topologies in the real world, including biological, technological, and social networks, lie between completely regular and completely random networks. They showed the importance of considering more complex network topology, which are strongly related to the function of networks. Furthermore, the networks including Internet [77], airline [3], sexual contact [78] and others are found to have common degree distribution, which obey the power law $p(k) = k^{-\alpha}$. The distribution indicates the existence of many tail nodes with a few connections and non-zero hub nodes with many connections to others in a network. Those hub nodes represent super-spreaders in probabilistic diffusion, which is not considered under the homogeneous mixing assumption. [62]. Therefore, the dynamical processes began to be studied in terms of complex network that defines pathway or contact process of interaction (Figure 2.2 (b)).

The underlying hypothesis of the approach to understand dynamical processes is that the different pathway or sequence of interactions brings different results. In addition more complex environment or more realistic situation can be introduced to the network-based approach, where the topology will be changed over the time or many kinds of attributes are set on nodes and links. However, introducing complex situation makes results obscure and also makes it difficult to induct the relationship between dynamical processes and network topology. Then, networks with static attributes are usually used in the study of dynamical processes on complex network.

The multi-agent system is another approach to study complex dynamical processes sophisticatedly. For example, in order to study a flu epidemic in a town or flocking behavior of moving agents, the multi-agent system can introduce multi-types of characters or action-rules on each agent and also make an artificial society with a number of agents (Figure 2.2 (c)). In agent based system, network topology usually emerged as a result of interactions between agents. This approach is useful to answer the question “Does the observable phenomena come from the difference in the network topologies or the difference of the dynamics of elements?” Furthermore, the agent based model is used to explore the evolution of networks [79, 80]. The hypothesis used here is that networked systems have topology (ex. hierarchy, rule, and norm in society) generated by the interaction of elements and the topology also imposes some sort of influence on them. The fluctuations of the behavior of elements invoked by the topology will make another topology. This relationship of different level interaction between a global topology and local elements is called micro-macro loop [81] (Figure 2.2 (d)). The agent based model intrinsically can draw the multi-scale interaction with network topology.

In this dissertation, it is assumed that there is a static rule defining the topology of a networked system. This means the network topology itself is not changed by dynamical processes and it has been static during dynamical processes. This assumption is not a trivial one, but it is applicable in the situations where the dynamical processes and network dynamics are mapped on different time scale. For example, computer virus usually spread silently at first via network without crashing any computers and connections to avoid countermeasures from users. Then, network-based approach is taken to study the dynamical processes and it is aimed to design optimal networks that promote or prevent the above mentioned dynamical processes by using new framework of network design proposed in the next chapter. After that, the network design problem on each dynamics is discussed in the following chapters. The analysis of the behavior of dynamical processes on dynamical networks is left as the next challenge of study.

Networks with modular structure or community structure are relevant to many social, biological, and industrial networks [82-84]. Modular networks consist of a number of modularized networks, where nodes within each module are densely connected but the connectivity of inter-modules is sparse. Typical examples of modular networks are metabolic networks or the Internet. Each modular network is defined in terms of its function or location and modular networks are combined in a hierarchical manner into a larger unit. Modular structure is a common strategy to form very large-scale networks in real world. Therefore, dynamical processes on modular networks are also studied in this dissertation after the study of each dynamical process on single network. This dissertation focuses on the kinds of topology of inter-modules which are optimal for dynamical processes. Two intuitive methods to interconnect modular networks are considered: i) random connection and ii) recursive connection. It is shown that the recursive connection is effective to coordinate the interaction patterns of inter-modules, where the structure of inter-modules becomes the same with optimal structure of the modular network.

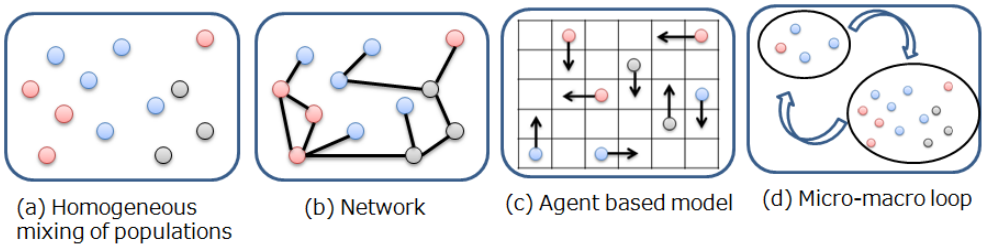

Figure 2.2 Several approaches to study dynamical processes.

Chapter 3

Network Optimization

3.1 Introduction to network optimization

Optimization is the standard policy of network design. The points to be optimized and the method to realize optimization may vary with the conditions that must be satisfied. If we focus on the problem of traffic jam on a highway network, there are many different approaches to prevent it. Examples are introducing a new fare structure, adjusting the maximum speed, making a new bypass for congestion area, encouraging people to use public transportation system. There are fundamentally four major types of optimization problems related to networked systems [85].

Type I: Optimization of topology [5, 86, 87]. Under fixed number of nodes and links a network is designed so that topological properties are optimized or adjusted as required. The optimization problem belongs to the category of graph theory (ex. minimization of average hop distance, maximization of clustering coefficient). This type of network design problem is studied as a method to model networks in the field of complex networks. For instance, the small-world network model by Watts-Strogatz have small average hop-distance and large clustering coefficients by the coexistence of the regularity and small randomness. The simple rule of degree-based preferential attachment of nodes can evolve scale free networks with small average hop-distance and power law in the degree distribution.

Type II: Optimization of parameters of dynamics. Under a static network topology, the parameters of nodes and links are optimized (ex. in a road network, finding the best setting of speed limit to reduce traffic jam).

Type III: Optimization of topology for given dynamics [88, 89]. Under given dynamics with fixed parameters, a network that maximizes the fitness value is designed. For example, scale free networks have good robustness against random failures of nodes, and random networks have good robustness against intentional attacks on nodes. Furthermore, the technical limitation of routers used on the internet makes hierarchical structure to maximize the data flow, which is called the Heuristically Optimized

Topology (HOT) [90]. The HOT is another mechanism of the emergence of the power law in degree distribution instead of the well-known mechanism of preferential attachment.

Type IV: Dynamics-driven network optimization [56, 80, 91]. Find the best network under dynamics affected by dynamical topology. In this case, the network topology affects the behavior of the dynamics and the change of the dynamics will affect the network topology again. A typical example of this case is a cascade failure such as a blackout. The surge of electrical current flow due to an accident or failure of an equipment will damage a power plant (node) or a transmission line (link) in power grid and the changes of the electric current flow cause further failure.

This dissertation focuses on a type III network optimization to find a network topology maximizing the performance under given dynamical processes. In this case the topology is unchanged, which means there is no birth-death process of nodes and links during the dynamics.

The optimization problem can be formulated as,

$$\max\big(F(\boldsymbol{\phi})\big)\ \ s.t.\, G(V,E) = m, \tag{3.1}$$

where $F(\boldsymbol{\phi})$ is the objective function also called fitness function on a network $G(V,E)$, and $\boldsymbol{\phi} = \phi(x_1, x_2, \cdots x_N)$ is a dynamical process with parameters x_i, where the number of parameters N depends on the dynamics. V is the set of nodes and E is the set of links. The network resource on V and E is constant m. From the form of equation (3.1), the problem seems to belong to equality constrained optimization that is solved by Lagrange multiplier. Therefore, if the problem can be formulated, the best network will be obtained mathematically as a solution of the extreme value problem, which maximizes $F(\boldsymbol{\phi})$. However, it is difficult to give such a constraint equation because the constraint is not simple and cannot be solved analytically in general.

Thus, it is necessary to adopt a looser definition of the word "optimization" by extending it to include a tendency of the network to improve its behavior. Under the definition, there are alternative methods: probabilistic meta-algorithm including the genetic algorithm and simulated annealing, which finds a better solution by the accumulation of the improvement. In essence, according to the no free lunch theorem, there is no difference between genetic algorithm and the simulated annealing to search for better solutions efficiently. However, the simulated annealing needs the gradient of the objective function and a proper schedule to control moving direction and moving distance for exploring an answer. Furthermore it can hold only single candidate answer. As a result, it will be complex and easy to be strapped to local optimal solutions. On the other hand, the genetic algorithm does not use the gradient of the objective function and does not need a scheduling management. Then, it is relatively simple and can explore the searching space globally using a set of many candidate answers simultaneously. Therefore, the genetic algorithm seems to be suitable for multimodal problems and a good enough solution that has been globally searched will be obtained. Accordingly the genetic algorithm (GA) is used here for network optimization.

3.2 Evolutionary optimization

A critical limitation of the optimization of networks is the lack of theoretical knowledge about the relationship between the topological properties and the index of network dynamics theoretically. Therefore, probabilistic meta-algorithm becomes the only way for the optimization of networks as mentioned in the previous subsection.

In this dissertation, evolutionary optimization by using GA is proposed to create optimal networks. In the optimization, the initial population of networks advances as results of accumulation of the improvement at each generation. In the algorithm, each node changes the linkage to others randomly to find a better network than the original one. The benefit of applying evolutionary optimization to network design is that the algorithm works without the knowledge of the optimal network topology. Setting the objective function, which implies how current network is near to an optimal one, is enough to run the algorithm.

Although the evolutionary optimization does not guarantee that the output is the best solution, it usually provides better solutions. It also shows whether there is still space for improvements in the current networks. Another benefit of the network design by evolutionary optimization is the sufficient flexibility toward optimization problems. The method can be applied to different problems and purposes if a proper objective function can be set.

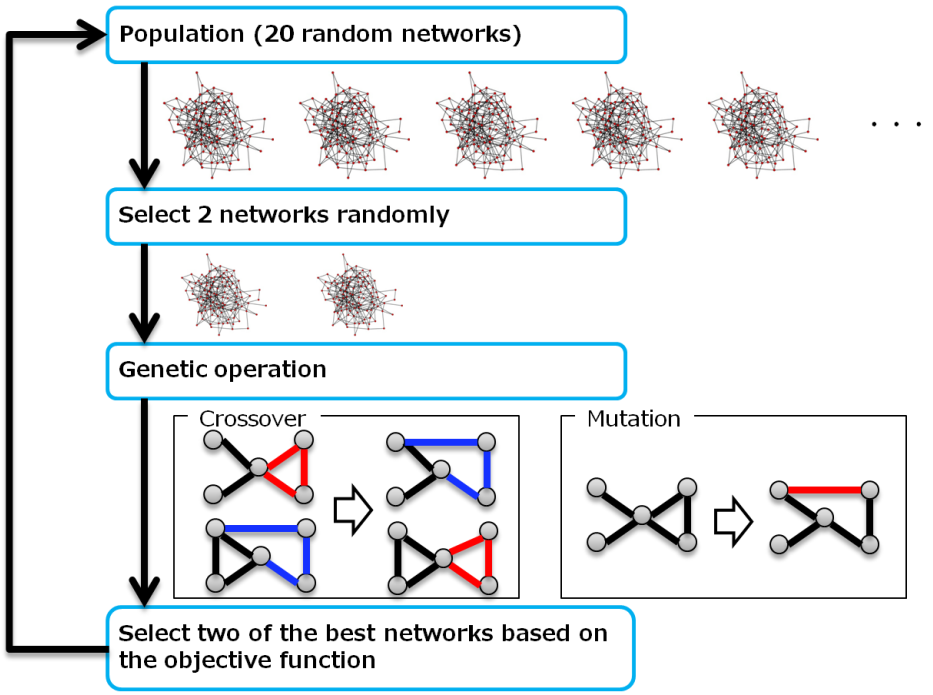

Figure 3.1 The procedures of evolutionary network optimization.

The evolutionary optimization consists of the following 7 steps as shown in Figure 3.1.

1. Create an initial population of networks.
2. Pick up two individuals (networks) randomly from the population as parent networks.
3. Create new networks from the parents by genetic operations, such as mutation and crossover.
4. Calculate the fitness of newly created networks and the parents' networks.
5. Select two networks to be put back into the population.
6. Calculate the fitness of the rest of the population
7. If the stop criterion was not met, go back to step 2. If the stop criterion was met, stop the algorithm and return the result.

The number of population and topology of each network is important to obtain a useful answer in a reasonable time. In this dissertation, 20 random networks are created as initial networks, because the best network, which has a similar topology to the optimal one, is unknown. In addition, only connected networks are considered to avoid meaningless results. Therefore, whether the network is disconnected is checked in all steps where it can happen.

In order to be able to apply genetic operators (mutations and crossover), each network is represented by the chromosome (Figure 3.2). It is a sequence of binary numbers from the adjacency matrix of a network. The adjacency matrix of an undirected network is a symmetric matrix. Therefore, the information of upper triangle of the matrix is enough to draw the network topology.

In the step of picking up parent networks to create children networks, the two networks are selected randomly as parents from the population. The random selection method works to minimize the gap of the fitness between two generations, and it is useful to maintain diversity in the population during the process of optimization. The parent networks are used to create several new networks with a genetic operation (uniform crossover). The number of new networks depends on the size of the search space.

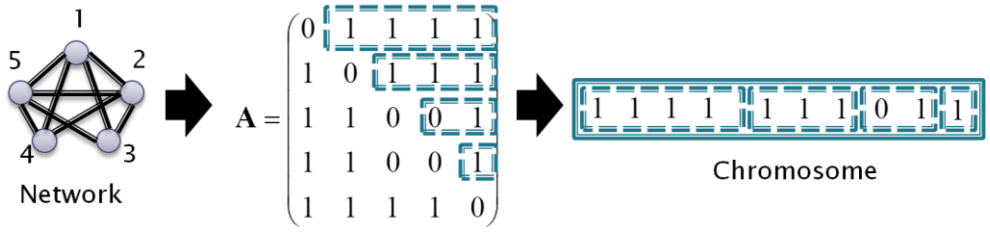

Figure 3.2 The chromosome of a network.

In step of evaluating newly created networks, two most suitable networks are selected from the created networks in the previous step and the parent networks. The selected two networks are inserted into the population again. Note that if the fitness of any child networks is worse than the parent networks, the parent networks are returned back into the population.

In the step of calculating the fitness, the population is evaluated by an objective function to check the distribution of the quality of networks. The evaluation results are used later for the termination of the evolutionary optimization.

In the step of stop criteria, it stops the whole genetic algorithm. As a stop criterion, the convergence of optimization is used. If all members have the same fitness and the value has not changed for more than ten iterations, the algorithm is stopped.

A big time complexity characterizes the proposed evolutionary optimization. In order to estimate the time complexity, the searching space of genetic algorithm and the calculation time of the maximum eigenvalue of the adjacency matrix are discussed. Each node has a binary state $(0,1)$. Then the total number of states of N nodes is $O(2^N)$. On the other hand, the calculation cost for the maximum eigenvalue is between $O(N^2)$ and $O(N^3)$, where the divide-and-conquer eigenvalue algorithm from the standard matrix computation library LAPACK [92] calculation is used. The simulated time complexity is defined as the average convergence time of evolutionary network optimization. From preliminary experiments shown as a function of the number of nodes in the Figure 3.3, it is about $O(N^{2.3})$, which is a result of over 10 simulations on the computer with Intel Core-i5 and 32 GB memory and there are 20 initial random networks having 500 nodes. The space complexity is $O(N^2)$, because the product of matrices is essential for the calculation of the maximum eigenvalue. It seems to be unrealistic or difficult to create large-scale networks by the evolutionary optimization. Thus I consider heuristic methods to create large-scale optimal networks in next section.

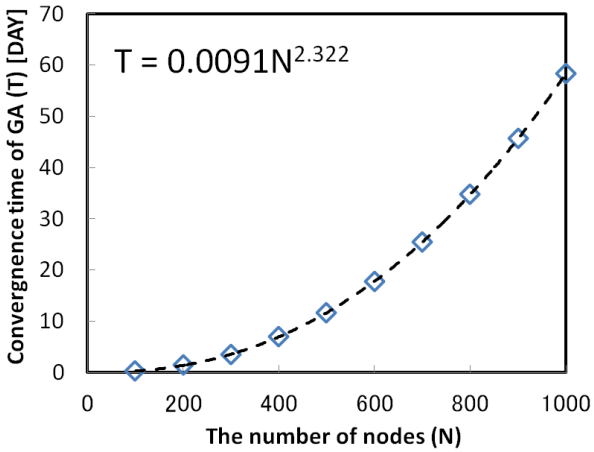

Figure 3.3 The convergence time of genetic algorithm as a function of the number of nodes in the network.

3.3 **Heuristic methods for network optimization**

This dissertation aims to design optimal network topologies to promote or prevent dynamical processes mentioned in Chapter 2. Heuristic method such as the network model is useful to understand how evolutionary optimized networks are evolved and to do mathematical analysis on the obtained networks. The network model also has enough scalability for the creating of a large-scale network. However, the evolutionary optimization is limited to medium size of networks with several hundred nodes.

The heuristic method (network model) is a set of procedures or rules to reproduce network topology that share the same properties and function with desired networks. As an example, the network model to make scale free network by Balabási Albert, of which degree distribution obeys the power law, is shown in the following 5 steps. In the model, the number of nodes and links grows over the time.

1. Create a small connected network (ex. network with 5 nodes and 7 links).
2. Calculate the fitness $\mathrm{f}(d_i)$ of each node i, where $\mathrm{f}(d_i) = d_i / \sum d_i$ and d_i denotes the degree of node i.
3. A new node is introduced to the network and linked to m nodes in a current network, which are stochastically selected based on the fitness value calculated in the previous step.
4. Iterate steps from step 2 to step 3 until the number of nodes meets the demand.

The random graph is another typical example of a network model in which nodes are connected randomly. In the random graph model, the required number of nodes without links are placed initially and whether a pair of nodes is linked or not depends on the probability p. The output of the model with $p = 1$ is a complete graph where each node is connected to all of the others and the output of the model with $p = 0$ is the set of isolated nodes.

The Watts-Strogatz model for a small world network is another type of network model, which has a link rewiring procedure. The ring-lattice network is prepared as an initial network and a few links are rewired randomly. By the controlling the number of rewired links, the network with small average hop-distance and large clustering coefficients is formed. The other sophisticated network models can be found in related studies [30, 93]. They can make network have arbitrary degree distribution or replicate topological properties in the real world. Furthermore some studies have developed dynamical network model, in which the networks are formed as a result of multi-agent interactions [79, 80].

As one of the side benefits of network models, the variety of optimized networks can be obtained by controlling the parameters in the network models. These trial experiments help us to understand the properties of optimized networks and may lead to find new properties that have not been realized yet.

3.4 **The recursive network design with modular networks**

The main advantage of recursive network design is that it is suited for creating a very large-scale network and it is easy to evaluate mathematical properties, such as degree distribution.

In the previous section, heuristic method (network model) is introduced to design a large-scale network. Although the heuristic methods which are obtained from the results of evolutionary optimization, can create large-scale optimal networks, it is still difficult to scale up to very large-scale networks due to computational time. Furthermore the optimization of a very large-scale network itself is sometimes unrealistic, for example it is restricted by geographical restrictions or organizational constraint.

Therefore, this dissertation proposes a new approach to design a very large-scale network (Figure 3.4) with four-steps. Firstly, the proposed evolutionary optimization is used to form optimal network on a given dynamical process, which has suitable size of nodes depending on the convergence time. Secondly, the essential properties of the obtained network are clarified. Thirdly, heuristic network model (a set of procedures), which can replicate the essential properties, is developed by using several techniques obtained in previous studies of network modeling. Finally, recursive network design is applied. Each modular network is optimized by using evolutionary optimization or heuristic network model. In order to interconnect those modular networks, the method of recursive connection is proposed, where the topology between modular networks is the same as the topology of modular network itself. By replicating the local topology of modular network globally, the optimal very large-scale networks can be designed.

The “Modular networks” is a realistic and efficient concept for network design along with the increase of the network size. Examples include biological systems [94, 95], WWW [94, 96], and social networks [97, 98]. The detail of recursive network design with modular structure is presented in Chapter 7.

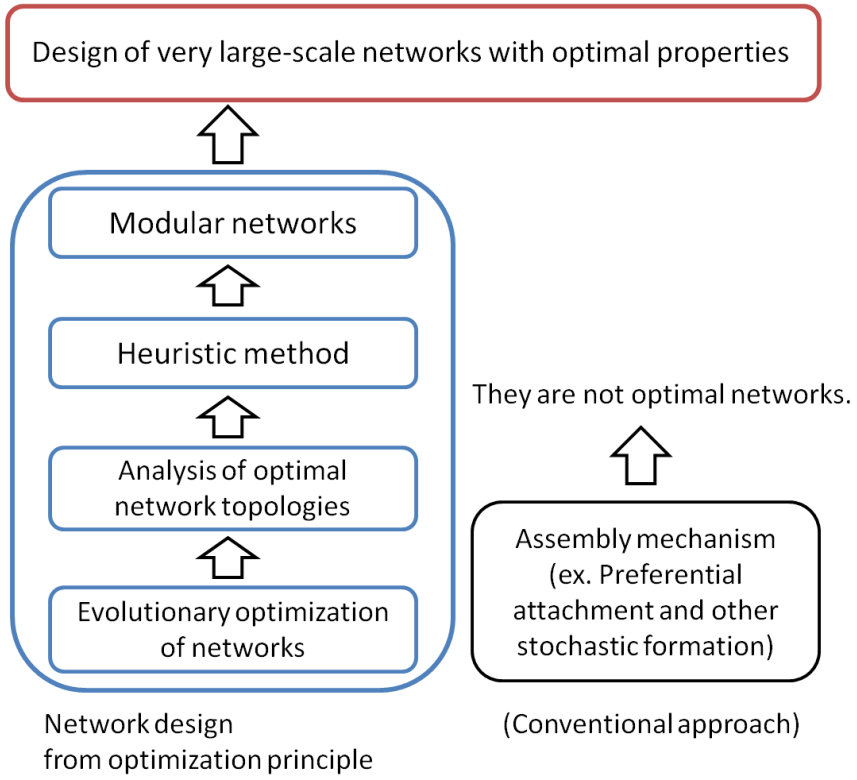

Figure 3.4 The comparison of the proposed approach with the conventional approaches for designing networks.

Chapter 4

Probabilistic Diffusion Dynamics

In this chapter, optimal networks are designed to promote or prevent probabilistic diffusion dynamics. The diffusion scenario defines whether the promotion or the prevention is suitable. Probabilistic diffusion largely corresponds to the size of the maximum eigenvalue of the adjacency matrix. The optimal network is designed, which has the largest or smallest maximum eigenvalue of the adjacency matrix, by using the proposed evolutionary optimization.

4.1 Diffusion models

In this section, three types of models of probabilistic diffusion process are introduced. The model of probabilistic diffusion initially has no concept of network topology, but the concept had been introduced along the recognition of the potent influence of network topology to the diffusion. Recently the new eigenvalue-based framework for probabilistic diffusion is developed, which no longer needs mean field assumptions to deal with probabilistic diffusion mathematically.

4.1.1 A homogeneous mixing model

Among researches concerning various diffusion processes, the spreading of virus has received the most attention due to the impact of the problem [3]. The meaning of the spreading is not interpreted as only bad effects but also good effects. For example, the information diffusion process by word of mouth can be viewed as a viral propagation in which virus spreads by a contact process between individuals [99]. At the beginning of the study, it is assumed that each person can interact with others directly, which is called a homogeneous mixing.

Two major diffusion models are well studied for the study of the contact processes. They are SIR model and SIS model. In SIR model, the population is classified into

three categories, susceptible (S), infected (I) and removed (R). The infected individual is removed from the population with the probability δ, and the removed people do not communicate with other people after that. The number of population who will be infected decreases along with the time evolution and there are no infected people finally. The dynamics of the SIR model is formulated as,

$$\frac{dS}{dt} = -\beta IS,$$

$$\frac{dI}{dt} = \beta IS - \delta I, \tag{4.1}$$

$$\frac{dR}{dt} = \delta I.$$

On the other hand, in the SIS model, the population is classified into only two categories, susceptible (S) and infective (I). A susceptible individual becomes infected by other neighboring infected individuals with infection rate β. The infected individual becomes susceptible again with the curing rate δ. The dynamics of the SIS model is formulated as,

$$\frac{dS}{dt} = -\beta IS,$$

$$\frac{dI}{dt} = \beta IS - \delta I. \tag{4.2}$$

Even if probabilistic diffusion is observed from the network based viewpoint, the network with high link density and small variance between populations meets the homogeneous mixing. However, many real network does not meet the mixing assumption of the homogeneous model. In many networks, the number of contactable nodes of each node is restricted to some extent by the network regulation, and then the effect of the network topology on the diffusion process should be considered.

In this dissertation, probabilistic diffusion is dealt with as a dynamical birth-death process with self-recovery using the SIS model, as shown in Figure 4.1. An infected agent diffuses its own state to its all adjacent agents in a single step with probability β, while at the same time an infected agent may recover or be initialized with probability δ. The ratio of the two factors β/δ is defined as the relative diffusion rate τ of the contact process.

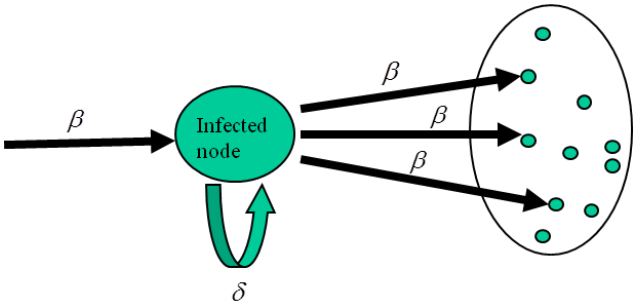

Figure 4.1 The diagram of the transition of the state of node: β is the infection rate and δ is curing rate.

4.1.2 A network based model

Kephart and White [65] introduced the concept of network-based approach and consider SIS model on a homogeneous network, in which all nodes have $\langle k \rangle$ links. Because the mean field approximation will fit very well in this case, the behavior of one node represents the whole network dynamics. The probability to become infected of a node corresponds to the fraction of infected nodes in a network.

The fraction of infected nodes at time t is denoted by $p(t)$. Then, $(1 - p(t))$ denotes the probability that node i is healthy and $kp(t)$ denotes expected value of infected neighboring nodes when node i has k neighboring nodes. The change of the fraction of infected nodes is occurred by two processes: 1) susceptible node becomes infected and 2) infected node becomes susceptible. Hence, the change of infected nodes can be formulated by using differential equation as,

$$\frac{dp(t)}{dt} = -\delta p(t) + \beta \langle k \rangle p(t)\big(1 - p(t)\big). \tag{4.3}$$

At a steady state $dp(t = \infty)/dt = 0$, the following relationship as shown in equation (4.4) is obtained from equation (4.3).

$$p(\infty)(\langle k \rangle \tau - 1 - \langle k \rangle \tau p(\infty)) = 0, \tag{4.4}$$

where $\tau = \beta/\delta$. The equation (4.4) has two solutions for $p(\infty)$. The trivial solution is $p(\infty) = 0$, where the infection rate β that is sufficiently small, thus the computer virus or epidemic will disappear. The another solution, which shows how many nodes are infected at a steady state, is

$$p(\infty) = \frac{\langle k \rangle \tau - 1}{\langle k \rangle \tau}. \tag{4.5}$$

The important index of epidemics, which decides whether epidemic will die out or survive, is the basic reproductive number R_o [100, 101]. The index shows the number of secondary infected people generated by one primary infected individual, and it can be estimated as,

$$R_o = \frac{\beta\langle k\rangle}{\delta}. \tag{4.6}$$

If $R_o > 1$, which means the number of infected individuals is larger than those who are recovered, the virus will survive and spread to the society. Then, the critical infection rate (tipping point) of the pandemic $\tau_c = \beta/\delta$ is obtained as,

$$\tau_c = \frac{1}{\langle k\rangle}. \tag{4.7}$$

On the networks with power law, the average degree $\langle k\rangle$ is no longer representative value for the tipping point due to the divergence of the fluctuation $\langle k^2\rangle$. When the size of network is infinitely or sufficiently large, the alternative tipping point τ_c is obtained as,

$$\tau_c = \frac{\langle k\rangle}{\langle k^2\rangle}. \tag{4.8}$$

This result may come as a surprise to many, because it implies the any epidemic, even if $\beta \simeq 0$, can spread on those networks [66, 77]. This is one of evidences that the network topology affects dynamical process.

The initial state of each node in the network is negligible at a steady state under this model, and it is clear that probabilistic diffusion easily occurs on networks with many links. Therefore, when the diffusion of bad things is considered, such as computer virus or flu, it is important to take a balance between the network performance, which is usually related to the number of links, and the robustness defined by equation (4.8) .

4.1.3 A diffusion model from eigenvalue viewpoint

Recently, a sophisticated mathematical framework is introduced, which can deal with probabilistic diffusion with no mean field approximation [20, 102]. Assuming the arrival of an infection along each link and the curing process of an infected node are independent Poisson processes with rate β and rate δ, respectively. The properties of probabilistic diffusion can be analyzed by using the continuous Markov chain theory.

Node i has either susceptible state $X_i(t) = 0$ or infected state $X_i(t) = 1$ at each time t. Each node changes its own state dynamically with the neighboring nodes that are connected to the node. Obeying the continuous Markov theory, it is assumed that the state vector of node i, $\mathbf{X}(t + \Delta t) = (Pr[X_i(t + \Delta t) = 0], Pr[X_i(t + \Delta t) = 1])^{\mathrm{T}}$, can be obtained by using the current state vector $\mathbf{X}(\mathrm{t})$ and the stochastic matrix $\mathbf{P}$ as shown in equation (4.9).

$$\mathbf{X}(\mathrm{t}+\Delta\mathrm{t}) = \mathbf{P}\mathbf{X}(\mathrm{t}),$$
$$\mathbf{P} = \begin{pmatrix} 1-\beta^*\Delta t & \beta^*\Delta t \\ \delta\Delta t & 1-\delta\Delta t \end{pmatrix}, \tag{4.9}$$

where it is assumed the transition probability from susceptible state to infected state $(0 \to 1)$ during time Δt, which is denoted by $\beta(\Delta\mathrm{t})$, can be approximated by linear function $\beta^*\Delta t$, if the time Δt is sufficiently small. The recovering probability during the time Δt is also assumed to be obtained by $\delta\Delta t$. The aggregative infection-rate β^* is estimated by the state of neighboring nodes as,

$$\beta^* = \beta \sum_{j=1}^{N} a_{ij} 1_{\{X_j(t)=1\}}, \tag{4.10}$$

where the indicator function $1_{\{x\}}$ equals 1 if the event x is true, else it equals zero. Equality of equation (4.10) holds theoretically when the infection rate β is sufficiently small. The coefficient a_{ij} is element of the adjacency matrix $\mathbf{A}$ of the network.

The element $\mathrm{p}_{i,j}$ of the i th row and j th column in the matrix $\mathbf{P}$ represents transition probability from state i to state j during the infinitesimal time Δt. The matrix $\mathbf{P}$ can be decomposed as,

$$\mathbf{P} = \begin{pmatrix} 1 & 0 \\ 0 & 1 \end{pmatrix} + \begin{pmatrix} -\beta^* & \beta^* \\ \delta & -\delta \end{pmatrix} \Delta\mathrm{t} = \mathbf{I} + \mathbf{Q}\,\Delta\mathrm{t}, \tag{4.11}$$

where $\mathbf{I}$ denotes the identity matrix and the matrix $\mathbf{Q}$ is called infinitesimal generator or transition matrix. If the process defined by equation (4.11) is applied to probabilistic diffusion directly, the explosion of problem space will occur: there can be $2^N - 1$ states because each node has either susceptible or infected $\mathrm{X_i(t)} = \{0 \text{ or } 1\}$. Hence, mean approximation is used to avoid the explosion of problem space [102]; $v_i(t) = Pr[X_i(t) = 1]$ is used instead of $1_{\{X_j(t)=1\}}$.

Then, equation (4.11) can be rewritten in terms of differential equation as,

$$\frac{dv_i(t)}{dt} = \big(1 - v_i(t)\big)\beta \sum_{j=1}^{N} a_{ij} v_j(t) - v_i(t)\delta. \tag{4.12}$$

From equation (4.12), $v_i(\infty)$ can be obtained at a steady state $dv_i(t)/dt = 0$ as,

$$v_i(\infty) = 1 - \frac{1}{1 + \tau \sum_{j=1}^{N} a_{ij} v_j(\infty)}. \tag{4.13}$$

Define $\mathbf{V}(t) = \big(v_1(t), v_2(t), v_3(t), \cdots, v_N(t)\big)^T$, the transmission rate of all nodes can be written from equation (4.12) as,

$$\frac{\mathrm{d}\mathbf{V}(t)}{dt} = \beta\mathbf{A}\mathbf{V}(t) - \mathrm{diag}\big(v_i(t)\big)(\beta\mathbf{A}\mathbf{V}(t) + \delta u), \tag{4.14}$$

where u is the all-one vector and $\mathrm{diag}\big(v_i(t)\big)$ is the diagonal matrix with elements $v_1(t), v_2(t), v_3(t), \cdots, v_N(t)$.

In a steady state; $\mathrm{d}\mathbf{V}(\infty)/dt = 0$, then the equation (4.14) can be rewritten as,

$$\mathbf{A}\mathbf{V}(\infty) - \mathrm{diag}\big(v_i(\infty)\big)\left(\mathbf{A}\mathbf{V}(\infty) + \frac{1}{\tau}u\right) = 0. \tag{4.15}$$

Define $\gamma \equiv \mathbf{A}\mathbf{V}(\infty) + \frac{1}{\tau}u$, then equation (4.15) can be transformed to

$$\gamma - \frac{1}{\tau}u = \mathrm{diag}\big(v_i(\infty)\big)\gamma, \tag{4.16}$$

or

$$\left(\mathbf{I} - \mathrm{diag}\big(v_i(\infty)\big)\right)\gamma = \frac{1}{\tau}u. \tag{4.17}$$

Ignoring the extreme case ($v_i(\infty) = 1$), the matrix $\mathbf{I} - \mathrm{diag}\big(v_i(\infty)\big)$ is invertible. Equation (4.17) can be solved for γ as,

$$\gamma = \frac{1}{\tau}\mathrm{diag}\left(\frac{1}{1 - v_i(\infty)}\right)u. \tag{4.18}$$

From the definition of γ and equation (4.18), equation (4.19) is obtained.

$$\mathbf{A}\mathbf{V}(\infty) = \frac{1}{\tau}\mathrm{diag}\left(\frac{1}{1 - v_i(\infty)} - 1\right)u. \tag{4.19}$$

The diagonal elements of right hand diagonal matrix are the summation of the geometric series as shown in equation (4.20), which are converged when the $\mathrm{v}_i(\infty) < 1$.

$$\frac{1}{1 - v_i(\infty)} - 1 = \frac{v_i(\infty)}{1 - v_i(\infty)} \leftrightarrow \sum_{k=1}^{\infty} v_i(\infty)^k. \tag{4.20}$$

Then, steady-state equation is obtained from equation (4.19) and equation (4.20) as,

$$\mathbf{A}\mathbf{V}(\infty) = \frac{1}{\tau}\sum_{k=1}^{\infty}\mathbf{V}(\infty)^k = \frac{1}{\tau}\mathbf{V}(\infty) + \frac{1}{\tau}\sum_{k=2}^{\infty}\mathbf{V}(\infty)^k. \tag{4.21}$$

In order to explore the tipping point of relative diffusion rate τ_c, it is set that $\mathbf{V}(\infty) = \varepsilon x$ $(\tau = \tau_c + \varepsilon)$ in equation (4.21), where x is the column vector that is linearly dependent of $\mathbf{V}(\infty)$. The following equation (4.22) is obtained.

$$\frac{1}{\tau}x + \frac{1}{\tau}\varepsilon x^2 + o(\varepsilon^2) = \mathbf{A}x. \tag{4.22}$$

When ε is sufficiently small in equation (4.22), the second and the third term in left

side are negligible, and equation (4.23) can be obtained.

$$\frac{1}{\tau}x = \mathbf{A}x. \tag{4.23}$$

The equation (4.23) shows that $1/\tau$ is eigenvalue of the adjacency matrix $\mathbf{A}$ and the x is eigenvector (steady-state vector) of the matrix $\mathbf{A}$. From the Perron-Frobenius theorem, the maximum eigenvalue $\lambda_{max}(\mathbf{A})$ of the adjacency matrix $\mathbf{A}$ is positive, of which the multiplicity is one, and only corresponding eigenvector is positive eigenvector. Then, $1/\tau = \lambda_{max}(\mathbf{A})$ and x is corresponding eigenvector of $\lambda_{max}(\mathbf{A})$. If $\tau < 1/\lambda_{max}(\mathbf{A})$, there is only effective solution $x = \mathbf{0}$. If $\tau > 1/\lambda_{max}(\mathrm{A})$, the effects of the second and third term of equation (4.22) are not negligible and there is positive steady-state vector. Therefore, the tipping point of relative diffusion rate τ_c can be obtained as,

$$\tau_c = \frac{1}{\lambda_{max}(\mathbf{A})}. \tag{4.24}$$

Equation (4.24) implies that a network with larger maximum eigenvalue $\lambda_{max}(\mathbf{A})$ is more susceptible to probabilistic diffusion.

Furthermore it is also clear that nodes with large eigenvector centrality c_i, which is i-th element of the eigenvector of $\lambda_{max}(\mathbf{A})$, will be infected fast and the diffusion starts from these nodes.

The advantage of the continuous markov chain model is that there is no assumption on the network topology and then it can be applied to arbitrary networks. The model uses only mean approximation about the state of each node $1_{\{X_j(t)=1\}} \rightarrow Pr[X_j(t) = 1]$. The influence of the approximation, however, is relatively small when the network has sufficient large number of nodes.

4.1.4 Properties of probabilistic diffusion dynamics

In probabilistic diffusion process, the infection processes of each infected node toward neighboring uninfected nodes are independent. Then, p_i the probability of un infected node i to become infected by neighboring infected nodes is formulated as,

$$p_i = 1 - (1 - \beta)^k, \tag{4.25}$$

where k is the number of neighboring infected nodes of node i. Figure 4.2 shows the probability of node i to become infected as a function of the number of neighboring infected nodes *k*. The point of this figure is that the probability of infection p_i is not zero even if there is only one infected node. Another point is that the accumulation of infected nodes extends the infection probability nonlinearly. Then, a hub node is very susceptible to the infection because the node has many pathways (links) to be attached to infected nodes. After the infection of a hub node, the hub node attempt to infect many neighboring nodes and works as a super spreader of virus.

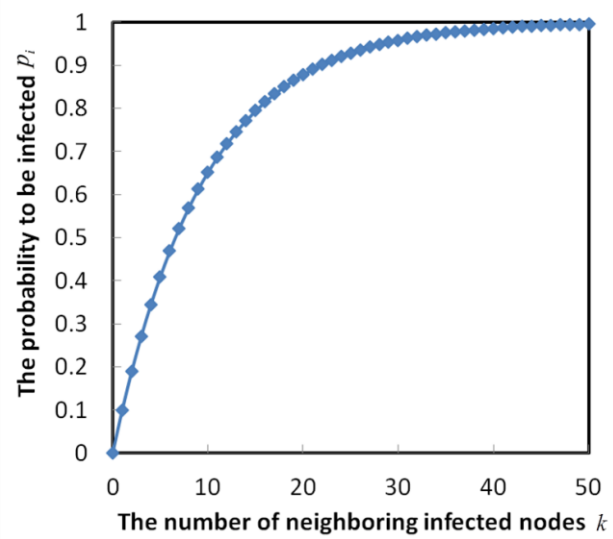

Figure 4.2 The probability of node i to be infected is plotted as a function of neighboring infected nodes, where β the infection probability of each infected node is 0.1.

The global effects of network topology can be seen as phase transition of the diffusion in probabilistic diffusion processes (Figure 4.3). If the relative infection rate $\tau = \beta/\delta$ is not larger than the tipping point τ_c, the diffusion process in a absorbing phase, and infected nodes will disappear. In the contrary case: $\tau > \tau_c$, the diffusion process is in active phase, and the infected nodes will survive, which spread into a finite fraction of nodes. The tipping point is changed by network topologies. A completely isolated graph where any nodes have no connection to others has infinite size of τ_c and a complete graph has very small τ_c. On the other hand the real networks have intermediate size of τ_c between the two extreme cases. The question of the tipping point is central in epidemics.

The difference of network topology makes different pathways to reach a steady state of diffusion processes, even if a steady state is same. In addition to studies on tipping point τ_c, the study on how network topology affects the time evolution is very important to predict a future state of nodes or deal with it effectively. For example, in the case an outbreak of foot-and-mouth disease, if the diffusion process draws shallow logistic curve, there is some time before extensive outbreak to prevent the spread of the disease: setting up no-go zones, spraying disinfectant at a farm or restriction of shipments, after the early detection of it. The study on the relationship between network topology and the time evolution of diffusion processes may be also applied into other applications: for example, the estimation of the underlying network topology from observed data (diffusion processes), which is usually unclear and essential for deep understanding of the dynamics (ex. human relationship in information cascade or sexual relationship in the spreading of AIDS).

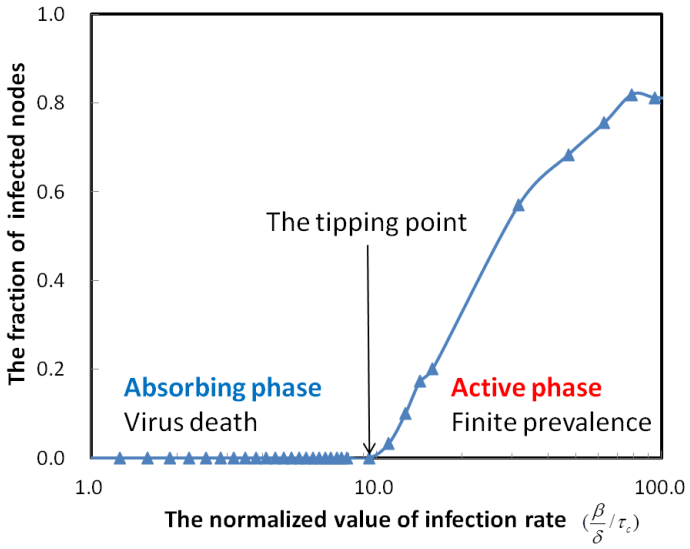

Figure 4.3 The fraction of infected nodes is plotted as a function of the normalized infection rate $\beta/\delta/\tau_c$ as the results of probabilistic diffusion simulation on random network with 500 nodes and 1000 links, where curing rate δ is 0.1 at all cases. τ_c is the inverse of maximum eigenvalue of adjacency matrix of CPA network proposed in following subsection 4.4.2.

Probabilistic diffusion on networks by equation (4.14) can be rewritten as

$$\frac{\mathrm{d}\mathbf{V}(t)}{dt} = -\delta\mathbf{V}(t) + \beta\mathbf{A}\mathrm{diag}\big(1 - v_i(t)\big)\mathbf{V}(t). \tag{4.26}$$

From equation (4.26), if the infection rate $\beta = 0$ or sufficiently small, the infection rate of each node decay exponentially from the initial infection rate $\boldsymbol{V}_o$, as shown in equation (4.27).

$$\mathbf{V}(t) = \boldsymbol{V}_o e^{-\delta t}. \tag{4.27}$$

If the relative infection rate $\tau(=\beta/\delta)$ is larger than the tipping point τ_c to take off in terms of the fraction of infected nodes at a steady state, the time evolution of the fraction of infected nodes is seemed to show logistic curve due to the symmetry of the equations between equation (4.3) and equation (4.26).

The fraction of infected nodes $\mathrm{y(t)}$ is obtained as

$$\mathrm{y(t)} = \frac{1}{N}\mathrm{u}^{\mathrm{T}}\mathbf{V}(t). \tag{4.28}$$

where N denotes the number of nodes in the network.

Figure 4.4 shows the time evolution of the diffusion on random network, as results of numerical calculation of equation (4.26) and confirms the intuition. In the calculation, infection vector is initialized: infection vector $\mathbf{V}(t=0)$ that has only one 1 element on a node with largest degree and other elements equal 0.

The changing rate of the fraction of infected nodes at an early stage from a trigger

of diffusion implies how much time is left for the countermeasures to prevent pandemic, if the diffusion is a bad event. When the infection rate of each node $v_i(t)$ is not so large, nonlinear term $\beta\mathbf{A}\mathrm{diag}(v_i(t))\mathbf{V}(t)$ in equation (4.26) is negligible. At that time, the changing rate of the fraction of infected nodes is given by

$$\frac{\mathrm{d}\mathbf{V}(t)}{dt} = (\beta\mathbf{A} - \delta)\mathbf{V}(t), \tag{4.29}$$

and it can be solved for $\mathbf{V}(t)$ as shown in equation (4.30).

$$\mathbf{V}(t) = \exp\big((\beta\mathbf{A} - \delta\mathbf{I})t\big)\mathbf{V}(0). \tag{4.30}$$

The term $\exp\big((\beta\mathbf{A} - \delta)t\big)$ can be rewritten as $\sum_{\mathrm{i}} \exp\big((\beta\lambda_i(\mathbf{A}) - \delta)t\big)\mathbf{z}_i\mathbf{z}_i^T$ where $\lambda_i(\mathbf{A})$ and $\mathbf{z}_i$ are *i*-th eigenvalue of the adjacency matrix $\mathbf{A}$ and corresponding eigenvectors corresponding to each eigenvalue from the maclaurin expansion of $\exp\big((\beta\mathbf{A} - \delta)t\big)$. From using the expression in equation (4.30), it is clarified how the difference of eigenvalues of the adjacency matrix affects the time evolution as shown in equation (4.31).

$$\mathbf{V}(t) = \sum_i \exp\big((\beta\lambda_i(\mathbf{A}) - \delta)\mathrm{t}\big)\mathbf{z}_i\mathbf{z}_i^{\mathrm{T}}\,\mathbf{V}(0). \tag{4.31}$$

The eigenvalue $\lambda_i(\mathbf{A})$ that meets $\beta\lambda_i(\mathbf{A}) - \delta > 0$ and corresponding eigenvector $\mathbf{z}_i$ contributes the spreading of the diffusion, and the impacts of the rest of eigenvalues (especially negative ones) exponentially decrease along with the time step. The analysis shows the meaning of the size of infection rate β and curing rate δ that decides how many positive eigenvalues of the adjacency matrix works positively and the impact of them toward the diffusion dynamics. Especially, the influence of the eigenvector of the maximum eigenvalue is dominant, because it is the only eigenvector with all positive components and all eigenvectors are normalized such as $\mathbf{z}_{\mathrm{i}}\mathbf{z}_{\mathrm{i}}^{\mathrm{T}} = 1\ \forall i$.

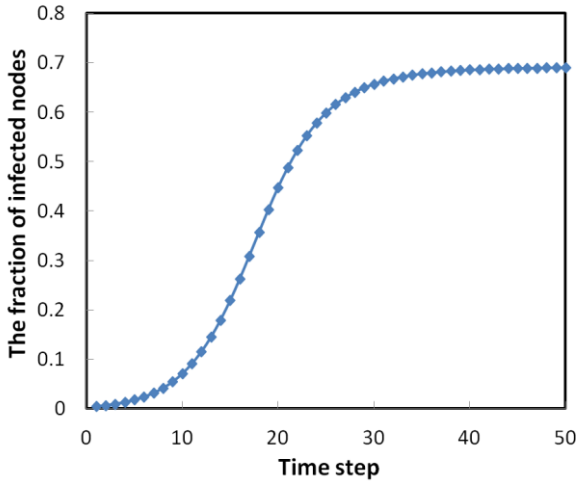

Figure 4.4 Time evolution of the fraction of infected nodes on random networks. Each point on line is a result of numerical calculation of equation (4.26). The random network has 500 nodes and 1000 links. One largest hub node is infected as a trigger of diffusion. Infection rate is $\beta = 0.097$ and curing rate is $\delta = 0.1$.

4.2 Evolutionary optimization of diffusion networks

In this dissertation, one of the main questions is "What kind of the network topology is best for the maximization of diffusion process?" The simple answer is complete graph having the maximum eigenvalue $\lambda_1(\mathbf{A}) = N - 1$, in which each node is connected to every other nodes. However, it becomes unrealistic to make complete graph with the increase of the size of network. Because it implies for example, a lot of costs is needed for the setting and the maintenance of links. Therefore, many networks in our life, such as social network, railway network and neuron network, adjust balance between the performance of the network and the number of links.

Let G be a connected graph with N nodes and L links. The simplest upper bound and lower bound for the maximum eigenvalue $\lambda_1(\mathbf{A})$ of the associated adjacency matrix $\mathbf{A}$ of network G is formulated as,

$$\langle k \rangle \leq \lambda_1(\mathbf{A}) \leq d_{max}, \tag{4.32}$$

where $\langle k \rangle$ represents average degree of the network, and d_{max} represents maximum degree of nodes in the network. The left side equality holds for a regular graph, in which all nodes have same number of links $\langle k \rangle$, and the right side equality holds for a complete graph. An upper bound of the maximum eigenvalue from the numbers of nodes and links is also found by Hong [103] as,

$$\lambda_1(\mathbf{A}) \leq \sqrt{2L - N + 1}. \tag{4.33}$$

From these equations (equation (4.32) and equation (4.33)), hub nodes, which makes d_{max} large, and sufficient number of links (L) is necessary to create a network having large maximum eigenvalue to maximize probabilistic diffusion.

A network is evaluated by maximum eigenvalue $\lambda_1(\mathbf{A})$ and average degree $\langle k \rangle$, which is associated with the number of links L ($\langle k \rangle = 2L/N$, where N denotes the number of nodes), and then the objective function for the maximization of probabilistic diffusion, which should be minimized by GA, is defined as,

$$E = \omega \frac{1}{\lambda_1(\mathbf{A})} + (1 - \omega) \frac{\langle k \rangle}{N - 1}, \tag{4.34}$$

where $\omega (0 \leq \omega \leq 1)$ is a parameter controlling the linear combination of the inverse of maximum eigenvalue $\lambda_1(\mathbf{A})$ and normalized average degree $\langle k \rangle/(N-1)$. Therefore, the objective function becomes the following equation (4.35) when the controlling parameter is set as $\omega = 1$ in equation (4.34).

$$E = \frac{1}{\lambda_1(\mathbf{A})}. \tag{4.35}$$

The optimal network by the objective function (equation (4.35)) is complete graph, which has a largest maximum eigenvalue $N - 1$ with the average degree $N - 1$.

On the other hand, in the case setting $\omega = 0$ in equation (4.34), the objective function becomes as,

$$E = \frac{\langle k \rangle}{N-1}. \tag{4.36}$$

The optimized network by the objective function (equation (4.36)) is a tree type network with average degree close to $2(N-1)/N \simeq 2$.

The minimization of objective function E (equation (4.34)) means the maximization of the maximum eigenvalue and the minimization of the average degree simultaneously. Here the connected graph is only considered, and the average degree of the network $\langle k \rangle$ has a value from $2(N-1)/N$ to $N-1$. In order to make the balance of the range of value between two terms in equation (4.34), the average degree is normalized by $N-1$.

"What kind of network is optimal to prevent the diffusion dynamics?" is another main question of this dissertation. From the above arguments, the network with smallest maximum eigenvalue of the adjacency matrix minimizes probabilistic diffusion. For that, the following equation (4.37) is used as objective function.

$$E = \omega \frac{\lambda_1(A)}{N-1} + (1-\omega)\frac{1}{\langle k \rangle}. \tag{4.37}$$

The evolutionary network optimization by genetic algorithm with two objective functions in equation (4.34) and equation (4.37) are used to find optimal networks for the maximization or minimization of probabilistic diffusion. The parameters on genetic algorithm MGG [104] is shown in Table 4.1.

Figure 4.5 shows the maximum eigenvalue of optimized networks using GA by changing controlling parameter ω in equation (4.34) and equation (4.37), which is compared to homogeneous network (random regular network), random network and scale free network with same or similar average degree. The optimized networks for maximization of probabilistic diffusion (GA (maximization)) have much larger maximum eigenvalues compared to that of scale free networks. It implies GA networks have lower threshold for probabilistic diffusion than that of scale free networks, which are supposed to be optimal to drive the diffusion easily. On the other hand, the optimized networks for minimization of probabilistic diffusion (GA (minimization)) have maximum eigenvalue as small as homogeneous network. The proposed optimization method can create networks with smallest maximum eigenvalue even if the average degree $\langle k \rangle$ is not integer.

Table 4.1 Parameters used for GA optimization

Genetic algorithm model	Minimum generation gap model [104]
Network size (The number of nodes)	500
Initial network topology of populations	Random network
Initial population size	100
'Child' population size	100
Objective function for the maximization of probabilistic diffusion	$\mathrm{E} = \omega \frac{1}{\lambda_1(\mathbf{A})} + (1-\omega)\frac{\langle k \rangle}{N-1}$
Objective function for minimization of probabilistic diffusion	$E = \omega \frac{\lambda_1(\mathbf{A})}{N-1} + (1-\omega)\frac{1}{\langle k \rangle}$
Crossover	Uniform crossover
Mutation	Not used
Selection	An elite selection strategy
The number of evaluations	Over 600,000

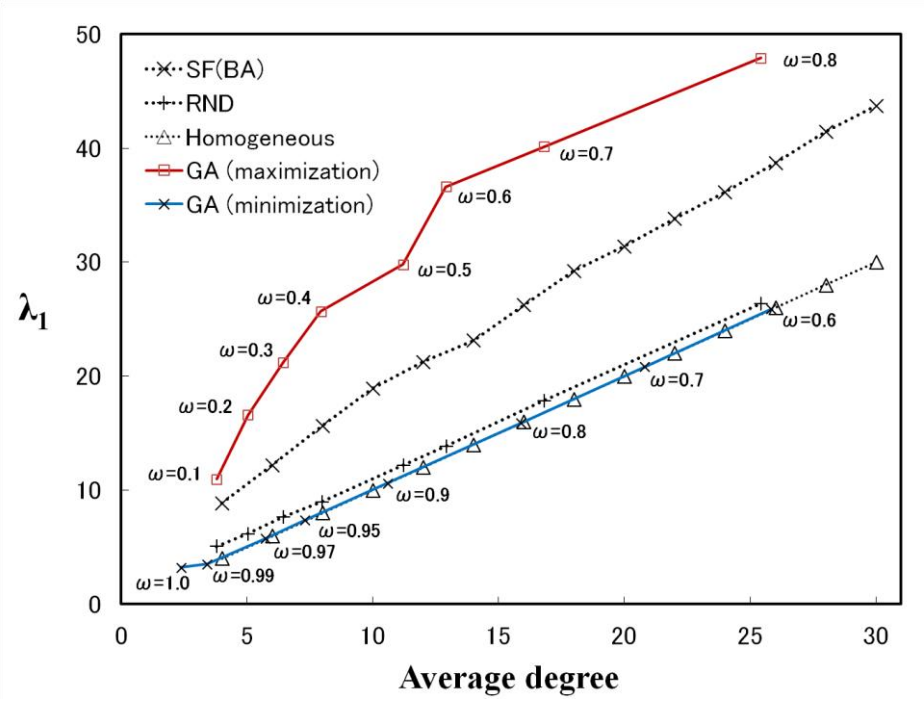

Figure 4.5 Maximum eigenvalue of optimized networks by GA (λ_1) is plotted as a function of average degree, which is compared to that of scale free network by BA model (SF(BA)), random network (RND), homogeneous network (random regular network (Homogeneous)). The value of parameter ω of equation (4.34) and equation (4.37) is shown at the side of each result.

4.3 **Topological properties of evolutionary optimized networks**

This section considers new question "What kind of network topology did GA optimization generate for maximizing or minimizing probabilistic diffusion?".

4.3.1 Optimal networks for maximizing probabilistic diffusion

In this subsection, I show topological properties of evolutionary optimized networks for the maximization of probabilistic diffusion. Let T be the ratio of maximum eigenvalue of optimized network λ_1^{GA} to that of random network λ_1^{R} which has same average degree as shown in equation (4.38).

$$T = \frac{\lambda_1^{\mathrm{GA}}}{\lambda_1^{\mathrm{R}}}. \tag{4.38}$$

In Figure 4.6, the ratio T is plotted as a function of average degree of the network. It is shown that the effectiveness T of the evolutionary optimization is changed with the average degree, and the optimized network at $\omega = 0.4$ in equation (4.34) has the largest ratio $T = 2.9$. It means at $\omega = 0.4$, the GA method created most effective network compared to networks at other conditions in terms of the size of maximum eigenvalue. Then the optimized network at $\omega = 0.4$ is suitable to understand the optimal topology for the maximizing probabilistic diffusion. Several topological analyses on the optimized network are done in the following paragraphs.

The topology of an optimized network at $\omega = 0.4$ in equation (4.34) is shown in Figure 4.7. Depicting network is usually useful method to understand how nodes are interconnected by links intuitively. It shows topological properties: a dense core at the center of the network, in which many links are wired to connect nodes forming a core, and many peripheral nodes with a few links connected to the center core. However, it is still obscure on the interconnectivity between nodes, which is important for the understanding of the topology.

Figure 4.8 shows how nodes are distributed on each networks of Table 4.2. In optimized network and scale free network, the over 70% nodes are within two hop distance from a hub node, which has most number of links. Figure 4.9 shows the degree distribution of the optimized network at $\omega = 0.4$ in equation (4.34). It shows the optimized network (GA) has a few hub nodes and many nodes with a few links as same as scale free network (SF(BA)) has.

Figure 4.10, Figure 4.11 and Figure 4.12 show degree of each node located at each hop distance from a largest hub node of networks in Table 4.2. They show hub nodes in optimized network are located around the largest hub node like scale free network. In random network, those nodes are separated.

Finally the rich-club connectivity [61] is used to characterize network topology, which shows link density between hub nodes. The rich-club connectivity is calculated as follows. In the original paper [61], nodes are divided into groups with same degree and look at interconnectivity between those groups. However, in this dissertation, nodes in the network are sorted by decreasing degrees and look at interconnectivity

between nodes to see the detail of the topology. The node rank r denotes the position of a node on the ordered list. r is normalized by the total number of nodes N.

The rich-club connectivity $\phi(r)$ is defined as the ratio of the total actual number of links $L(r)$ to the maximum possible number of links between members of the rich-club ($n(r)$ nodes), as shown in equation (4.39).

$$\phi(r) = \frac{\mathrm{L(r)}}{\mathrm{n(r)C_2}}. \tag{4.39}$$

As an example, the rich-club connectivity $\phi(r)$ of optimized network at $\omega = 0.4$ in equation (4.34) is calculated and compared it to both scale free network and random network in Table 4.2 (Figure 4.13). It shows the rich-club connectivity $\phi(r)$, which is a function of cumulative fraction of nodes r, on a log-log scale. As shown, hub nodes of the optimized network by GA are connected each other very well. The top 10% rich nodes in optimized network have 33.6% of the maximum possible number of links, compared to $\phi(r = 10\%) = 14.2\%$ in scale free network and $\phi(\mathrm{r} = 10\%) = 5.5\%$ of random network.

From the above results, optimized networks by GA and scale-free networks share several network properties: the existence of hub nodes and the deployment of hub nodes around the nodes with largest degree. However, optimized networks only have remarkable large rich-club connectivity.

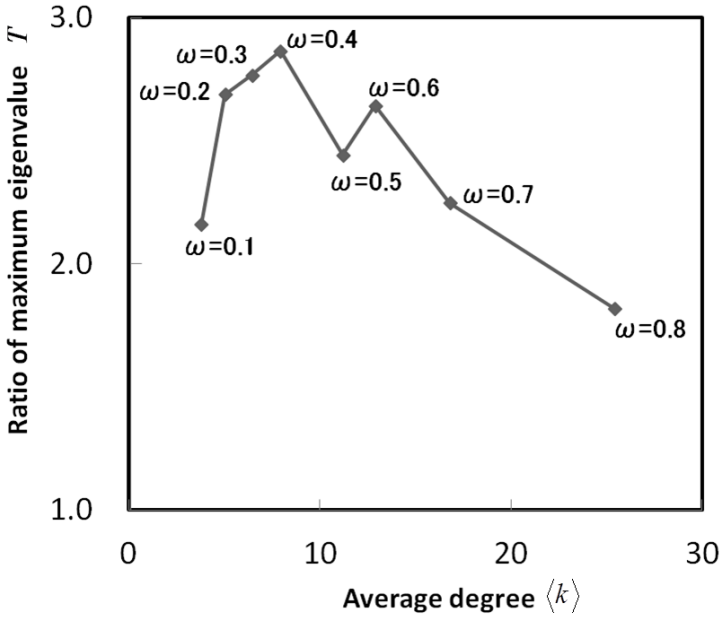

Figure 4.6 Ratio T of maximum eigenvalue of optimised networks to random networks with the same average degree is plotted as a function of average degree $\langle k \rangle$. The value of parameter ω of equation (4.34) is shown at the side of each result.

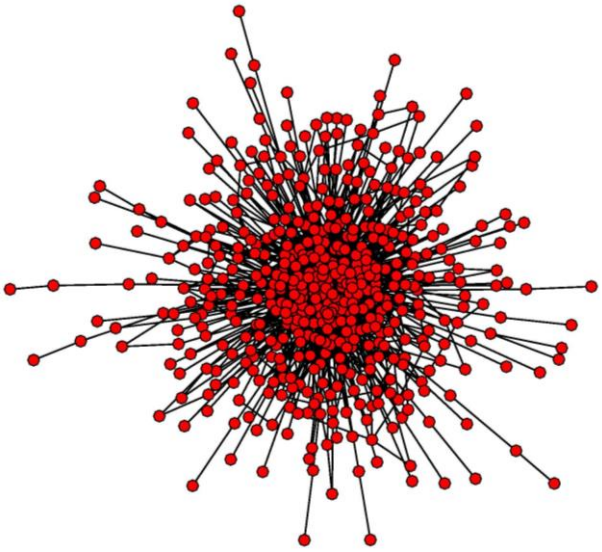

Figure 4.7 The snapshot of the optimized network at $\omega = 0.4$ in equation (4.34) for maximization of probabilistic diffusion (500 nodes, 1984 links ($\langle k \rangle = 7.936$))

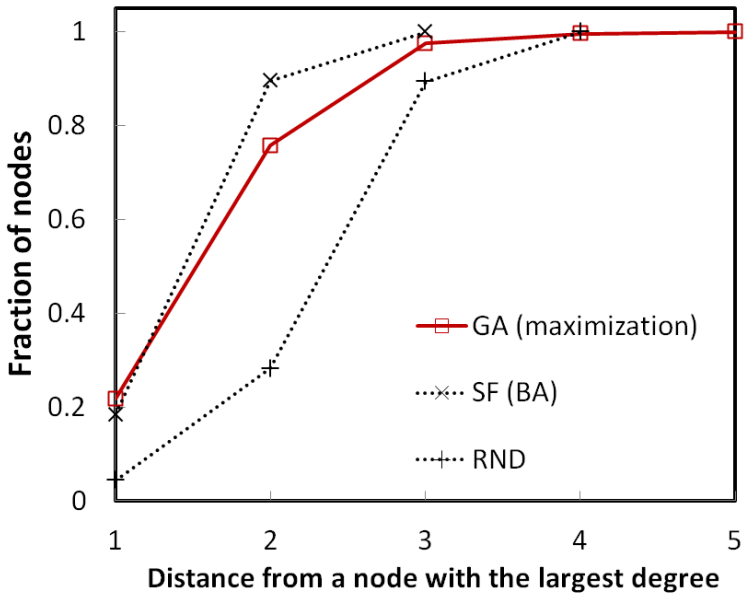

Figure 4.8 The fraction of nodes is plotted as a function of the hop distance from a node with largest degree in optimized network by GA (ω = 0.4 in equation (4.34)) (500 nodes, 1984 links ($\langle k \rangle = 7.936$)), which is compared to a random network and a scale free network with the same average degree.

Table 4.2 The property of networks

	Evolutionary optimized network at $(\boldsymbol{\omega = 0.3})$ in equation (4.34)	Scale-free network	Random network
The number of node	500	500	500
The number of link	1984	1984	1984
The average distance	3.2	2.9	3.2
The maximum eigenvalue of adjacency matrix	25.7	16.0	9.0

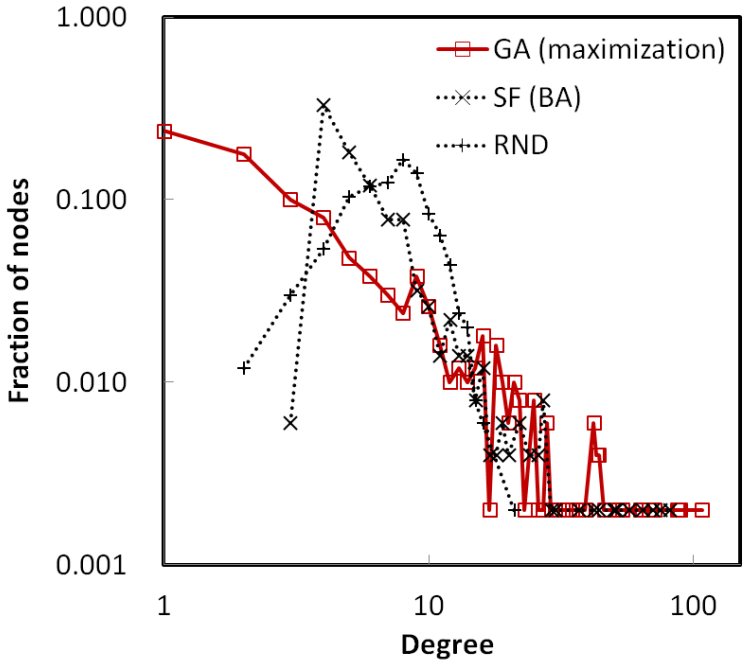

Figure 4.9 The degree distribution of an optimized network by GA (ω = 0.4 in equation (4.34)) (500 nodes, 1984 links ($\langle k \rangle = 7.936$)) is shown, which is compared to a random network and a scale free network with the same average degree.

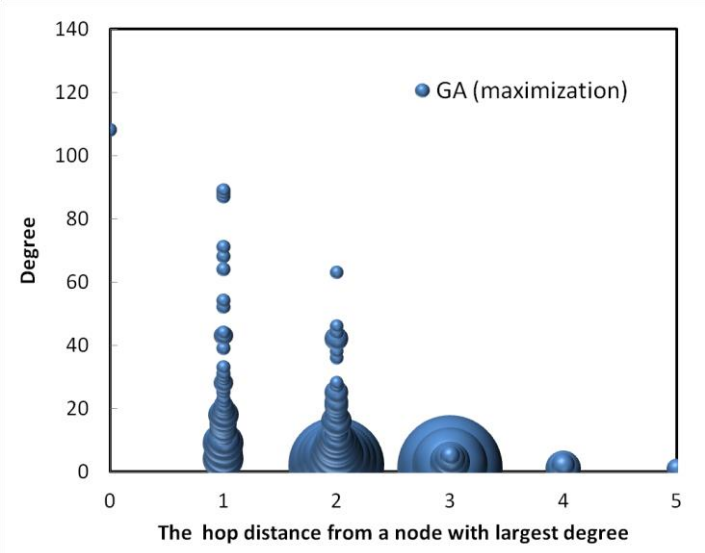

Figure 4.10 A node degree is plotted as a function of the hop distance from a node with largest degree in an optimized network by GA (ω = 0.4 in equation (4.34)) (500 nodes, 1984 links ($\langle k \rangle = 7.936$)) Notes: The size of each circle is drawn in proportion to the number of nodes plotted in the same position. The size of circle at 0 distance means there is one node with about 108 degrees.

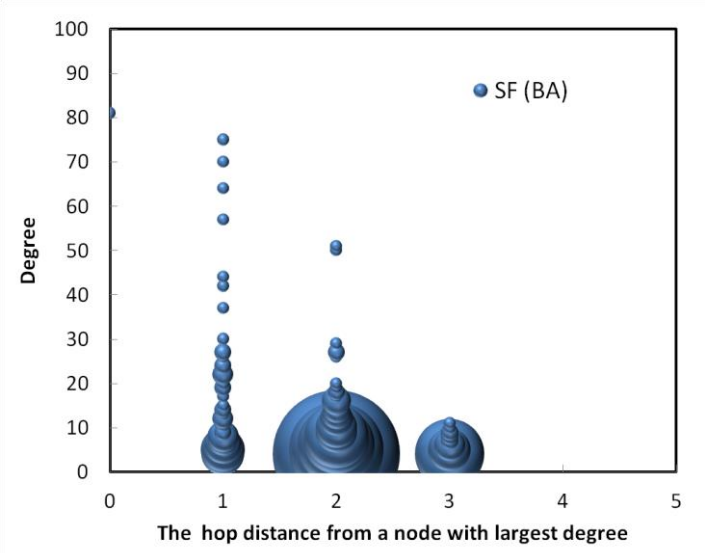

Figure 4.11 A node degree is plotted as a function of the hop distance from a node with largest degree in a scale free network (SF (BA)) with 500 nodes and 1984 links ($\langle k \rangle = 7.936$) Notes: The size of each circle is drawn in proportion to the number of nodes. The size of circle at 0 distance means there is one node with 81 degrees.

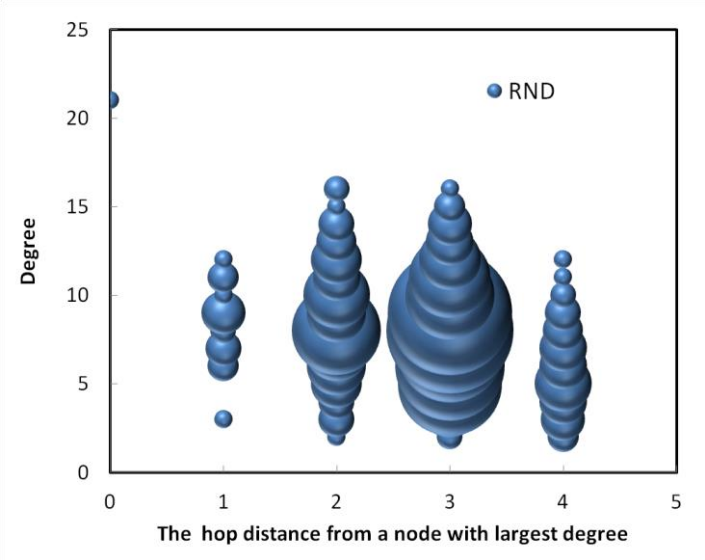

Figure 4.12 A node degree is plotted as a function of the hop distance from a node with largest degree in a random network (RND) with 500 nodes and 1984 links ($\langle k \rangle = 7.936$) Notes: The size of each circle is drawn in proportion to the number of nodes. The size of circle at 0 distance means there is one node with 21 degrees.

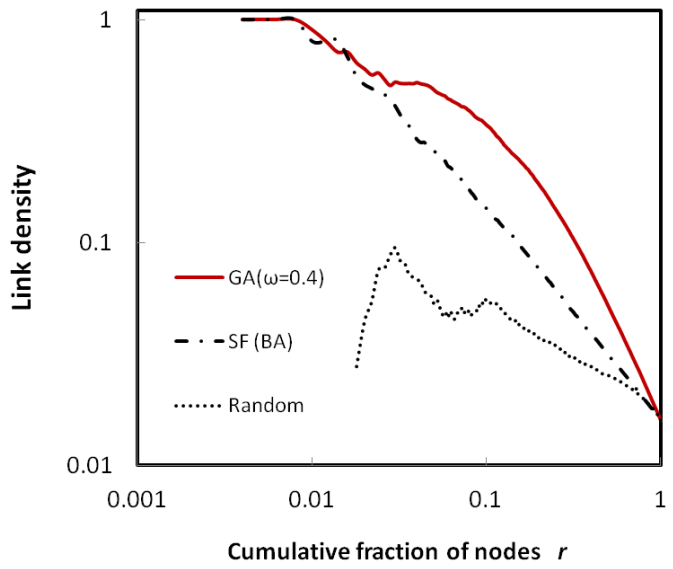

Figure 4.13 Rich club connectivity of networks in Table 4.2 (500 nodes, 1984 links ($\langle k \rangle = 7.936$)), which is link density between nodes that rank in top r% in decreasing order in terms of degree, is plotted as a function of r.

4.3.2 Optimal networks for minimizing probabilistic diffusion

In Figure 4.14 and Figure 4.15, the degree distribution of evolutionary optimized networks for the minimization of probabilistic diffusion is plotted, of which the number of node is 500 and the average degree is $\langle k \rangle = 10.6$ and $\langle k \rangle = 15.9$ respectively. They show optimized networks are almost regular network, in which many nodes have same number of links. The standard deviation of their degree distributions is very small, which are 0.51 ($\langle k \rangle = 10.6$) and 0.37 ($\langle k \rangle = 15.9$) respectively. Although the *k* random regular network, of which average degree is *k*, is known as network having smallest maximum eigenvalue $k - 1$, there is no method to make network having smallest maximum eigenvalue when the average degree is not integer number. The proposed evolutionary network optimization can create optimal networks with smallest maximum eigenvalue under arbitrary average degree.

Note that homogeneous (random regular) network is used as optimal network for the minimization of probabilistic diffusion in the following simulations, because the average degree is usually set as an integer.

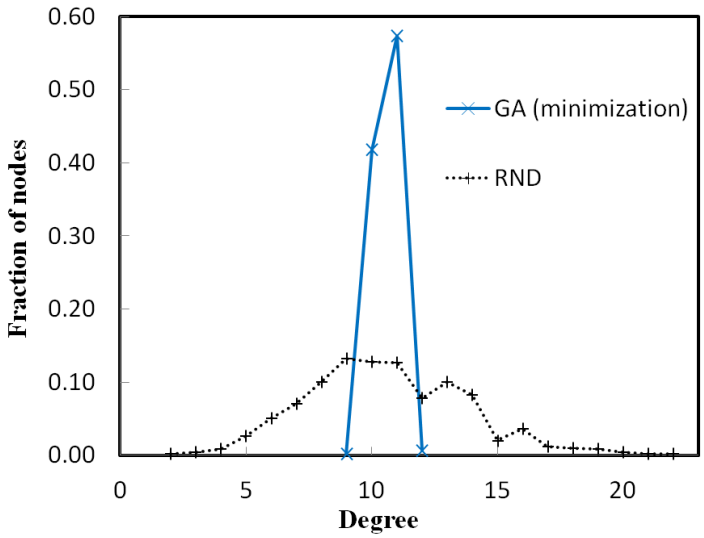

Figure 4.14 The degree distribution of an optimized network by GA (ω = 0.9 in equation (4.37)) (500 nodes, 2646 links ($\langle k \rangle = 10.6$)) is shown, which is compared to a random network with same average degree.

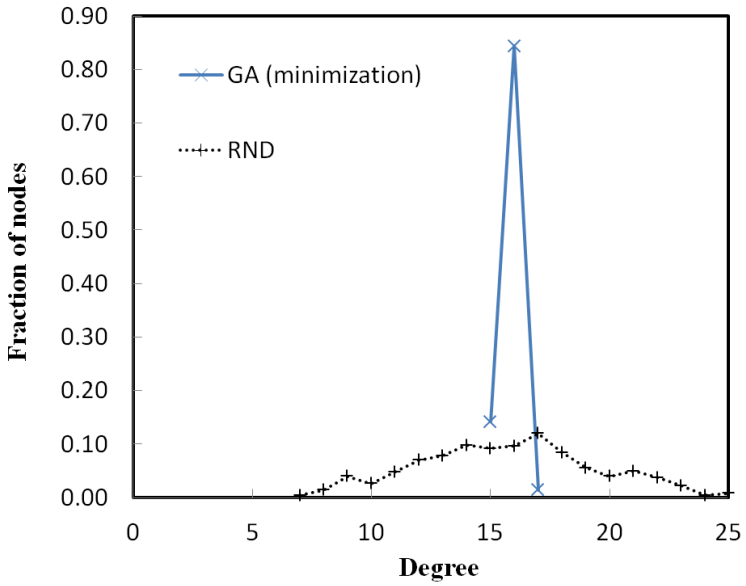

Figure 4.15 The degree distribution of an optimized network by GA (ω = 0.8 in equation (4.37)) (500 nodes, 3968 links ($\langle k \rangle = 15.9$)) is shown, which is compared to a random network with same average degree.

4.4 Heuristic models for designing a large-scale network

Evolutionary network optimization (on a PC) can be applied to small-scale networks (~ 500 nodes), because the time complexity increases with the number of nodes. In this section, two heuristic models are proposed to create large-scale networks for maximizing probabilistic diffusion.

4.4.1 The KN model

The Komatsu-Namatame (KN) network model creates a network which has hub nodes and the cluster of them (Figure 4.16). These topological features are observed in evolutionary optimized networks for the maximizing of probabilistic diffusion. The KN model can be classified to one of growing network models, in which constant number of nodes and links are introduced into a current network at each time step (Figure 4.17).

At first, the small network is prepared as initial network. A new node i is introduced at each discrete time $t = i$ and it is connected to a node by using preferential attachment with the probability $\Pr(k)$ as shown in equation (4.40). Under the preferential attachment scheme, a node with many links has large probability to be connected to a new node and this mechanism makes hub nodes.

$$\Pr(k) = \frac{d_i}{\sum_i d_i}. \tag{4.40}$$

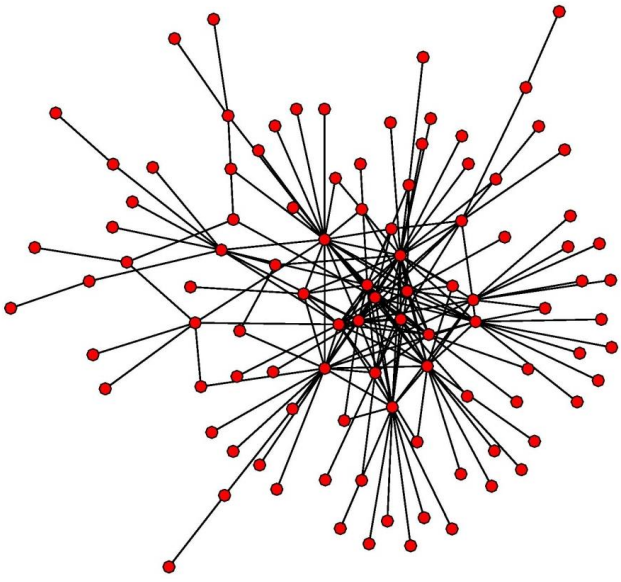

Figure 4.16 KN network (100 nodes and 194 links): The cluster of hub nodes is formed at the center of the network.

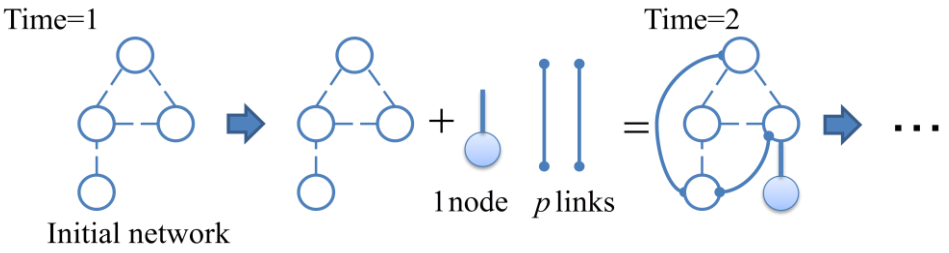

Figure 4.17 The procedure of growing networks by the proposed KN model

At the same time $t = i$, p new links are introduced and they are used to connect two nodes that are not connected directly. A pair of nodes to be connected is also selected by a preferential attachment mechanism. Then, those links are usually used to connect a pair of hub nodes and the procedure makes cluster of hub nodes in the network. As a result, KN network has large rich club connectivity that is observed in optimized network for maximizing probabilistic diffusion (Figure 4.18).

By using mean field theory or master equation method, the degree distribution $p(k)$ of KN model networks can be obtained as,

$$p(k) = \left(1 + \frac{1}{2p+1}\right) k^{-\left(2+\frac{1}{2p+1}\right)}. \tag{4.41}$$

Then, $p(k)$ obeys power law and its power index converges to 2 along with the increase of the number of p. Let *N* denote the number of introduced nodes until now and $\langle k \rangle$ denote the average degree of the network. The relationship between $\langle k \rangle$ and p can be written as shown in equation (4.42) when the *N* is sufficiently large.

$$\langle k \rangle = \frac{2N(1+p)+l}{N+n} \simeq \frac{2N(1+p)}{N} = 2(1+p). \tag{4.42}$$

where *n* and *l* denotes the number of nodes and links in the initial network respectively. The number of introduced links at each time p decides the average number of links and the power index of the degree distribution of the KN model networks, which changes from 3 ($p = 0$) to 2 ($p = \infty$).

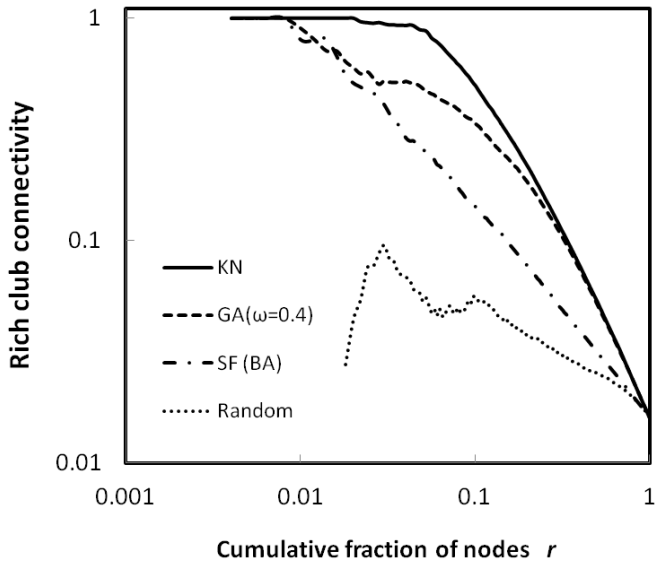

Figure 4.18 Rich club connectivity of networks in Table 4.2 and KN network that has same number of nods and links with other networks (500 nodes, 1984 links ($\langle k \rangle = 7.936$)).

4.4.2 The partial complete graph model

The partial complete graph model is the extreme case of the KN network model, which has most dense cluster of hub nodes. In other words, a part of the network is complete graph K_n where n represents the number of nodes in the complete graph. This type of network can be seen in mathematical study to maximize the spectrum radius of the eigenvalue of the adjacency matrix.

The model consists of only two steps to build a network, as shown in Figure 4.19. Let *N* denote the number of nodes and *L* denote the number of links in the network. At first, the *n*-complete graph K_n is made as a core of a network, in which *n* nodes are connected each other completely and each node has $n-1$ degrees. Any node needs at least one link to connect itself to other node. There is ${}_nC_2$ links in the complete graph K_n, and the formula on L can be obtained as,

$$L = \frac{n(n-1)}{2} + N - n. \tag{4.43}$$

By isolating n, the maximum size of complete graph n_{max} is obtained as,

$$n_{max} = \left\lfloor \frac{3 + \sqrt{9 + 8(L - N)}}{2} \right\rfloor, \tag{4.44}$$

where the floor function $\lfloor x \rfloor$ is used to get maximum integer limited to x ex. $\lfloor 20.2 \rfloor = 20$.

Secondly, the rest of nodes $N - n_{max}$ are attached to the complete graph $K_{n_{max}}$ by using arbitrary methods. Here, two type methods are considered; one is preferential attachment (Complete graph and Preferential Attachment: CPA) and another one is random attachment (Complete graph and Random Attachment: CRA). Figure 4.20 show the examples of CPA and CRA, which have 100 nodes and 200 links. All peripheral nodes are attached to one of nodes in the complete graph or to other peripheral nodes.

The center complete-graph works to maximize the number of contact processes under the fixed network resources (nodes and links), and then diffusion processes is easily in active phase, which is defined in Figure 4.3, even if it has small relative infection rate $\tau\ (= \beta/\delta)$. Surprisingly, the difference of methods to attach peripheral nodes to the complete graph does not affect the tipping point of the network for probabilistic diffusion. It is confirmed by the comparison of maximum eigenvalue and numerical simulations in the following sections.

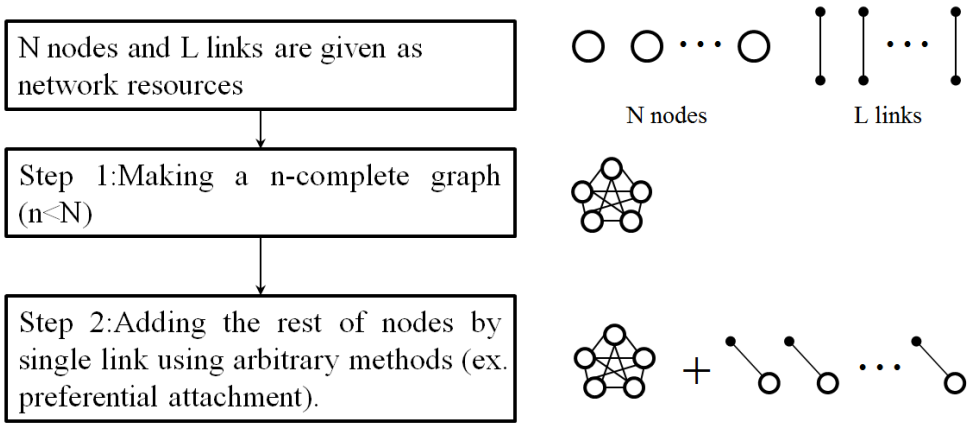

Figure 4.19 The procedures of building proposed networks.

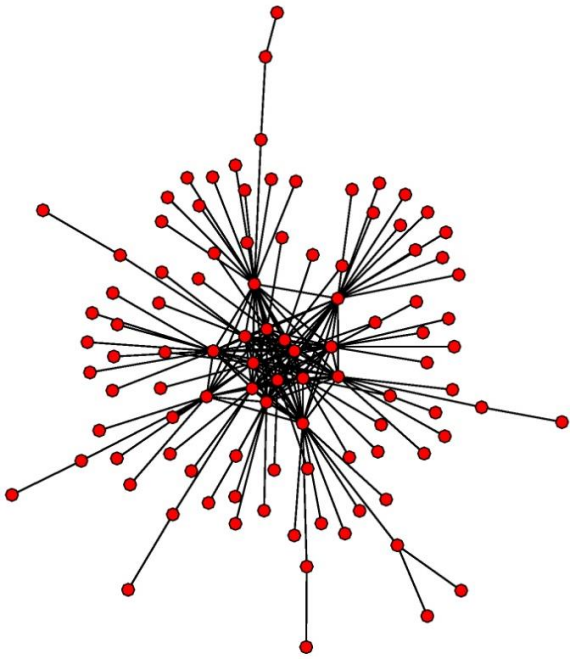

(a) The network that consists of complete graph and preferentially attached nodes (CPA)

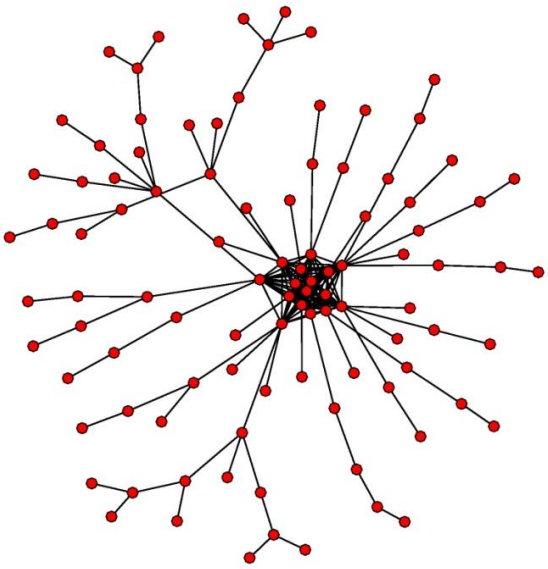

(b) The network that consists of complete graph and randomly attached nodes (CRA)

Figure 4.20 The least susceptible networks: the networks have 100 nodes and 200 links. the number of nodes in the center core is 16.

4.4.3 Comparison of maximum eigenvalues

The maximum eigenvalue of the adjacency matrix defines the tipping points for probabilistic diffusion to take off, and the size depends on the extent of the dense cluster in networks (Figure 4.21). CPA and CRA has complete graph at the center of the network, of which the size is maximized in those networks, and their maximum eigenvalue will converges to the theoretical upper limit along with the average degree. The difference of how nodes, which are not member of complete graph, are added in step 2 (Figure 4.19) will make little change in the size of maximum eigenvalue drastically. From the results, it is clear that the maximum eigenvalue of the adjacency matrix is an index showing the existence of cluster of hub nodes. The difference on the method to connect peripheral nodes to the complete graph does not affect tipping point, but it affects communication efficiency (the average hop distance) between nodes (Figure 4.22). The CPA networks have relatively small average hop distance compared to other networks having same average degree, but the CRA networks have largest average hop distance.

KN network also has relatively large maximum eigenvalue, which is larger than maximum eigenvalue of scale free network. The scale free network is usually said it is most susceptible to probabilistic diffusion (ex. virus spreading on social or computer networks), because the threshold of pandemic on scale free network closes to zero when the size of network (the number of nodes in network) diverges. In the real world, however, the network size is limited to some constant number, which is usually due to the network resource or time restriction. Under such situation, the difference of the threshold for spreading between networks having degree distribution with power law (KN and SF (BA)) becomes clarified, which is the inverse number of maximum eigenvalue. It is known that the Internet has rich club connectivity (the cluster of hub nodes). The results of KN networks show such topological feature of Internet makes it more susceptible to virus spreading than previously believed.

Scale free networks by Balabási-Albert model (SF(BA)) is used in many papers as benchmark networks with low threshold in probabilistic diffusion simulation. The maximum eigenvalue, however, is only 1.5 to 2 times larger than random networks (RND), which are thought to be robust to probabilistic diffusion. This results implies it is needed to evaluate the network properties by not only the type of degree distribution and but also appropriate index (the maximum eigenvalue) that influences the network dynamics directly.

The increase of maximum eigenvalue of the homogeneous networks with the average degrees shows the pandemic can occur on any kind of networks except special networks, of which the average degree is constant (ex. line graph). The lower limit of maximum eigenvalue is bounded by average degree, and then the increase of the average degree decreases the threshold of the pandemic.

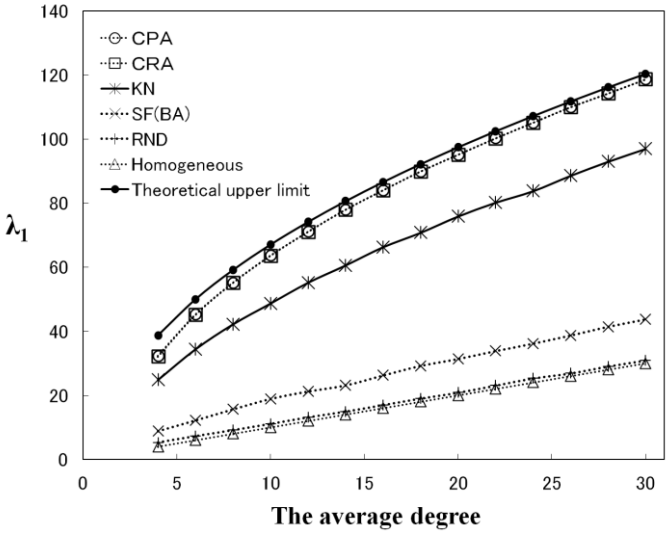

Figure 4.21 The maximum eigenvalue of adjacency matrix of each network with 500 nodes is plotted as a function of the average degree of it: CPA: Complete graph and preferential attachment, CRA: Complete graph and random attachment, KN: KN network, SF(BA): Scale free network by Balabási-Albert model, RND: Random network, Homogeneous; Regular random network, Theoretical upper limit is defined by equation (4.33).

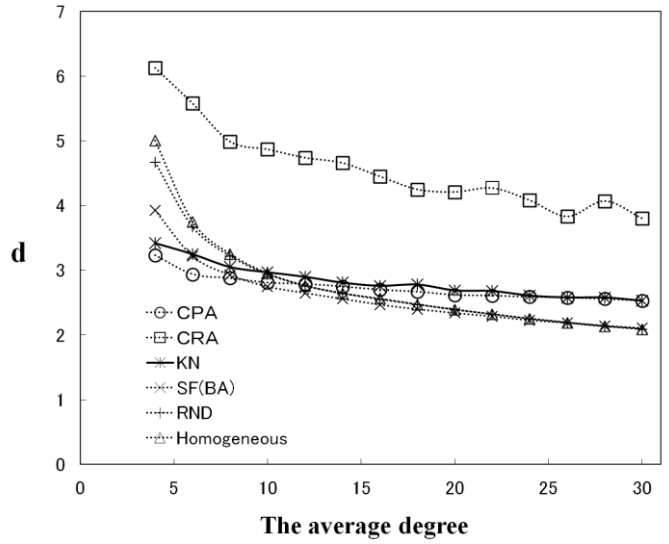

Figure 4.22 The average hop distance d of each network is plotted as a function of the average degree: CPA: Complete graph and preferential attachment, CRA: Complete graph and random attachment, KN: KN network, SF(BA): Scale free network by Balabási-Albert model, RND: Random network, Homogeneous; Regular random network.

4.4.4 Diffusion thresholds

The maximum eigenvalue $\lambda_{max}(\mathbf{A})$ of adjacency matrix $\mathbf{A}$ of network is dominant eigenvalue for probabilistic diffusion taking place on networks, because it decides the tipping point ($= 1/\lambda_{\max}(\mathbf{A})$) (with SIS model) to take off and is related to how hub nodes are interconnected, which also affects the deterministic diffusion (it is discussed in Chapter 5). The maximum eigenvalue $\lambda_{max}(\mathbf{A})$ is equal or larger than average degree $\langle k \rangle$ and the value increases with the average degree. If the network has infinity nodes and certain average degree, the maximum eigenvalue also becomes infinity and it means the comparison of the maximum eigenvalue has no meaning because any network becomes diffusive with no threshold. For example, probabilistic diffusion can occur on even homogeneous network, which is least diffusive network when networks are compared under a finite network size.

In the real world, however, the network size (the number of nodes) is finite due to several reasons including the finite network resources and the finite time of network design. In these cases, the maximum eigenvalue is not infinite and the comparison of it between networks is meaningful. Here, the new index is used, which is the normalized maximum eigenvalue, $\langle k \rangle/\lambda_{\max}(\mathbf{A})$ to capture the properties of how network topology affects process taking place on networks. The range of this index is given as,

$$0 < \frac{\langle k \rangle}{\lambda_{\max}(\mathbf{A})} \leq 1. \tag{4.45}$$

The right hand equality holds when the network is completely homogeneous and the index becomes smallest when the network topology is partially compete graph like CPA and CRA. From topological point of view, the index shows how network is homogeneous.

In Figure 4.23, the critical threshold value τ_c of SIS model of different networks that have different average degree from 4 to 30 is plotted as a function of $\langle k \rangle/\lambda_{\max}(\mathbf{A})$. From the results, it is clear that τ_c is changed linearly with the normalized maximum eigenvalue $\langle k \rangle/\lambda_{\max}(\mathbf{A})$, and the network with less homogeneity becomes more diffusive when the network has same average degree. Along with the increase of $\langle k \rangle/\lambda_{\max}(\mathbf{A})$, the tipping point in any average degree cases are moved from bottom to top, because the value of the homogeneous network is largest $\tau_c = 1/\lambda_{max}(\mathbf{A}) = 1/\langle k \rangle$ compared to other networks. The increase of average degree makes networks more homogeneous and finally all networks become complete graph, which is most diffusive network.

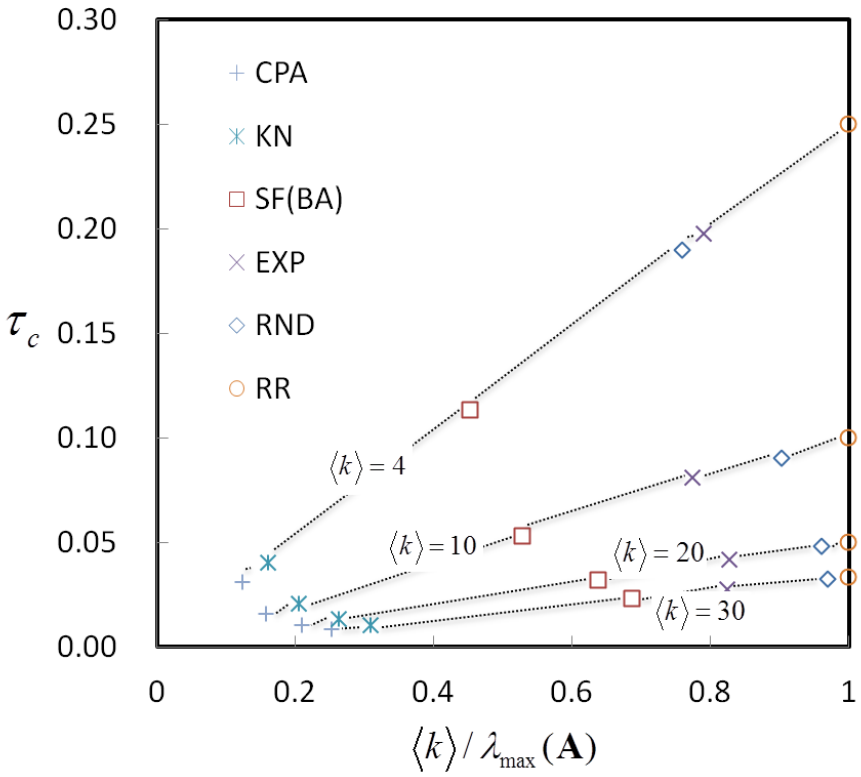

Figure 4.23 The critical threshold value τ_c of SIS model on different networks is plotted as a function of normalized maximum eigenvalue $\langle k \rangle / \lambda_{max}(\mathbf{A})$.

4.5 **Simulation on optimized networks**

In this section, a set of simulation results is given. The simulations are conducted to confirm diffusion processes will take off easily on networks by proposed models (CPA, CRA, KN), compared to scale-free network and random network.

Scale-free networks used in this study are generated by Balabási-Albert model. Random graphs are generated by Erdos-Reny model. Each network has 500 nodes, and the average degree is 4.

Each simulation begins with making only one node infected, which has most number of links in the network. Simulation proceeds in steps of one time unit. During each time step, all infected nodes attempt to infect each of its neighbors with probability β simultaneously. In addition, every infected nodes go back to be susceptible again with probability δ. The attempt of infection on a already infected node has no effect. Each simulation will be done when diffusion process is in a steady state $dI(t)/dt = 0$. Unless otherwise specified, each simulation plot is averaged over 100 individual runs. In each simulation, infection rate β and recovering rate δ are set as,

$$\beta = Score \times \frac{\delta}{\lambda_1(\mathbf{A}_{CPA})}, \qquad \delta = 0.1, \tag{4.46}$$

where Score is a scaling parameter to decide infection rate based on the threshold $\tau_c(= 1/(\lambda_1(\mathbf{A}_{CPA})))$ of a network which is a CPA network with largest maximum eigenvalue and same number of nodes and links. Score parameter is varied from 1 to 100.

During probabilistic diffusion processes by SIS model, the state of each node is changing between $x_i = 0$ and $x_i = 1$. When a relative infection rate $\tau = \beta/\delta$ is sufficiently small, all nodes becomes $x_i = 0, \forall i$ at a steady state. When τ is very large, a steady state of all nodes are $x_i = 1, \forall i$. Then, this simulation clarifies the tipping points of τ^* of each network and the behavior of probabilistic diffusion after $\tau > \tau^*$.

In Figure 4.24, the fraction of infected nodes at a steady state on networks by proposed models is plotted as a function of score, which is compared to other networks. It is clear that each network has different tipping points τ^*, and the magnitude relationship is shown in equation (4.47), which is the same relationship of the inverse of maximum eigenvalue of each network.

$$\tau^*_{CPA} = \tau^*_{CRA} < \tau^*_{KN} < \tau^*_{SF(BA)} < \tau^*_{RND} < \tau^*_{Homogeneous}. \tag{4.47}$$

The network with the large maximum eigenvalue of the adjacency matrix is prone to probabilistic diffusion and the infection process will survive for a long time. In other words, the dense cluster is foothold for probabilistic diffusion to survive at a steady state.

Many of recent studies make effort to estimate a tipping point value τ^* accurately, but in the real world the fraction of infected nodes is also important to

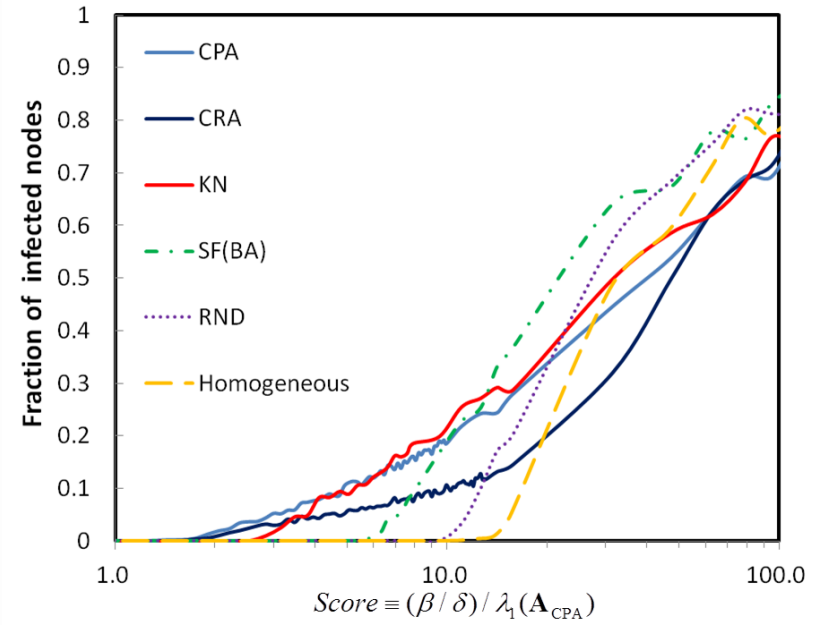

Figure 4.24 The fraction of informed nodes at steady state is plotted as a function of the score. Each network has 500 nodes and same average degree $\langle k \rangle = 4$.

understand the diffusion processes. From the simulation results, even if τ exceeds a tipping point τ_c, all nodes are not necessarily infected. In order to make all nodes infected, τ should be increased sufficiently. This result can be explained mathematically. The maximum eigenvalue is dominant when $\tau \simeq \tau^*$, but it is need to consider the influence of following terms, which are more than second order, of the equation (4.47) when $\tau > \tau^*$.

Figure 4.25 shows the time evolution of the diffusion processes from an initial state (time $= 0$) to a steady state on networks having different epidemic threshold τ_c. For example, in a case that diffusion is simulated with $\beta = 0.097$ and $\delta = 0.1$ (Figure 4.25 (b)), if maximum eigenvalue that meets the condition $\lambda_1(\mathbf{A}) \geq \delta/\beta = 1.03$, the diffusion will take off. The time evolution shows logistic curve (s-curve), which is also observed in the diffusion by Kephart and White model, and the exact curve of time evolution seems to depend on each network topology.

From equation (4.31), it is clear that the spectrum of eigenvalues and the size of infection rate β and curing rate δ decide the behavior of time evolution of diffusion processes. The network with large maximum eigenvalue has the tendency to have high changing rate of infected nodes at an early stage of the diffusion. In a case that the order of maximum eigenvalue between networks represents an order of rest of eigenvalue similarly, the changing rate of the fraction of infected nodes can be compared by the value of maximum eigenvalue. Figure 4.26 shows top 10 maximum eigenvalue of the adjacency matrix of networks. The magnitude relationship of maximum eigenvalue of SF(BA), RND, and Homogeneous networks shows the

relationship of following eigenvalue and then the order of changing rate of infected nodes is the same to the order of maximum eigenvalue. In any other case, however, the magnitude relationship of maximum eigenvalue of networks necessarily does not represent the order of the rest of eigenvalues, and it is difficult to discriminate the changing rate by maximum eigenvalue simply. The CRA network has larger maximum eigenvalue compared to KN network, but the rest of eigenvalues are smaller than those of KN network. Figure 4.27 (a) shows results of numerical calculation of the time evolution of the fraction of infected nodes from equation (4.31). The fraction of infected nodes on CPA network is larger than KN network at first, however, after time step $= 2$, KN network has more infected nodes in it. This result comes from the distribution of the eigenvalues and the tendency is confirmed by results of numerical simulations in Figure 4.27 (b).

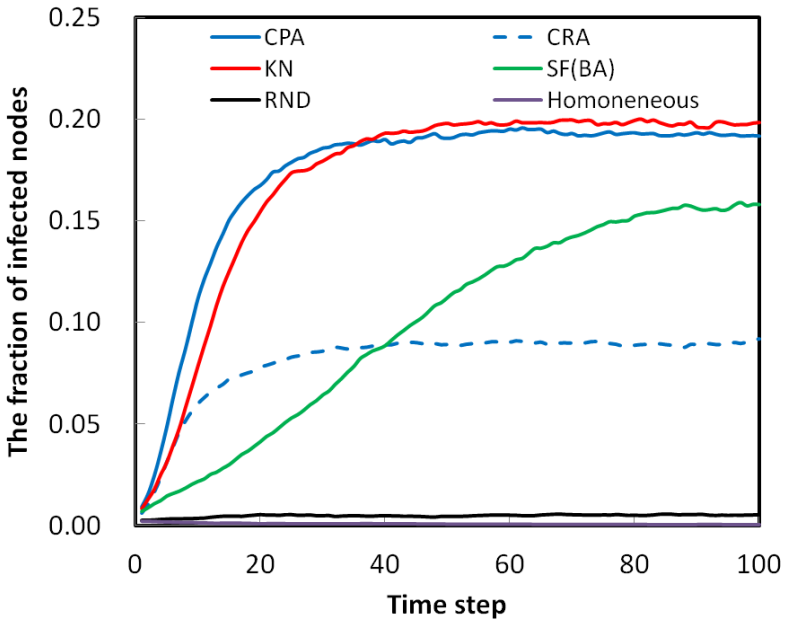

(a) $Score \simeq 10: \beta = 0.030, \delta = 0.1$

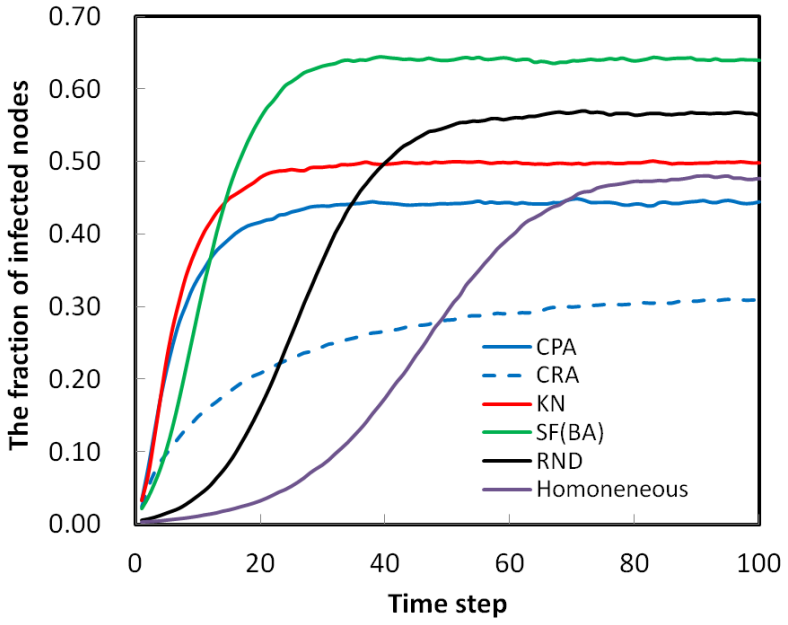

(b) $Score \simeq 30: \beta = 0.097, \delta = 0.1$

Figure 4.25 The time evolution of the fraction of infected nodes: The score based on the maximum eigenvalue of a CPA network is set as 10 and 30 respectively. All networks have 500 nodes and 1000 links ($\langle k \rangle = 4$).

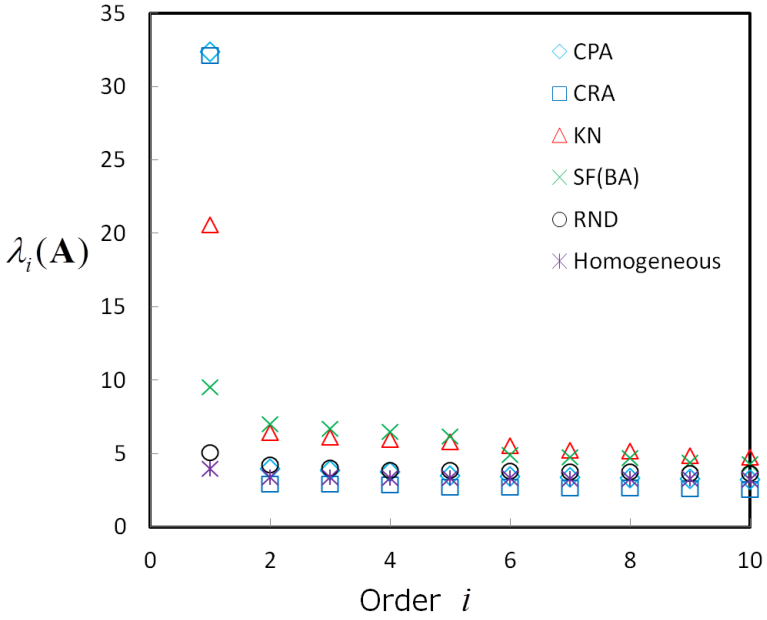

Figure 4.26 The i th maximum eigenvalue of adjacency matrix of networks. All networks have 500 nodes and 1000 links ($\langle k \rangle = 4$).

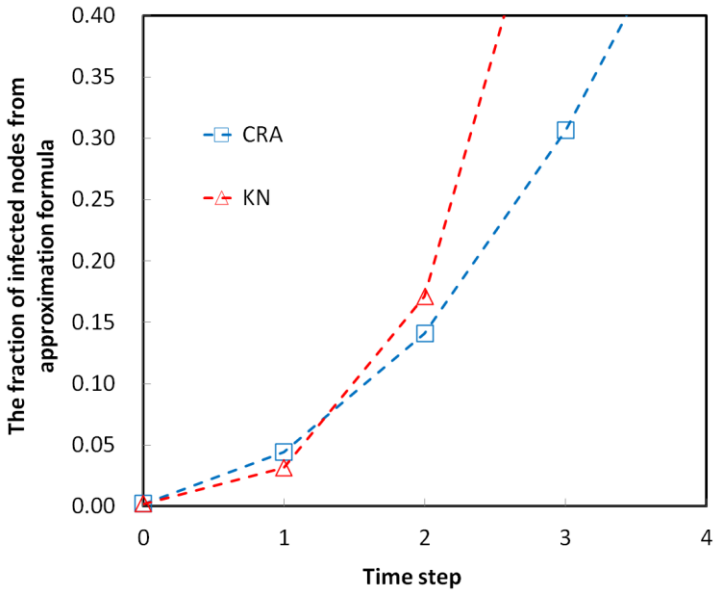

(a) Results of numerical calculation about the time dependence of the fraction of infected nods by using approximation formula (4.31): The infection rate $\beta = 0.0971$ and the curing rate $\delta = 0.1$ are settled as same in Figure 4.25 (b) $Score = 30$.

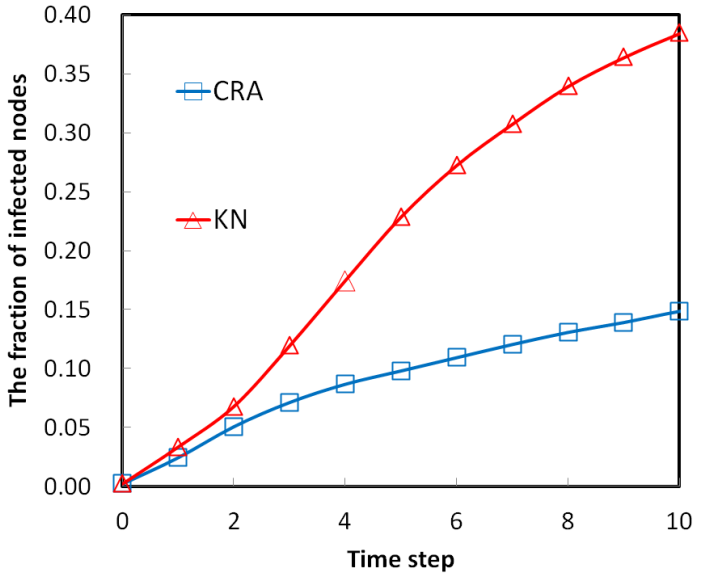

(b) The simulation results in Figure 4.25 (b) $Score = 30$ is rewritten on small scale to see the changing rate of infected nodes at early stage clearly.

Figure 4.27 The comparison of the changing rate of infected nodes at early stage of the diffusion on CRA network and KN network to see the influence of the difference of the spectrum on eigenvalue of adjacency matrix.

Chapter 5

Cascade Dynamics

In Chapter 5, cascade dynamics on a threshold model is discussed, which is usually applied to study evolution of collective behaviors. Example includes diffusion of innovation and cascade failure such as chain bankruptcy. After introducing basic properties of cascade dynamics, optimal networks for maximizing cascade dynamics are formed by evolutionary optimization. The optimized networks have specific patterns of interconnection between nodes. Topological analysis of the optimal networks and numerical simulations on them show that the specific topological pattern controls the pathway of cascade dynamics to spread into the whole network via a cluster of vulnerable nodes. It is also demonstrated that optimal networks for minimizing cascade dynamics are optimal networks for maximizing probabilistic diffusion.

5.1 **A threshold model**

As mentioned in section 2.1, there are two types of cascade models, an overload model and a threshold model. Here, cascade dynamics on a threshold model is considered.

A threshold model includes no probabilistic dynamics and the difference brings another type of diffusion properties, which is called robust but fragile. Let a given networked system have N agents (nodes) and L links and all agents have certain threshold ϕ_i $(i = 1,2,3, \cdots N)$. All agents face a situation whether they will adopt a new innovation $s_i = 1$ or keep the present manner $s_i = 0$. Agents change their own state from and to the space $S = \{0,1\}$ based on the fraction of adjacent agents who adopt innovation at the previous time step. If the adoption rate of neighboring nodes is larger than the threshold ϕ_i, the agent will become the adoption state $s_i = 1$ at the next time step. The dynamics is summarized by equation (5.1).

$$s_i(t+1) = \begin{cases} 1 & \frac{\sum_{j \in N_i} s_j(t)}{d_i} \geq \phi_i \\ 0 & \frac{\sum_{j \in N_i} s_j(t)}{d_i} < \phi_i \end{cases} . \quad (5.1)$$

where $j \in N_i$ denotes a set of adjacent agents of agent i.

Cascade dynamics by the model is progressive, where the direction of change in state is one way, for example, no agents turn back to be initial state after it changed. Initially, no agents adopt innovation $s_i = 0, \forall i$. The state of a few agents are forcely changed from 0 to 1 as a trigger of cascade dynamics and changes of the state of some neighboring agents is induced by them, which makes further changes of the state of other agents recursively. When a sequence of the change, or so-called "cascade", is spread to the almost of all agents, such a result is called "global cascade". This threshold model is usually used in the studies including diffusion of innovation, opinion formation and the spread of the specific state into the network.

The dynamics by threshold model can be considered as coordination games on networks, in which agents play a 2×2 coordination game with each neighbor and revise the own state using a deterministic myopic-best response to maximize his current payoff that is decided by the fraction of neighbors choosing same state. In this framework, selecting 0 or 1 means, for example, adopting innovation or conservatism, selecting new product A or old product B, and accept or reject. The characteristic property of this cascade model is the decision rule based on the locality and the proportion of agents. Thanks to this simplicity, the model can be applied on many situations, in which each agent makes a binary decision. The payoff of each state for agents is summarized in symmetric matrix (Table 5.1).

Table 5.1 A payoff matrix of a coordination game: agent i and agent j can select 0 or 1 respectively, and the payoff depends on a combination of a selection by agent i and agent j. If agents select same one, they will get profit a or b. However, if agents select different ones, they will get no profit. The value at left side in each cell represents the profit of agent i and the value at right side in each cell represents the profit of agent j.

i \ ***j***	1	0
1	a, a	0, 0
0	0, 0	b, b

Let $U(s_i, s_{j\in N_i})$ be a total payoff after a 2×2 coordination game with neighboring agents as shown in equation (5.2), which is obtained using the summation of a payoff of each coordination game $u(s_i, s_j)$.

$$U(s_i, s_{j\in N_i}) = \sum_{j\in N_i} u(s_i, s_j). \tag{5.2}$$

The best response of each agent depends on the fraction of neighbors choosing 1. If the fraction r is larger than the threshold ϕ, then the best response of agent *i* is to choose 1, which means agent *i* adopts innovation. Otherwise agent *i* choose 0. The threshold value ϕ is decided by, for example, how attractive the innovation or opinion is for agents. The dynamics of a choosing state by agents is summarized by equation (5.3).

$$\mathrm{s_i} = \begin{cases} 1 & r > \phi \\ 0 & r < \phi \end{cases}, \phi = b/(a+b). \tag{5.3}$$

5.2 **Cascade window**

Watts [21] showed that there exists a condition of global cascade by using generating function, which is in terms of the threshold ϕ and the average degree (the average number of adjacent agents) z. Under the condition, global cascade could occur and the diffusion of innovation is achieved. They named this condition (area) as cascade window.

The size of a cluster of vulnerable nodes which have small degrees and are affected easily by even a single adopting node, decides whether the cascade spreads to the entire network by a trigger.

In order to obtain the condition for global cascade, a calculation of a cluster size of vulnerable nodes is done by generating function which is well-used approach to calculate a cluster size in the percolation theory. A generating function on the degree distribution $G_0(x)$ is defined as,

$$G_0(x) \equiv \sum_{k=0}^{\infty} P(k)x^k, \tag{5.4}$$

where $P(k)$ represents degree distribution of the network.

The average degree (1st moment) $\langle k\rangle$ of the degree distribution $P(k)$ is given by $G_0(x)$ as shown in equation (5.5).

$$\langle k\rangle = \sum_{k=0}^{\infty} kP(k) = G'_0(1). \tag{5.5}$$

The n-th moment is also given by equation (5.6).

$$\langle k^n \rangle = \sum_{k=0}^{\infty} k^n P(k) = \left(x \frac{d}{dx} \right)^n G_0(1) \Big|_{x=1}. \tag{5.6}$$

The probability distribution that a node has degree k, which is pointed from a randomly selected link, is $kP(k)/\langle k \rangle$. The generating function of this distribution is given by equation (5.7).

$$\begin{aligned} &\frac{\sum_{k=0}^{\infty} kP(k)x^k}{\langle k \rangle} \\ &= \frac{0P(k)x^0 + 1P(1)x^1 + 2P(2)x^2 + 3P(3)x^3 + \cdots}{\langle k \rangle} \\ &= \frac{xG'_0(x)}{\langle k \rangle}. \end{aligned} \tag{5.7}$$

The generating function of the probability distribution that a node has degree k except a following link, which is pointed from a randomly selected link, is given by equation (5.8).

$$\begin{aligned} G_1(x) &\equiv \frac{P(1)x^0 + 2P(2)x^1 + 3P(3)x^2 + \cdots}{\langle k \rangle} \\ &= \frac{G'_0(x)}{\langle k \rangle}. \end{aligned} \tag{5.8}$$

The probability distribution of it, which is the summation of the degree of m nodes that are randomly selected from a network, is given by $G_0(x)^m$. In the case $m = 2$, for example, $G_0(x)^2$ is given as,

$$\begin{aligned} \mathrm{G}_0(x)^2 &= \left[\sum_{k=0}^{\infty} P(k)x^k \right]^2 \\ &= P(0)P(0)x^0 + (P(0)P(1)+P(1)P(0))x^1 \\ &+ (P(0)P(2) + P(1)P(1) + P(2)(0))x^2 + \cdots, \end{aligned} \tag{5.9}$$

where each coefficient of variable x^k implies the probability of the summation of the degree of two node is k.

$H_1(x)$ the generating function of the distribution of the size of the vulnerable cluster is defined as shown in equation (5.10) by using the recursiveness of the topology (Figure 5.1) and the property of the generating function (equation (5.9)).

$$\begin{aligned} H_1(x) &\equiv f\big(H_1(x)\big) \\ &= xq_0 + xq_1 H_1(x) + xq_2 [H_1(x)]^2 + xq_3 \big[H_{1(x)}\big]^3 + \cdots \\ &= xG_1\big(H_1(x)\big), \end{aligned} \tag{5.10}$$

where coefficient q_k represents the degree distribution of a node except a following link, which is connected to randomly selected link.

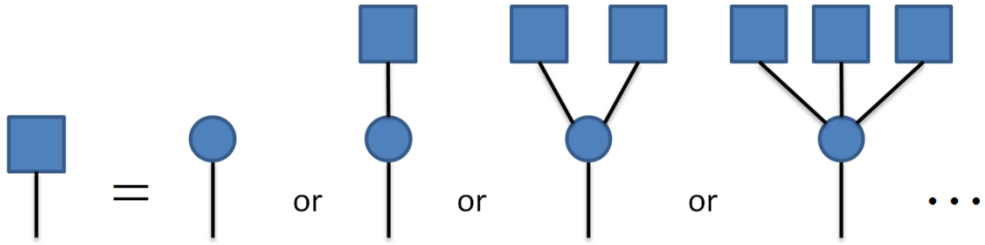

Figure 5.1 The recursiveness of network. The network topology can be explained the combination of itself.

The generating function $H_1(x)$ can be rewritten from a viewpoint of nodes as,

$$H_0(x) \equiv xG_0\big(H_1(x)\big). \tag{5.11}$$

The average cluster size $\langle n \rangle$ including a randomly selected node is given as,

$$\begin{aligned} \langle n \rangle &= H_0'(1) \\ &= G_0\big(H_1(1)\big) + G_0'\big(H_1(1)\big)H_1'(1) \\ &= 1 + G_0'(1)H_1'(1), \end{aligned} \tag{5.12}$$

where $H_1'(1)$ is

$$\begin{aligned} H_1'(1) &= G_1\big(H_1(1)\big) + G_1'\big(H_1(1)\big)H_1'(1) \\ &= 1 + G_1'(1)H_1'(1) \\ &= \frac{1}{1 - G_1'(1)}. \end{aligned} \tag{5.13}$$

Then, equation (5.12) can be rewritten as,

$$\begin{aligned} \langle n \rangle &= 1 + \frac{G_0'(1)}{1 - G_1'(1)} \\ &= 1 + \frac{\langle k \rangle G_0'(1)}{\langle k \rangle - G_0''(1)}. \end{aligned} \tag{5.14}$$

The degree distribution of vulnerable node is given by

$$P_v(k) = \xi_k P(k), \tag{5.15}$$

where $\xi_k = \lfloor 1/\phi \rfloor$ and $\lfloor x \rfloor$ denotes a floor function ex. $\lfloor 5.2 \rfloor = 5$.

The average size of a vulnerable cluster is given as,

$$\langle n_v \rangle = 1 + \frac{\langle k \rangle G_v'(1)}{\langle k \rangle - G_v''(1)}, \tag{5.16}$$

where $G_v\ (x) = \sum \xi_k P(k) x^k$.

The equation (5.16) will diverge when $\langle k \rangle = G_v''(1)$. It implies a cluster size of vulnerable nodes is sufficiently large for a cascade dynamics to spread into the whole network via the cluster of vulnerable nodes. Then the condition of global cascade is given as,

$$\sum_{k=0}^{\lfloor 1/\phi \rfloor} k(k-1)P(k) = z, \tag{5.17}$$

where the constant z represents the average degree $\langle k \rangle$.

Figure 5.2 shows the example of the theoretical cascade window of different network topologies from the cascade condition by Watts [21] (equation (5.17)). Inside the cascade window, an initial trigger node can make global cascade, but outside the cascade window the trigger has little influence and it cannot make global cascade.

It is clear that even if networks have same average degree z, they have different size of cascade window due to the difference on their degree distribution. This implies that the size of the cascade window is influenced by underlying network topology.

Young modeled the diffusion of innovation using a threshold model and studied the cascade condition on the lattice network [12, 13, 105] and Watts showed the importance of agents having small degree to maximize cascade window [106]. From their results, it is important that there is a large cluster which consists of agents with a small number of links. López used a mean-field approximation for modeling cascade phenomena on a threshold model and said that a network with intermediate variance in degree distribution maximizes the size of cascade window because the limitation make a network have a cluster of vulnerable nodes as Young and Watts introduced. López showed the relationship between the topology and the size of cascade window which is that an exponential network has wider cascade window compared to a scale free network [107] that is most susceptible to probabilistic diffusion [77]. Figure 5.2 compares theoretical cascade windows. It is shown that the exponential network actually has larger cascade window compared to scale free network by KN model. However, a scale-free network by Barabási-Albert model has a wider cascade window than it of an exponential network (Figure 5.2). This implies that the conclusion by López about cascade window is partially true, which is that a network with intermediate deviation in its degree distribution, has the largest cascade window.

From Figure 5.2, the inequality on the size of the cascade window is obtained as,

$$\phi_{\mathrm{KN}} < \phi_{\mathrm{RND}} < \phi_{\mathrm{EXP}} < \phi_{\mathrm{SF(BA)}}. \tag{5.18}$$

This result brings another fundamental questions such as “Is the scale free network by Barabási-Albert model the best network to maximize the cascade window?”, “Contrary to maximization of the cascade window, what kind of network is optimal to prevent cascade dynamics?” and “How do we design networks which meet our requirements on the size of cascade window?”. Answering these questions is the first step to understand relationship between cascade phenomena and network topologies. In this dissertation, the optimal networks are studied, which maximize the cascade window for good cascade and minimize the cascade window for bad cascade.

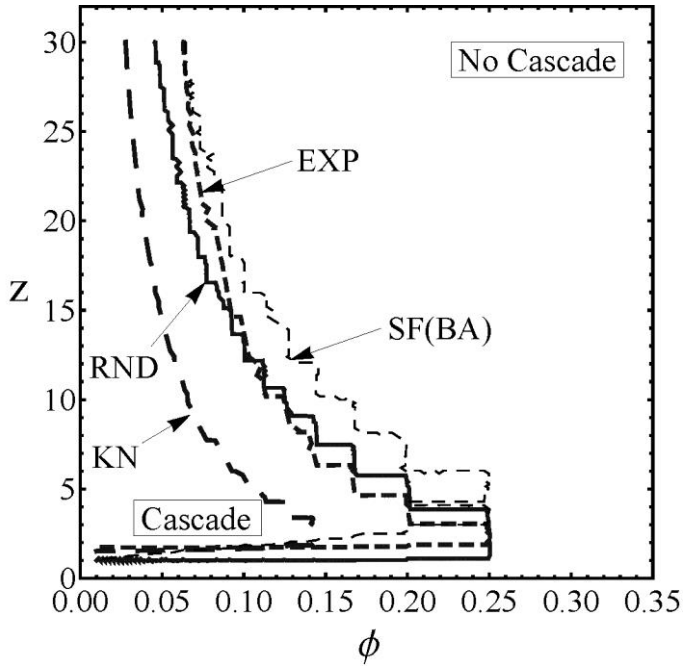

Figure 5.2 The cascade window as a function of the threshold value ϕ of agents and the average degree z of networks: scale free network by KN model (KN), random network (RND), exponential network (EXP), and scale free network by BA model (SF(BA)).

In cascade dynamics, the accumulation of adopting nodes has completely different effects compared to probabilistic diffusion. The changing probability on a state of a node is a nonlinear function under cascade dynamics on a threshold model; if the fraction of neighboring-adopting agents is under a threshold value of a node, nothing will happen, and if the fraction is over a threshold of a node, it is inevitable that a node i will adopt. This local dynamics decides the role of a hub node on cascade dynamics. In order to change the state of a hub node, large fraction of neighboring nodes should have adopted it, and then a hub node works as obstacles for a good cascade or firewall for a bad cascade (Case 1 in Figure 5.3). Of course, a hub node can transfer the influence to many neighboring nodes simultaneously (Case 2 in Figure 5.3). However, it rarely occurs due to small fraction of hub nodes, and it also has limited effect when the average degree of a network is not small because neighbors of a hub node are not usually vulnerable nodes under the condition.

The cluster of vulnerable nodes which will adopt it even if only one of neighboring node has adopted it, have important role to get past a firewall (a hub node) (Case 3 in Figure 5.3). If the cascade dynamics begin from a vulnerable node, the sequence of adaptations can continue in a cluster of vulnerable nodes. When the substantial fraction of vulnerable nodes has adopted it, a center hub node will adopt it. A vulnerable node cannot make a hub node adopt directly, but the accumulation of adaptations of vulnerable nodes can do it. After that, the hub node will affect the rest of

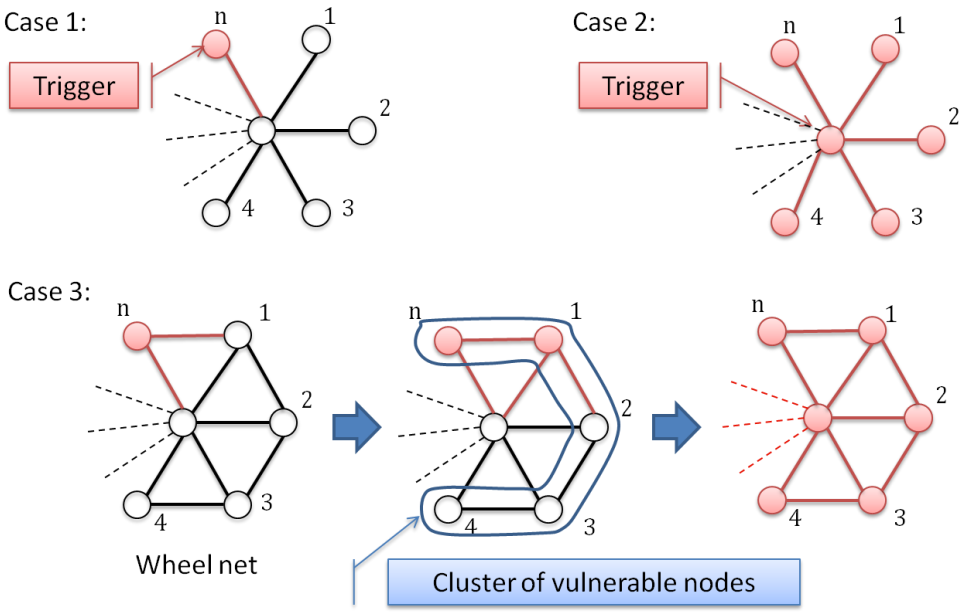

Figure 5.3 The effects of network topology on cascade dynamics.

neighboring un-adopted nodes efficiently. In this respect, the cluster of vulnerable nodes works as a catalyst of cascade dynamics and a hub node works as both a firewall and an accelerator.

Cascade dynamics on a threshold model has different phase transition compared to probabilistic diffusion. Figure 5.4 shows an example of the phase transition on scale free network by Barabási-Albert model. At around $\phi = 0.3$, the cascade does not spread globally, and the average size of cascade is the same to a trigger node. Along with the decrease of the threshold value, the average size of cascade will increase, but the information from the average size does not show what actually happen on the network. For example, the average cascade size is still very small ($= 0.7\%$) at the threshold $\phi = 0.22$, but the global cascade is observed at least two times as results of 1000 iterative numerical simulations. In probabilistic diffusion, the fraction of infected nodes at a steady state is increased continuously from a tipping point, but under cascade dynamics the prevalence to the whole network may occur at a tipping point and it will not happen always. This property of cascade dynamics is called “robust but fragile” and it makes difficult to predict the results of cascade dynamics.

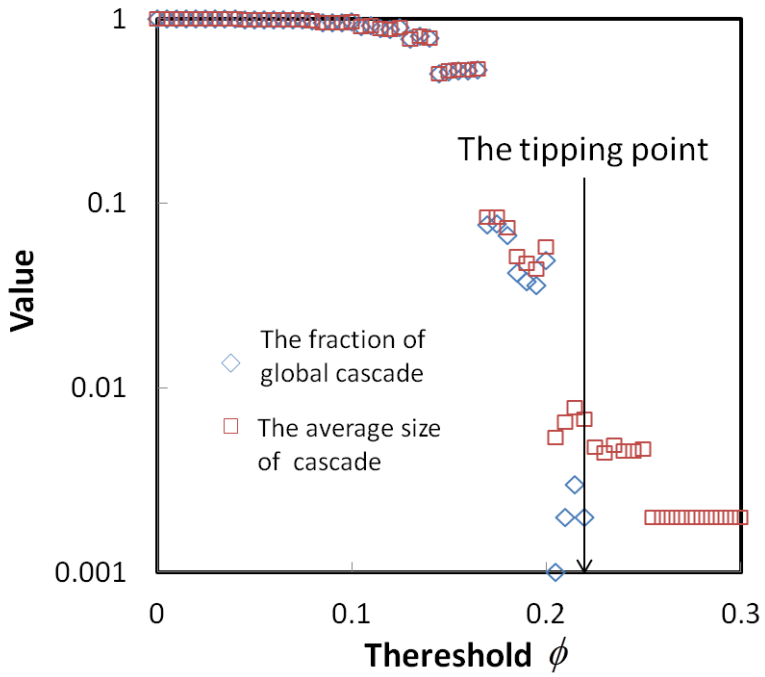

Figure 5.4 The fraction of global cascade and the average size of cascade is plotted as a function of a threshold value of each node ϕ, which is changed from 0.3 to 0, as the results of cascade dynamics on a scale free network by BA model with 500 nodes and 2000 links. The tipping point, which defines the cascade window, is 0.22, where two global cascades are firstly observed in over 1000 iterative simulations.

5.3 Evolutionary optimization for maximizing cascade window

In this section, an optimal network for maximizing cascade window is designed by evolutionary optimization. The formula to obtain cascade window ϕ^* have already been introduced (equation (5.17)), but it is difficult to use it as objective function in evolutionary optimization. The variable k in the left side of equation (5.17) is discrete number ($k = 0, 1, 2, \ldots$), and then the k, which makes the left side of the equation equal to the right side average degree z, cannot be found by numerical computation. On the other hand, there is alternative method that has only inequality in the formula.

(1) Defining the objective function

Cascade window size ϕ^* can be estimated analytically, where global cascade can occur, by the mean-field analysis of cascade phenomena [107].

All nodes face a problem of selection whether to adopt innovation or not. The probability $\theta(t)$ that a node adopts innovation, which is selected by following a randomly selected link, is given as,

$$\theta(t) = \sum_{k} \frac{kP(k)}{\langle k \rangle} \rho_k(t), \tag{5.19}$$

where $\rho_k(t)$ is the fraction of nodes having degree k, which adopt innovation at time $= t$.

Then, the probability that a node having degree k has k_1 adjacent nodes who have adopted it is given as,

$$ {}_kC_{k_1}\theta^{k_1}(1-\theta)^{k-k_1}. \tag{5.20}$$

The changing rate of $\rho_k(t)$ is given by

$$\begin{aligned} &\frac{d\rho_k(t)}{dt} \\ &= \big(1-\rho_k(t)\big)\sum_{k_1=0}^{k} P(s=adopt,k_1,k)C_{k_1}\theta^{k_1}(1-\theta)^{k-k_1} \\ &-\rho_k(t)\sum_{k_1=0}^{k} P(s=reject,k_1,k)C_{k_1}\theta^{k_1}(1-\theta)^{k-k_1}, \end{aligned} \tag{5.21}$$

where $P(s=adopt,k_1,k)$ and $P(s=reject,k_1,k)$ represents the probability that a node will select adopt or reject respectively when a node having degree k has k_1 adjacent nodes who have adopted it, which is given by equation (5.1).

The $\rho_k(t)$ at equilibrium state $d\rho_k(t)/dt = 0$ is given as,

$$\rho_k(t) = \sum_{k_1=0}^{k} P(s=adopt,k_1,k)C_{k_1}\theta^{k_1}(1-\theta)^{k-k_1}. \tag{5.22}$$

Then, the recurrence formula of $\theta(t)$ is given as shown in equation (5.23) by using equation (5.19) and equation (5.22).

$$H(\theta) \equiv \theta(t) = \sum_{k} \frac{kP(k)}{\langle k \rangle} \sum_{k_1=0}^{k} P(s=adopt,k_1,k)C_{k_1}\theta^{k_1}(1-\theta)^{k-k_1}. \tag{5.23}$$

At the beginning of the spread of cascade dynamics, $\theta(t) \approx 0$, and the condition $dH(\theta)/dt|_{\theta\approx 0} > 1$ is essential for the cascade to expand.

Therefore, the condition of the global cascade is formulated as,

$$\phi^* = \arg\min_{\phi\in[0,1]} \frac{1}{\langle k \rangle}\sum_{k\geq 1}^{\lfloor 1/\phi \rfloor} k^2P(k)\,, \quad \text{s.t}\ \frac{1}{\langle k \rangle}\sum_{k\geq 1}^{\lfloor 1/\phi \rfloor} k^2P(k) > 1\,. \tag{5.24}$$

When the function $H(\theta)$ is convex upward, the global cascade will occur by a few trigger nodes (Figure 5.5).

In order to maximize the cascade window ϕ^* for good cascade, it is needed to find the network having the largest ϕ^* and then equation (5.24) is used as an objective function for evolutionary optimization proposed in Chapter 3.

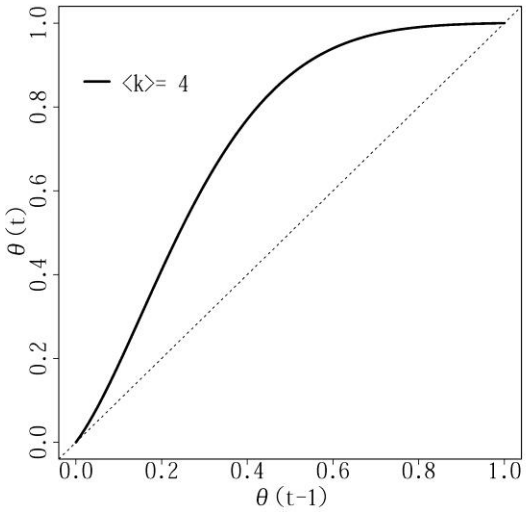

Figure 5.5 The diagram of changes of the probability θ on a random network: average degree is $\langle k \rangle = 4$, the threshold of nodes is $\phi = 0.25$.

(2) Cascade window of evolutionary optimized networks

Table 5.2 shows the summary of settings of evolutionary network optimization by GA for maximizing cascade window ϕ^*. The accumulation of the improvement by optimization cycle outputs a network having large fitness value along with the increase of the evaluation number (Figure 5.6). The optimization results are shown in Figure 5.7 (circle), in which the average degree of networks is changed from 4 to 30. As above mentioned, the scale free network by BA model seems to be most suitable to maximize cascade window, but evolutionary optimization can find networks that have the widest cascade window, which is labeled as GA in Figure 5.7.

Table 5.2 Parameters for genetic algorithm

Genetic algorithm model	Minimum Generation Gap model [104]
Network size (number of nodes)	500
Initial population size	20
“Child” population size	20
Objective function	Equation (5.24)
Crossover	Uniform crossover
Mutation	Not used
Selection	An elite selection strategy
The number of evaluations	Over 20000

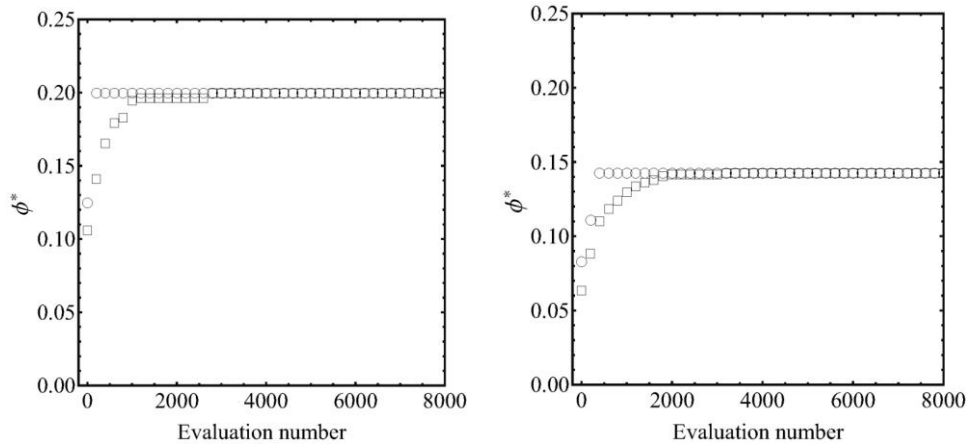

(a) $\langle k \rangle = 10$ (b) $\langle k \rangle = 20$

Figure 5.6 The fitness value of a network as a function of the evaluation number: ○:The largest fitness value of the population, □:The average fitness value of the population.

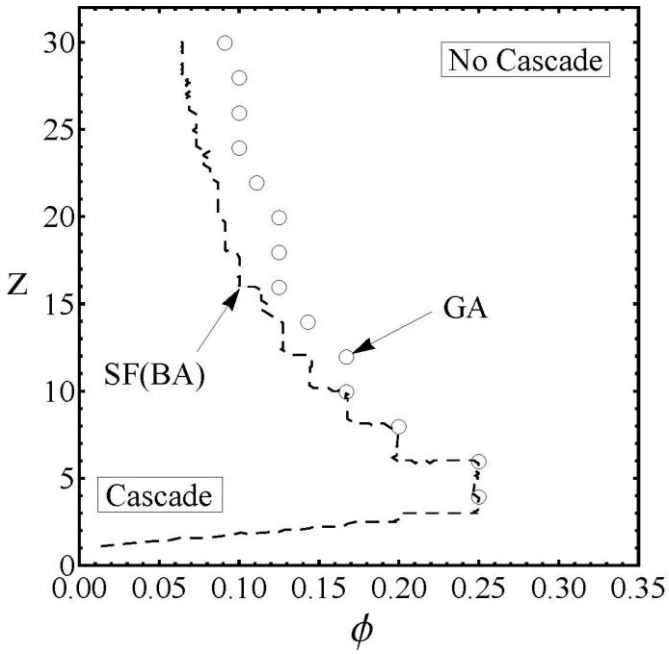

Figure 5.7 The theoretical cascade windows from Lopez formula (equation (5.24)) is plotted as a function of the threshold value of agents ϕ and average degree of a network z, which are based on their degree distributions of networks: SF(BA) (Scale-free network by Barabási-Albert model) and GA (Evolutionary optimized network).

5.4 **Heuristic models for optimizing cascade dynamics**

This section proposes heuristic models for maximizing or minimizing cascade dynamics. The heuristic models can form large-scale networks, and networks by the models can have an arbitrary average degree. The theoretical comparison on cascade window size between heuristic model networks and evolutionary optimized networks shows that the heuristic models are more optimal to maximize or minimize cascade dynamics.

5.4.1 P model for maximizing cascade

In this subsection, the probabilistic growing network model ”P model” for maximizing cascade dynamics is proposed, which is based on the network properties of evolutionary optimized networks. The evolutionary optimization is powerful method to create required networks, but the time complexity is relatively big. For example, when we create a large-scale network, the method requires a lot of computation time to propose a solution. Meanwhile, a heuristic model (network model), in general, has relatively small time complexity compared to the evolutionary optimization method. Furthermore, a heuristic model is useful to clarify and confirm what necessary structure for maximizing cascade of innovation is.

P model replicates the topological properties of evolutionary optimized networks to maximize cascade dynamics. In next section, it will be shown that the optimized network has a cluster of hub nodes and a cluster of vulnerable nodes. A fundamental idea under the P model is creating each cluster by growing network mechanism. The typical example of growing network is BA model, of which degree distribution obeys power law. In BA model, at each time, a newly introduced node is connected to existing m nodes by preferential attachment, and it has a few hub nodes and many vulnerable nodes.

In P model, at each time, one new node and c new links are introduced to a currnet network, and they are connected to hub nodes or vulnerable nodes, which depends on controlling parameter probability p. With probability $1-p$, a new node is connected to m hub nodes and new c links are used to interconnect hub nodes. With probability p, new node is connected to m vulnerable nodes and new c links are used to interconnect vulnerable nodes. Therefore, if p is close to 0, almost all nodes and links are connected to hub nodes. On the other hand, if p is close to 1, they are basically connected to vulnerable nodes. By changing the probability p from 0 to 1, we can control the size of cluster of hub nodes and cluster of vulnerable nodes to find the best network for maximizing cascade window. The good side effect of the growing network model is that a created network should be a single connected network, and we do not need to consider disconnection of nodes. The more detail of P model is explained in the following paragraphs.

In the P model, a small connected network with a few nodes is prepared initially. At each time step, the creation of a cluster of either vulnerable nodes or hub nodes is

selected stochastically with probability p. If the creation of a cluster of hub nodes is selected, a newly introduced node is connected to m hub nodes in a current network, and new c links are used to connect hub nodes. The probability, which is that existing nodes will have a new neighboring node or new links, is defined by equation (5.25). Then a node having many links has higher probability to be selected.

$$p(d_i) = \frac{(d_i)^{\beta}}{\sum (d_i)^{\beta}}. \tag{5.25}$$

If the creation of the cluster of vulnerable nodes is selected, a newly introduced node is connected to m vulnerable nodes in a current network, and c links are used to connect vulnerable nodes. The probability, which is that existing nodes will have a new neighboring node or new links, is given by the function of their degree defined by equation (5.26). Then, a node having few links has higher probability to be selected.

$$p(d_i) = \frac{\left({}^{1}/_{d_i}\right)^{\beta}}{\sum \left({}^{1}/_{d_i}\right)^{\beta}}. \tag{5.26}$$

The variable m and c define average degree z of a formed network ($z \simeq 2(c + m)$), and the exponent β in equation (5.25) and equation (5.26) changes what kind of nodes are selected. Note that β has effective range on its value. If β is too large, same pair of nodes are selected at each iteration, but multi links between same pair of nodes is not permitted. If β is too small, each selection of nodes based on equation (5.25) and on equation (5.26) equal to random selection. As a result, the network cannot grow or make a cluster of nodes with sufficient size. In following simulations, $\beta = 2$ is set, which is decided from results of the preliminary experiments ($\beta = 1, 2, 3$). In addition, $m = 2$ is set, which is effective to form a cluster of vulnerable nodes efficiently. Of course we can set $m = 1$, but it makes a created network have a chance to have nodes with a single link. These nodes do not contribute to maximizing cascade dynamics, because these nodes do not transmit a state of an adjacent node to another node. How to make a network by P model is summarized as follows and in Figure 5.8.

Step 1 Prepare a small connected network having a few nodes.
Step 2 Go to step 3 with probability $1 - p$ or go to step 4 with probability p.
Step 3 Add a new node with m links and new c links to hub nodes with probability defined by equation (5.25). After that, go to step 5.
Step 4 Add a new node with m links and new c links to vulnerable nodes with probability defined by equation (5.26). After that, go to step 5.
Step 5 Go to Step 2 if a stop criterion, which is usually defined by the number of nodes, is not met.

Figure 5.9 shows the theoretical cascade window size ϕ of P model network from equation (5.24) as a function of a parameter p. The network by P model has 500 nodes, and settings of parameters are $\beta = 2, m = 2$. It is shown that the size of

cascade window ϕ depends on a parameter p and a network with the largest cascade window can be obtained by controlling p. If a controlling parameter is set as $p = 0$, P model forms only a cluster of hub nodes and has narrow cascade window. If $p = 1$, P model forms only a cluster of vulnerable nodes and has cascade window that is almost same size with random network. The cascade window of P model is maximized at intermediate p ($= 0.1$~0.3). Figure 5.10 shows the theoretical cascade window of P model networks with best parameter p at each average degree z from equation (5.24). It is shown that the P model networks have same or larger size of cascade window compared to evolutionary optimized network (GA network).

5.4.2 CPA and CRA model for minimizing cascade

In general it is natural that equation (5.24) is used as objective function of evolutionary optimization to minimize cascade window. However, the evolutionary optimization requires a lot of computation time to propose a solution. Then, it is efficient to use another method when there is alternative method.

From the definition of a threshold model (equation (5.3)), hub nodes (nodes with many links) and a cluster of them prevent the cascade. A hub node is stable toward the change of state of neighboring nodes, because a hub node still has many other un-changed nodes. When a network has a cluster of hub nodes, hub nodes have stable hub nodes as adjacent nodes and cascade is hard to occur.

The study of probabilistic diffusion in Chapter 4 showed that the maximum eigenvalue of the adjacency matrix of a network is an index which shows how hub nodes are interconnected in a network.

Then, a network with large maximum eigenvalue of the adjacency matrix (ex. partial complete graph and KN networks in Chapter 4) will be effective to minimize the spread of cascade dynamics. This intuitive idea is studied in this subsection.

Figure 5.11 compares the theoretical cascade window between partial complete graph (CPA, CRA), KN network and random network, which is based on degree distribution of them. The figure shows that networks by the heuristic models (CPA, CRA, KN), which have large cluster of hub nodes, have narrow cascade window. Especially, the partially complete graph (CPA, CRA) has very narrow cascade window, and it denotes the cascade phenomena hardly spreads on those networks.

The results in this chapter aiming to find network topologies that maximize or minimize the cascade window are summarized by the same manner of López [107] as

$$\phi^*_{\mathrm{CPA}} = \phi^*_{\mathrm{CRA}} < \phi^*_{\mathrm{KN}} < \phi^*_{\mathrm{RND}} < \phi^*_{\mathrm{EXP}} < \phi^*_{\mathrm{SF(BA)}} < \phi^*_{\mathrm{GA}} < \phi^*_{\mathrm{P\ model}}. \qquad (5.27)$$

where $\phi^*_{\mathrm{P\ model}}$ denotes the cascade window of the network by P model. Note that KN network can be considered as a network by the proposed P model with controlling parameters as $\beta = 1, m = 1, p$=0.

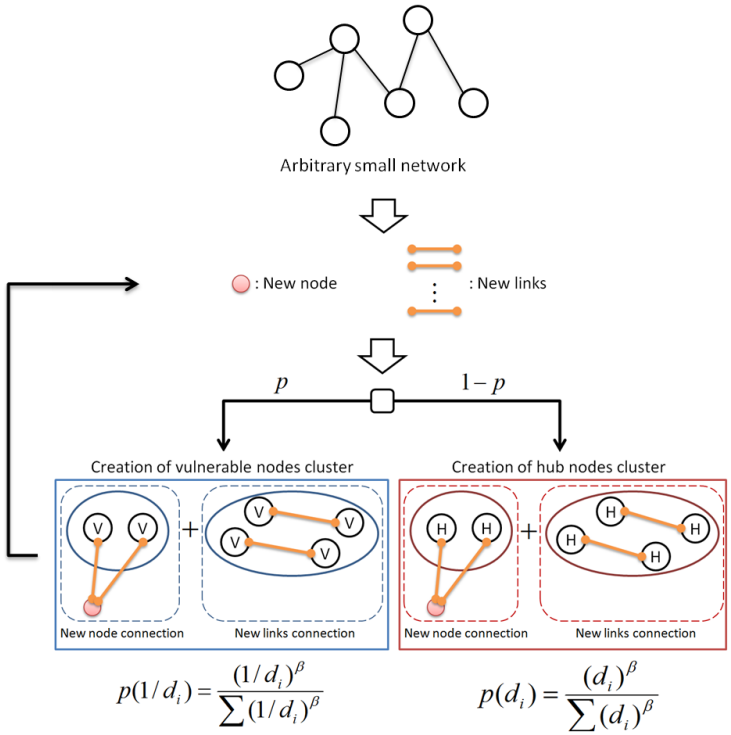

Figure 5.8 The diagram of the procedure of P model. p represents the probability to use newly introduced node and links for making a cluster of hub nodes. The encircled character V and H represent vulnerable node and hub node in the network respectively.

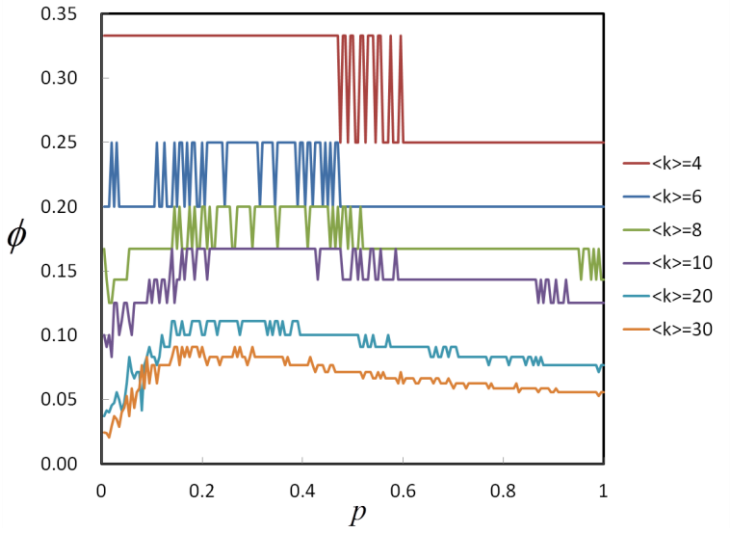

Figure 5.9 The theoretical cascade window ϕ is plotted as a function of controlling parameter p of P model. Each line corresponds to results of each network with average degree $\langle k \rangle$ and 500 nodes. Note that parameters of P model are $\beta = 2$ used in equation (5.25) and equation (5.26) and $m = 2$ that is number of nodes connected to a newly introduced node.

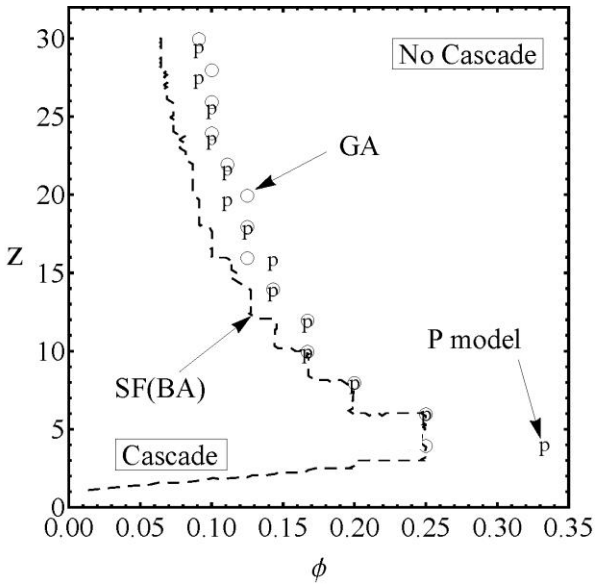

Figure 5.10 The theoretical cascade window of P model network model with best parameter p by Lopez formula equation (5.24) is plotted as a function of the threshold value ϕ of agents and the average degree z of networks, which are compared to the results of evolutionary optimized network (GA) and Scale-free network by Barabási-Albert model (SF(BA)).

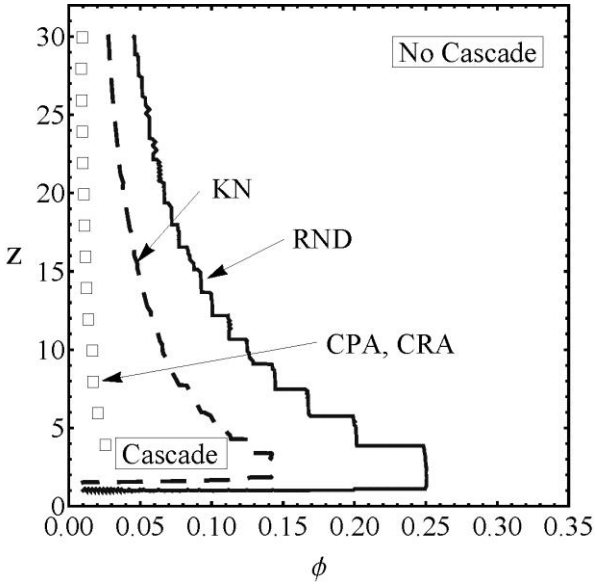

Figure 5.11 The theoretical cascade windows by Lopez formula (equation (5.24)) that is based on the degree distribution of networks is plotted as a function of ϕ the threshold value of agents and z average degree of network: CPA (Complete graph with Preferential Attachment in Chapter 4), CRA (Complete graph with Random Attachment in Chapter 3), KN (KN network in Chapter 4), and RND (Random network).

5.5 **Analysis of optimized networks**

What kind of interaction among agents is formed by evolutionary optimized network topology to enhance cascade dynamics? Figure 5.12 shows evolutionary optimized network topology, but it is too complex to interpret the properties directly. Then, the topological properties of GA networks are revealed by using the degree distribution and the proposed maps denoting how nodes are interconnected.

Figure 5.13 and Figure 5.14 show complementary cumulative density and cumulative density of the degree distribution of each network having average degree $\langle k \rangle = 10$ and $\langle k \rangle = 20$ respectively. It is clear that optimal networks for maximizing cascade window by P model and GA networks have hub nodes, which usually works like a "brake" in cascade dynamics except the case the cascade begins from hub nodes, like networks by KN model and networks by CPA model, which have very small cascade window. The nodes with a few neighbors, which are usually called as leaf nodes or vulnerable nodes, are basically susceptible to the change of states of neighboring nodes. However, both of networks by KN model and networks by CPA model have a lot of vulnerable nodes like networks by P model for maximizing cascade window and GA networks. Then, only the amount of hub nodes and vulnerable nodes cannot define the size of cascade window. It imposes another new topological analysis on us to find out what elements make the spread of cascade dynamics easy or difficult.

Therefore, the mapping method of the linkages between nodes in network is proposed (Figure 5.15). A point is plotted on (d_i, d_j) when node i having d_i links and node j having d_j links are connected. Each point may have different diameter, which is proportional to the logarithm of the frequency of the cases. For the better understanding visually, the figure is converted to be symmetry. Figure 5.16 and Figure 5.17 show how nodes are interconnected in networks, which have different average degree $\langle k \rangle = 10$ and $\langle k \rangle = 20$ respectively. For example, in the network by P model with the best p that maximize ϕ, there are a cluster of vulnerable nodes in the dashed circle and a cluster of hub nodes like as evolutionary optimized (GA) network (Figure 5.16 (a)). The center of the cluster of vulnerable nodes is $(5,5)$, which is most near from the origin of axes compared to other networks. The nodes in the cluster have small number of links and the cumulative fraction of those nodes is more than 60% (see at degree=10 in Figure 5.13 (b)). Cascade dynamics is driven via the vulnerable cluster, which are sensitive to the change of state of neighboring nodes, and the accumulation of the activated nodes in the cluster will change the state of the rest of nodes including hub nodes. Therefore, cascade dynamics can spread easily if a few nodes in a vulnerable cluster are activated.

In a network by KN model, it is shown that there are hub nodes and they are densely interconnected. The network also has many vulnerable nodes, which are susceptible to cascade dynamics, but they are mainly connected to hub nodes and then they are isolated.

In a network by CPA, it is clear that there are one big cluster of hub nodes (core)

and nodes connected to the core (peripheral nodes). The peripheral nodes have no direct connection each other and then cascade dynamics cannot spread via peripheral nodes.

Same maps on networks with different average degree $\langle k \rangle = 20$ are also plotted in Figure 5.17 and the results are same with Figure 5.16.

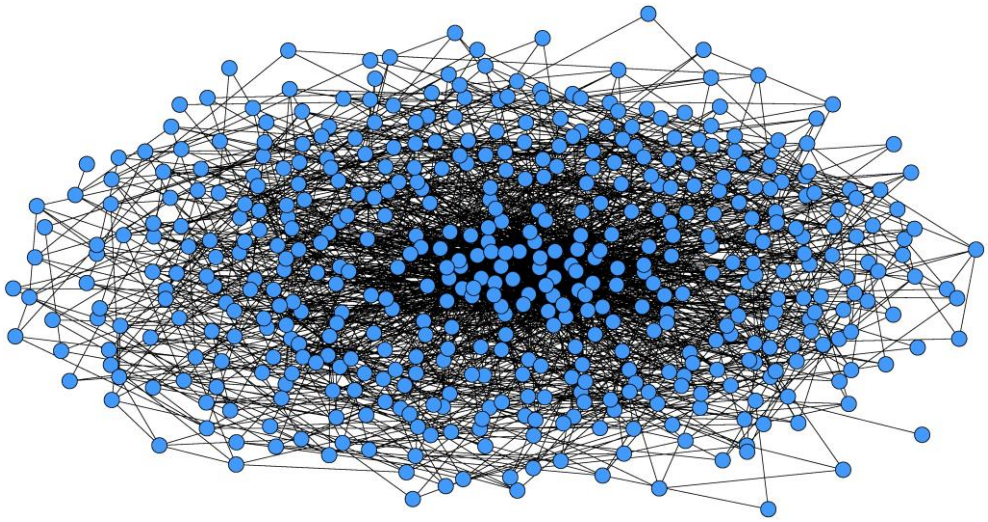

Figure 5.12 Evolutionary optimized network: The network is output in the case the number of nodes is 500 and the average degree $z = 20$.

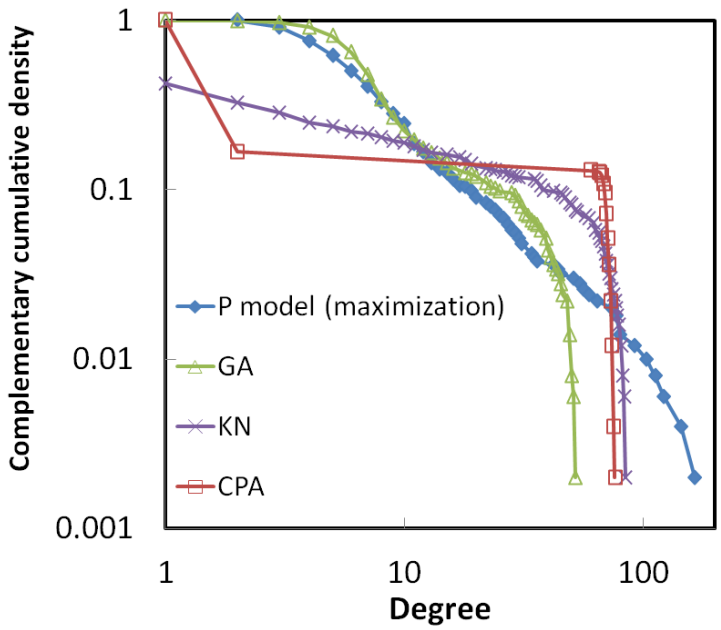

(a) Complementary cumulative density

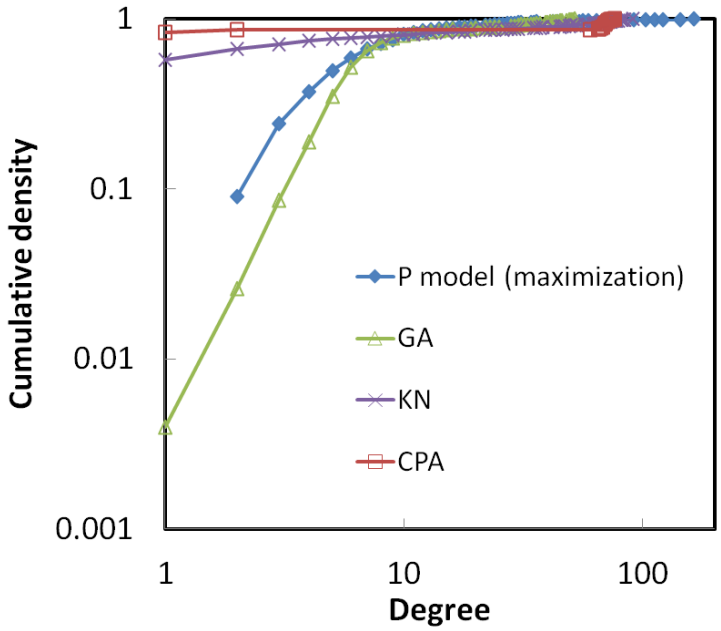

(b) Cumulative density fraction

Figure 5.13 The complement cumulative density and cumulative density in terms of degree of network by P model with the best p that maximizes cascade window (P model (maximization)), the evolutionary optimized network (GA), KN network (KN) and CPA network (CPA). All networks have 500 nodes and same average degree $\langle k \rangle = 10$.

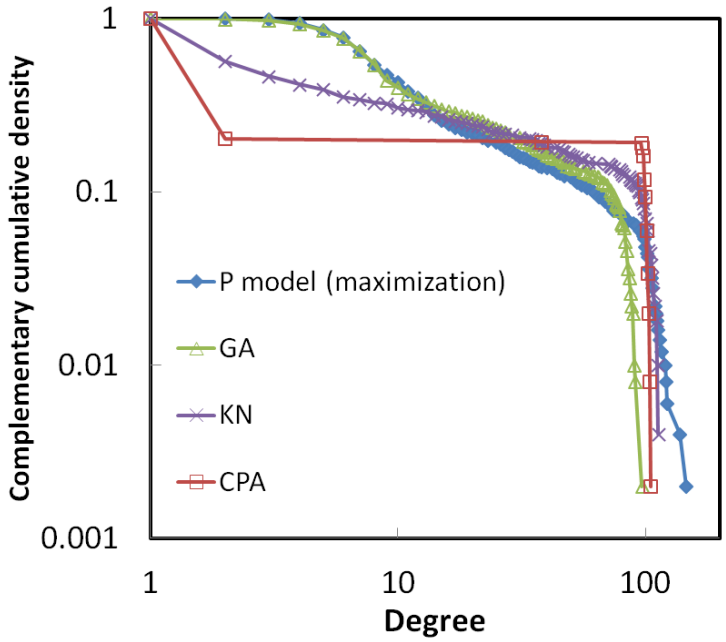

(a) Complementary cumulative density

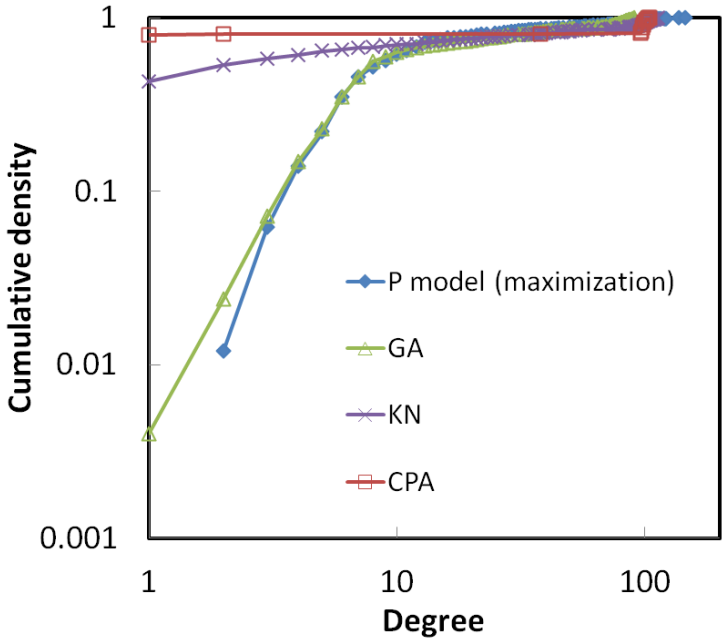

(b) Cumulative density fraction

Figure 5.14 The complement cumulative density and cumulative density in terms of degree of network by P model with the best p that maximizes cascade window (P model (maximization)), the evolutionary optimized network (GA), KN network (KN) and CPA network (CPA). All networks have 500 nodes and same average degree $\langle k \rangle = 20$.

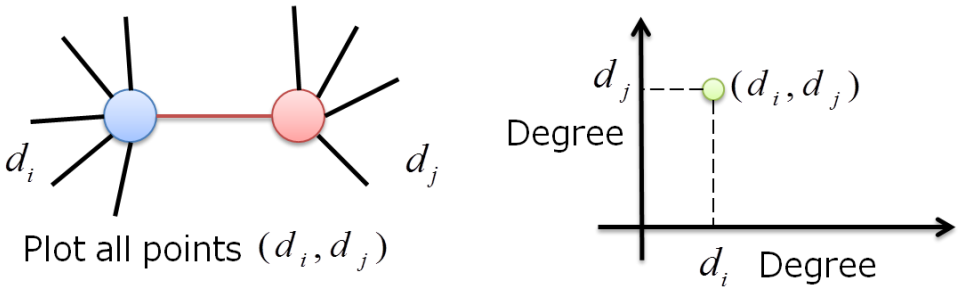

Figure 5.15 The mapping of linkages between nodes in a network.

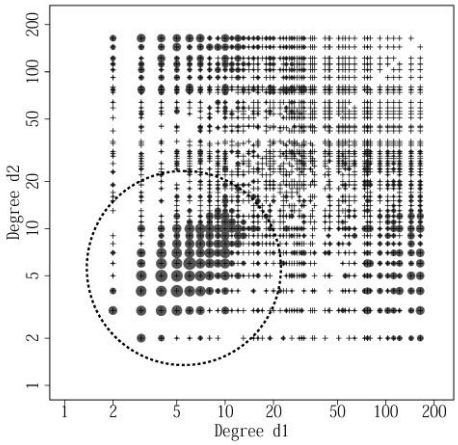

(a) P model (maximization)

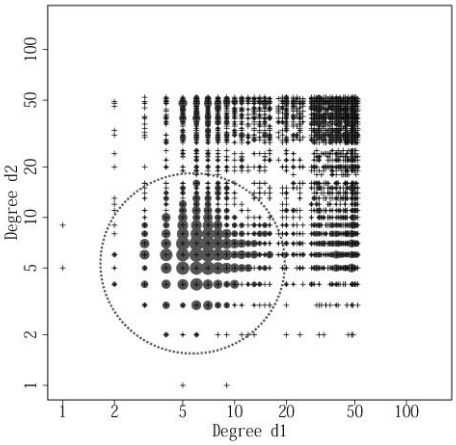

(b) GA network

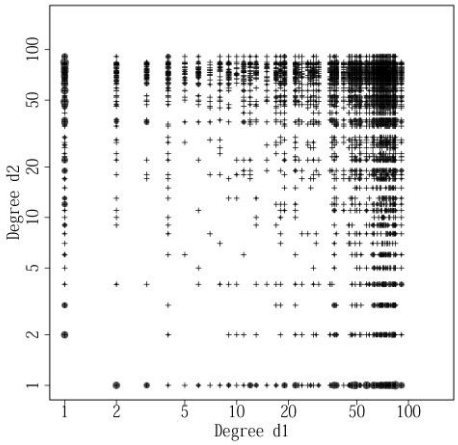

(c) KN network

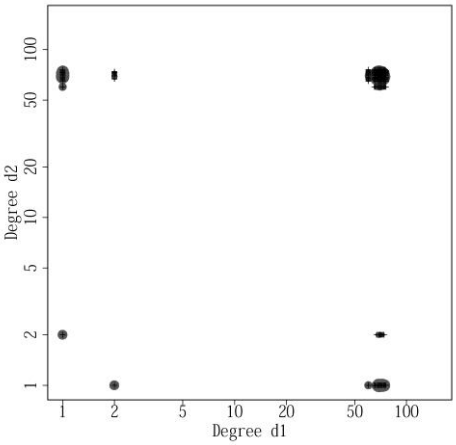

(d) CPA

Figure 5.16 This map shows the relationship of degrees between nodes, which are connected by links. The average degree of each network is $\langle k \rangle = 10$. The diameter of each point on the map is proportional to the logarithm of the frequency.

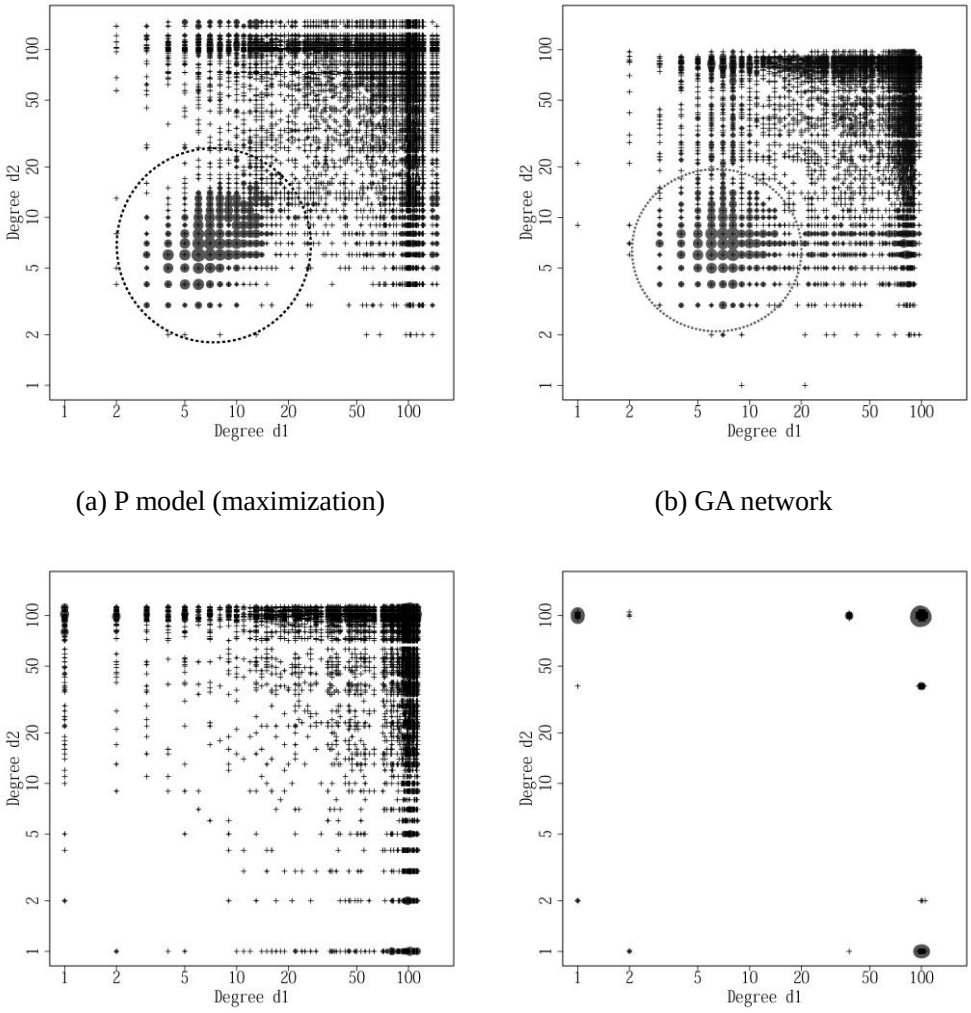

(a) P model (maximization)

(b) GA network

(c) KN network

(d) CPA network

Figure 5.17 This map shows the relationship of degrees between nodes, which are connected by links. The average degree of each network is $\langle k \rangle = 20$. The diameter of each point on the map is proportional to the logarithm of the frequency.

5.6 **Simulation on optimized networks**

In this section, a set of simulation results is given. The simulations are conducted to confirm the influence of network topology to cascade dynamics (cascade phenomena) directly. The formula by Lopez (equation (5.24)) is useful mathematical tool to estimate cascade window. However, the formula cannot consider how nodes are interconnected and just use statistical information: the degree distribution of network. Then, it is needed to validate the results in former sections by simulations.

Seven different networks are compared (CPA (Complete graph with preferential attachment), CRA (Complete graph with random attachment), KN (KN network), RND (Random network), EXP (Exponential network), SF(BA) (Scale free network by Balabási-Albert model), GA (Evolutionary optimized network)), and all networks have 500 nodes. The average degree is changed from 4 to 30.

Initially, the state of all nodes (agents) is 0 and the state of only one node, which is selected randomly, is changed from 0 to 1 as a trigger of cascade dynamics. All agents update those states simultaneously depending on a threshold model (equation (5.1)). Same simulation is done over 1000 times and the average proportion of agents choosing 1 is observed.

5.6.1 Analysis of cascade process

The process of cascade phenomena from the beginning of it to a steady state is studied to check the idea that a vulnerable cluster is the gateway for the diffusion of cascade on networks. Figure 5.18 is a combination graph. Each triangle denotes the degree of a node that changes own state to adopt innovation at corresponding time. In the case the cascade process begins from a trigger that is a vulnerable node, cascade phenomena proceed via a vulnerable cluster until the cumulative fraction of adopting agents plotted by solid line with small circle exceeds certain critical mass. After that, hub nodes begin to adopt innovation and the cascade is spread to the whole network finally. The process of the cascade which begins from a hub node, is the same: the cascade phenomena proceed in a vulnerable cluster initially and cumulative fraction of adopting agents draw s-shaped curve, which implies there is a critical mass for global cascade. The difference of the starting position of cascade dynamics only affects the number of adopting nodes by a trigger at first step. Of course this difference could change the results drastically when the hub node has a lot of vulnerable nodes.

It is also shown that it took relatively long time steps until hub nodes begin to adopt and all agents adopt innovation. This is because vulnerable nodes have a few links and the direct impact of the adoption by each vulnerable node is small. Then, it needs many steps for the cascade to spread to the entire network. This feature of the cascade phenomena implies why there is a long lag time between an innovation’s first appearance and the time when a substantial number of people have adopted it.

From these results of numerical simulations and study of evolutionary optimized network topologies, it is clear that the coexistence of a cluster of hub nodes and a

cluster of vulnerable nodes drives cascade phenomena at wide conditions. When the total number of nodes and links is fixed respectively, the existence of a cluster of hub nodes decreases the average degree of nodes in a vulnerable cluster, which enhances the sensibility of the cluster toward cascade dynamics, and a large vulnerable cluster also essential to make hub nodes adopt innovation by adopting-agents besieging them.

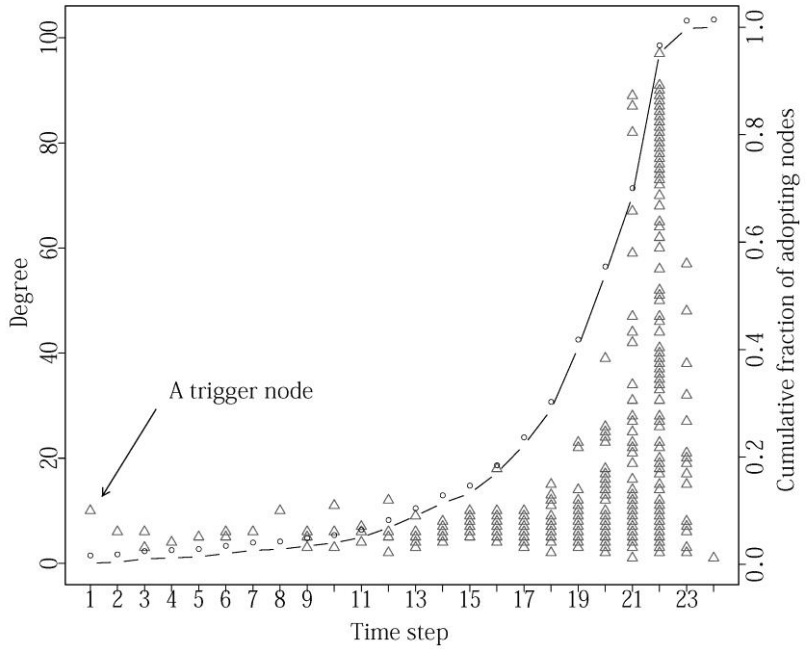

(a) A trigger is a vulnerable node

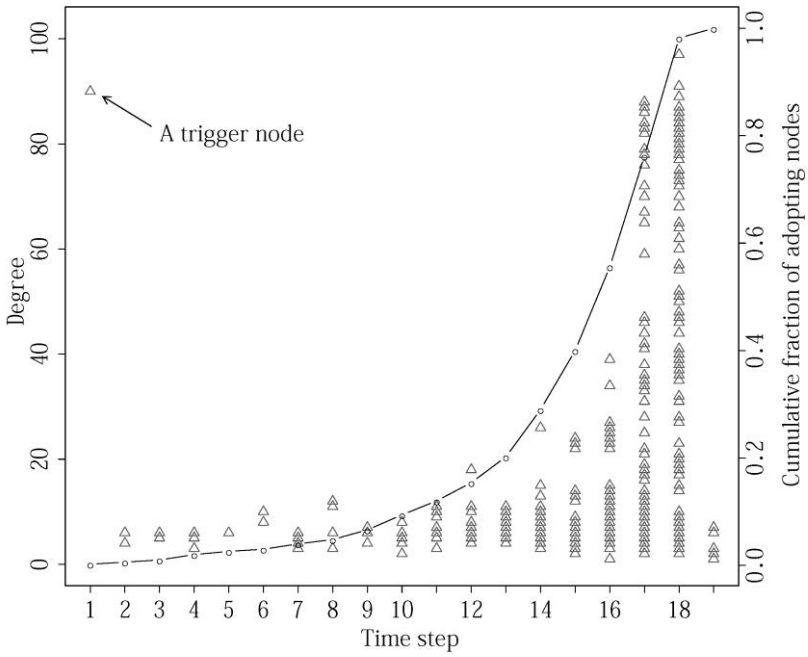

(b) A trigger is a hub node

Figure 5.18 This figure shows the process of cascade dynamics on evolutionary optimized networks, which begins from a trigger node. The network has 500 nodes and the average degree is $\langle k \rangle = 20$.

5.6.2 Comparison of cascade window

This subsection compares cascade window of networks. In Figure 5.19, the border line with points is plotted, on which global cascade is observed, at least one time out of 1,000 trials. It is very clear that the GA network has the largest cascade window compared to other network topologies at wide condition in terms of average degree z and partial complete graph (CPA and CRA) has the narrowest cascade window. The results implies the network topology influence whether global cascade will occur even if network and each node has same average degree z and threshold ϕ respectively. The results also reflect the trend of the theoretical cascade window as shown in Figure 5.7 and Figure 5.11.

It is interesting that KN network and SF(BA) network, of which degree distribution obey power law and have hub nodes, have opposite effects on the cascade window. SF(BA) network tends to expand the cascade window, but KN network narrow cascade window. It is intuitive and easy to understand the reason in the case of KN network, because almost all nodes are interconnected via the center hub cluster that is very stable toward the change of neighboring node's state. In the case of SF(BA) network, however, it is needed to understand the effects of the cluster of vulnerable nodes, of which degree is less than average degree in the network. The cluster of vulnerable nodes is also the reason that GA network has the largest cascade window.

The performance of P model networks is also validated by numerical simulations. Figure 5.20 shows the size of cascade window of P model network is same or larger compared to it of GA network. These results support the intuitive idea that the cluster of vulnerable nodes could enhance cascade under even severe condition, where each node has high threshold and the average degree of network is high.

The cascade windows of networks are also considered from eigenvalue view point in Figure 5.21. The ratio $\langle k \rangle / \lambda_{\max}(\mathbf{A})$ is defined by equation (4.45) to understand how a cluster of hub nodes affects tipping point on probabilistic diffusion. The figure shows the cascade window expands with the increase of the ratio and become largest at the intermediate size of the ratio. After that it decreases again. This result corresponds to the change of cascade widow of P model with parameter p shown in Figure 5.9. In P model, the cascade window is maximized at intermediate p, and its topological meaning is finding the optimal size of a cluster of hub nods to maximize cascade window.

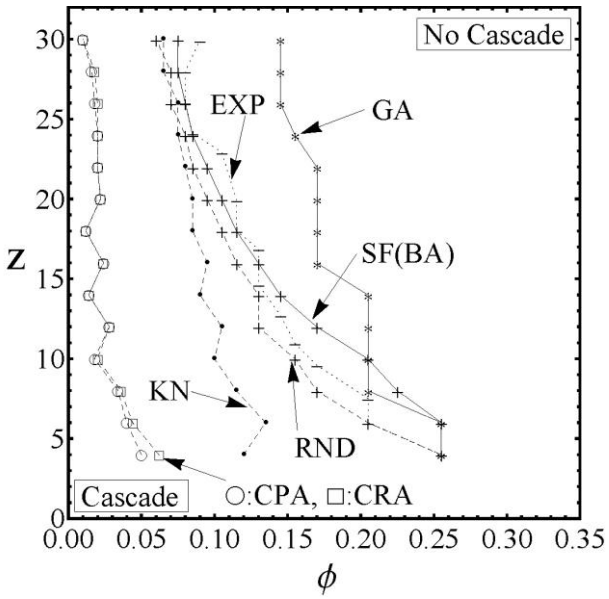

Figure 5.19 The cascade window on networks from numerical simulations is plotted as a function of the threshold value ϕ of agents and average degree z of network.

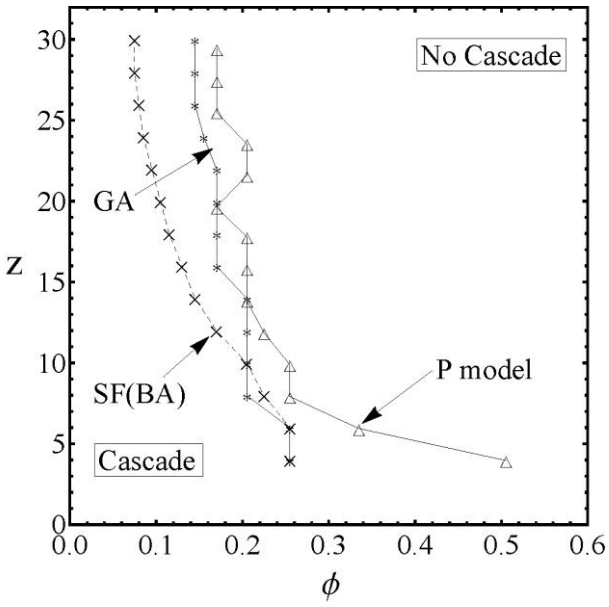

Figure 5.20 The cascade window of P model network from numerical simulations is plotted as a function of the threshold value ϕ of agents and the average degree z of networks, which is compared to the results of evolutionary optimized network and exponential network.

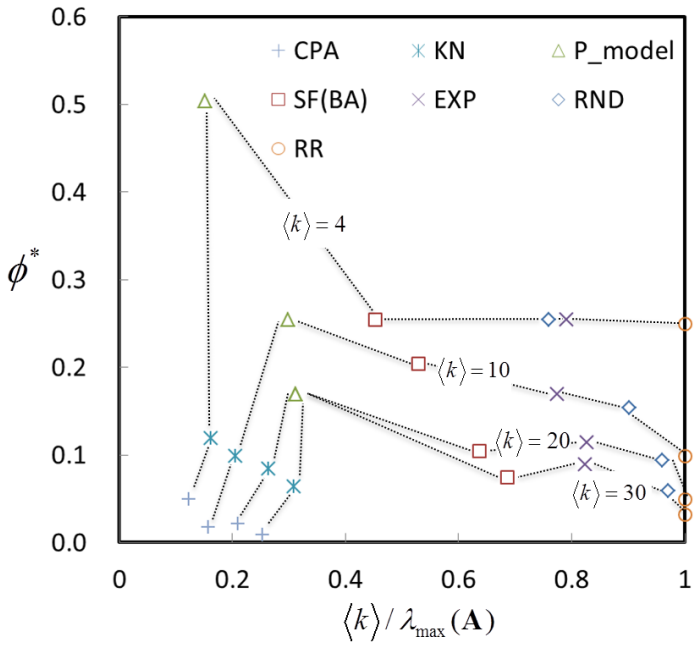

Figure 5.21 The cascade window ϕ^* of networks from simulation results is plotted as a function of the ratio of average degree to maximum eigenvalue $\langle k \rangle / \lambda_{\max}(\mathrm{A})$.

5.6.3 Comparison of the frequency of global cascade

The cascade window shown in previous subsection indicates the area where the global cascade can occur in terms of the relationship between threshold value of nodes and average degree of a network. However, it lacks a point of view about the frequency or how often the global cascade will occur inside the cascade window.

Figure 5.22 shows the density (or ratio) of global cascade on networks by P model, in which all agents finally accept. The cascade will spread to a whole network when average degree $\langle k \rangle$ and threshold ϕ is inside the cascade window. However, near the border of the cascade window, global cascade does not usually occur. The density is about from 0.001 to 0.01 as results of 1000 numerical simulations. Furthermore, near the border of cascade window, the size of each cascade is usually small except global cascade.

The tendencies that the frequency of global cascade will decrease near the border of the cascade window are common properties of all simulated networks except homogeneous network where all nodes have same degree (Figure 5.22 - Figure 5.29). It implies that near the border of the cascade window, the sequence or the process of global cascade is limited to a few cases. Therefore, the network is scarcely affected when the initially activated node is not optimal one for global cascade.

If concerned network has condition that is on the border of cascade window, the global cascade may not occur in many cases. When the global cascade represents bad phenomena (ex. diffusion of rumor or the sequence of bankrupt), it will not explained to pay for preventing or mitigating the loss of the global cascade by the usual thinking scheme of cost and benefit because the expected loss of it is not sufficiently large. This is not unusual case especially in the artificial systems. Those systems are usually designed to maximize the utility and minimize the cost for creation of systems including the cost for safety. As a result, we may have to accept the entire loss by global cascade in the worst case.

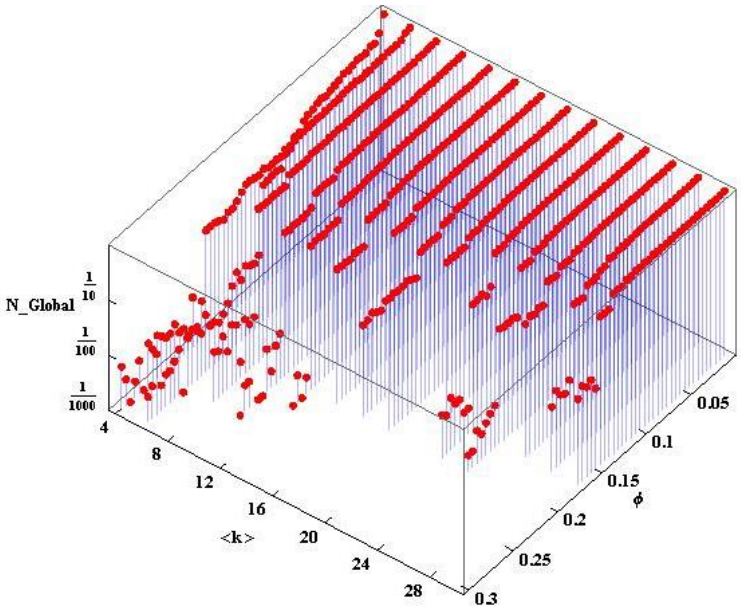

Figure 5.22 The density of global cascade on networks by P model with best parameter p to maximize cascade window, in which all nodes finally accept. The only one node is selected randomly as initially accepted node for each simulation. The network has 500 nodes. The average degree $\langle k \rangle$ is changed from 4 to 30 and the threshold ϕ is changed from 0.00 to 0.30.

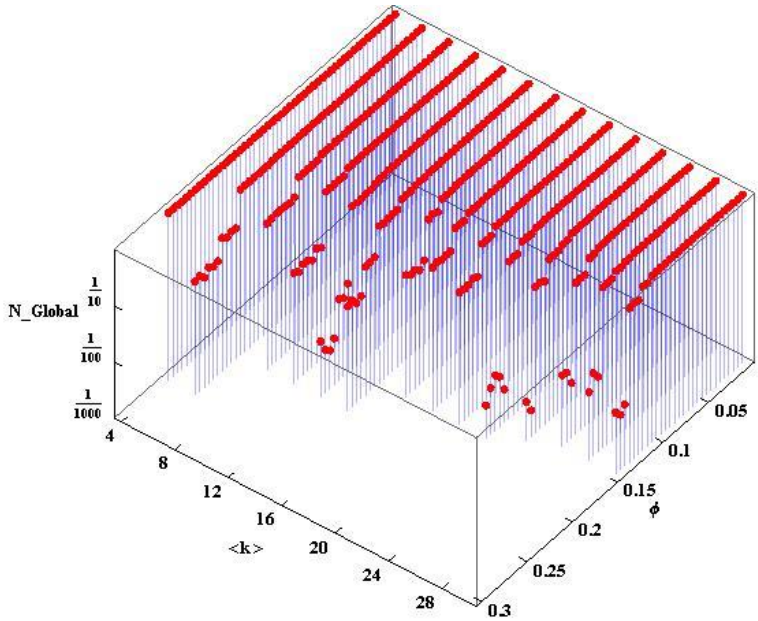

Figure 5.23 The density of global cascade on GA networks, in which all nodes finally accept. The only one node is selected randomly as initially accepted node for each simulation. The network has 500 nodes. The average degree $\langle k \rangle$ is changed from 4 to 30 and the threshold ϕ is changed from 0.00 to 0.30.

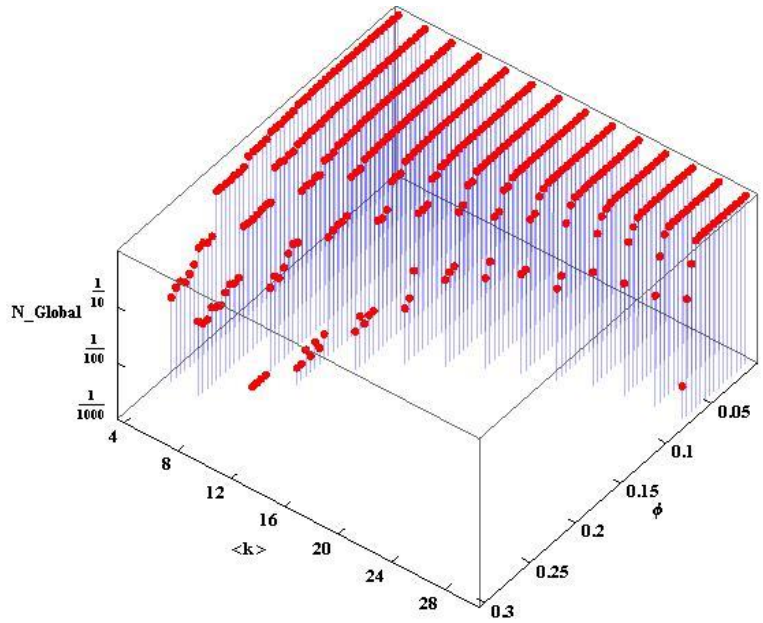

Figure 5.24 The density of global cascade on SF(BA) networks, in which all nodes finally accept. The only one node is selected randomly as initially accepted node for each simulation. The network has 500 nodes. The average degree $\langle k \rangle$ is changed from 4 to 30 and the threshold ϕ is changed from 0.00 to 0.30.

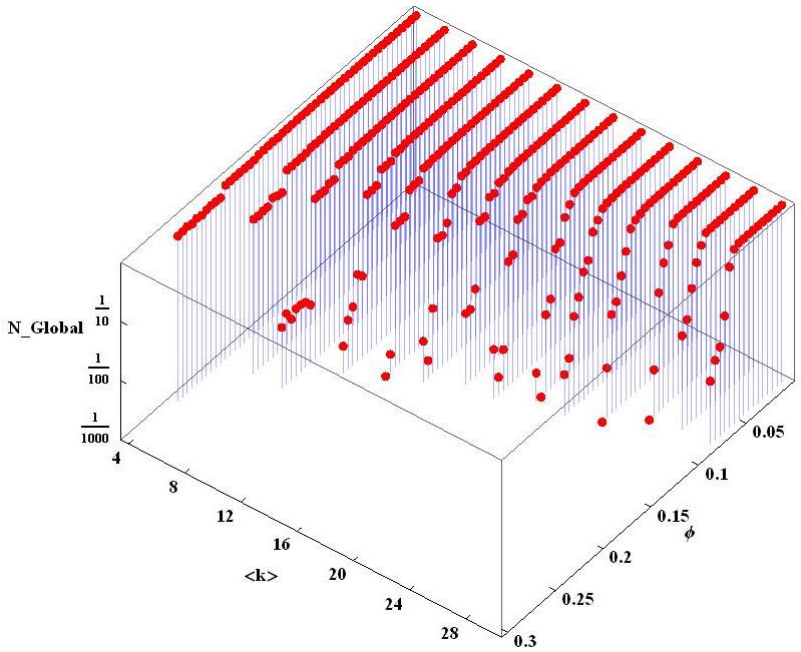

Figure 5.25 The density of global cascade on EXP networks, in which all nodes finally accept. The only one node is selected randomly as initially accepted node for each simulation. The network has 500 nodes. The average degree $\langle k \rangle$ is changed from 4 to 30 and the threshold ϕ is changed from 0.00 to 0.30.

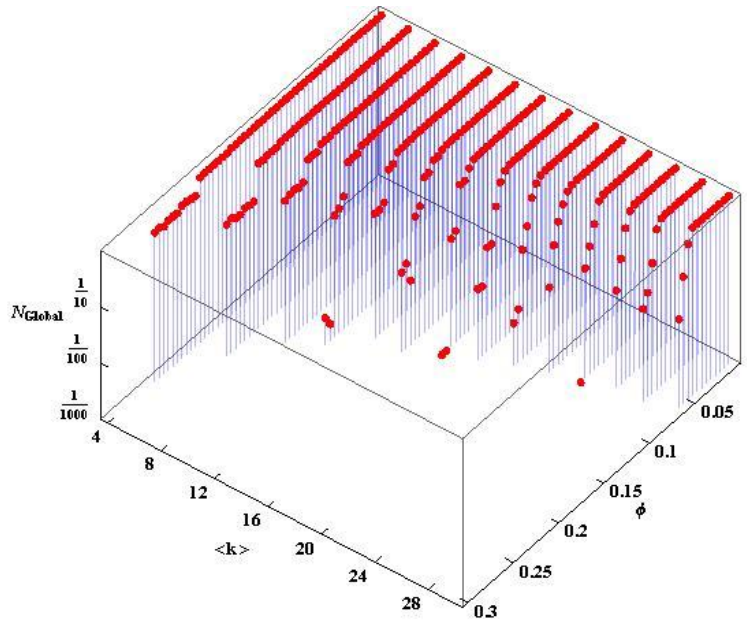

Figure 5.26 The density of global cascade on random networks, in which all nodes finally accept. The only one node is selected randomly as initially accepted node for each simulation. The network has 500 nodes. The average degree $\langle k \rangle$ is changed from 4 to 30 and the threshold ϕ is changed from 0.00 to 0.30.

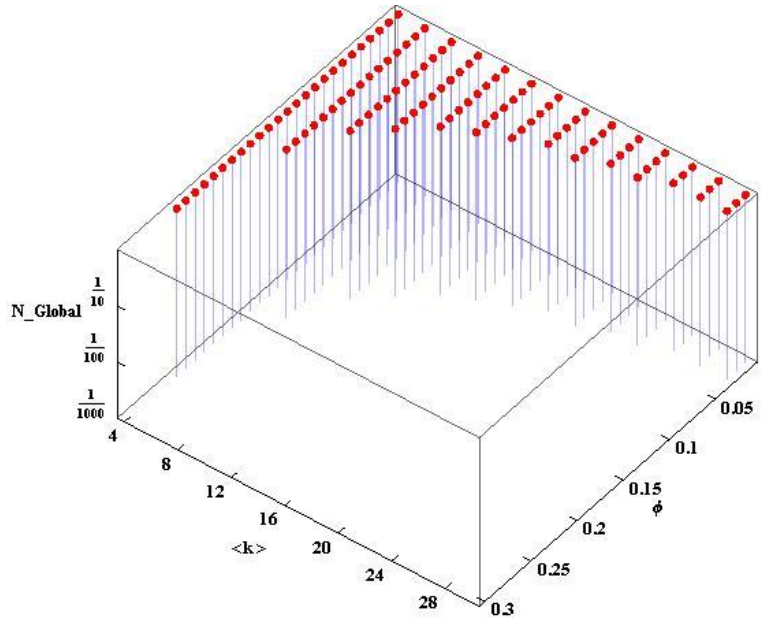

Figure 5.27 The density of global cascade on homogeneous networks, in which all nodes finally accept. The only one node is selected randomly as initially accepted node for each simulation. The network has 500 nodes. The average degree $\langle k \rangle$ is changed from 4 to 30 and the threshold ϕ is changed from 0.00 to 0.30.

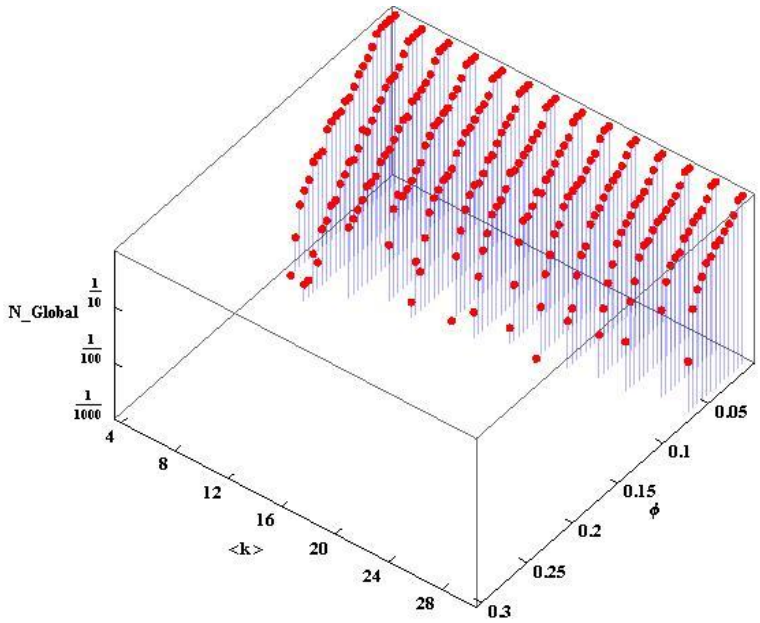

Figure 5.28 The density of global cascade on KN networks, in which all nodes finally accept. The only one node is selected randomly as initially accepted node for each simulation. The network has 500 nodes. The average degree $\langle k \rangle$ is changed from 4 to 30 and the threshold ϕ is changed from 0.00 to 0.30.

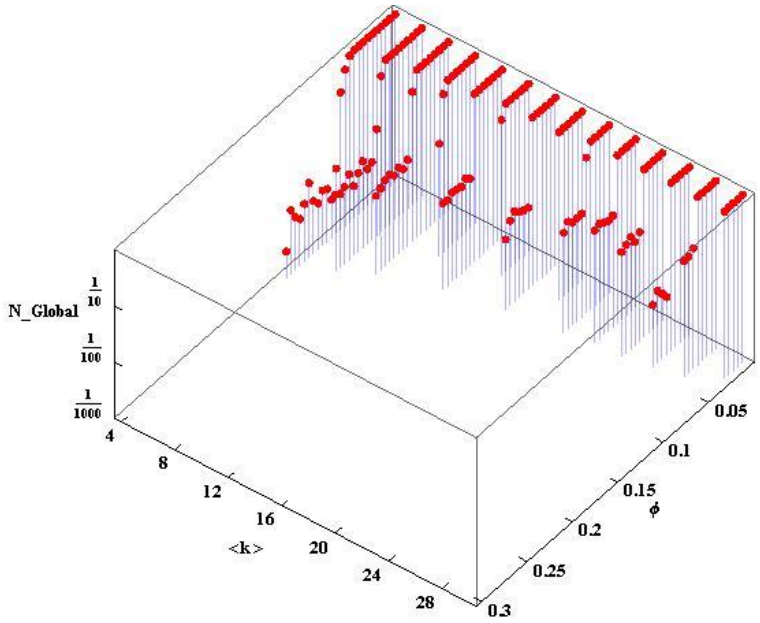

Figure 5.29 The density of global cascade on CPA networks, in which all nodes finally accept. The only one node is selected randomly as initially accepted node for each simulation. The network has 500 nodes. The average degree $\langle k \rangle$ is changed from 4 to 30 and the threshold ϕ is changed from 0.00 to 0.30.

5.6.4 Comparison of the average cascade size

The average number is usually a useful statistic index to understand the properties of concerned phenomena. Examples include the average death rate due to harmful effects of medicines, the average height of tsunami after terrible earthquake, and the mean time before failure of new products. This subsection studies the average cascade size on networks with the frequency of global cascade, which has been already considered in previous section. The results show that the global cascade can occur even the average cascade size is almost 0. This gap between the frequency of global cascade and the average size of cascade may lead underestimation of the probability of events driven by cascade dynamics.

Figure 5.30-Figure 5.37 show the average cascade size $\langle s \rangle$ from reiterative simulation over 1000 times. In each simulation, no nodes accept initially and one randomly selected node is forced to accept as a trigger of cascade dynamics. The average degree of the network and the threshold value of nodes are changed to observe their influence.

The results of networks by P model with best parameter p to maximize cascade window is shown in Figure 5.30. It is very interesting that the average cascade size is relatively small at small average degree $\langle k \rangle$ even if the network has largest cascade window as shown in Figure 5.20. This result comes from the drastic decrease of number of global cascade as shown in Figure 5.22. A network by P model at small average degree has star like structure and then the global cascade only start from the hub node. The specific structure reduces the frequency of global cascade. As results, the average cascade size becomes very small even the network has largest cascade window. It is the typical case we may misunderstand the influence of events driven by cascade dynamics.

Except networks by P model, there are roughly two common properties of average cascade size on networks. First one is that the average cascade size will jump from almost 0 to 1 nonlinearly when the threshold ϕ becomes smaller than the certain point at any average degree. Second is that the width of the threshold where the average cascade size is almost 1 becomes narrow along with the increase of the average degree. Both of them are not observed in probabilistic diffusion process. Especially, the latter property that a network with smaller average degree is more diffusive in threshold dynamics is interesting, which is a contrary result in probabilistic dynamics (equation (4.8)).

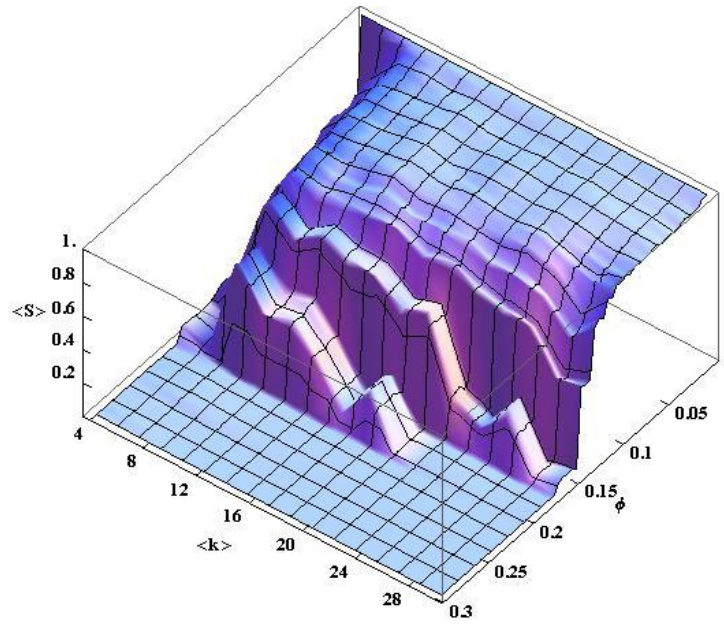

Figure 5.30 The average cascade size from reiterative simulation over 1000 times on networks by P model with best parameter p to maximize cascade window. The only one node is selected randomly as initially accepted node for each simulation. The network has 500 nodes. The average degree $\langle k \rangle$ is changed from 4 to 30 and the threshold ϕ is changed from 0.00 to 0.30.

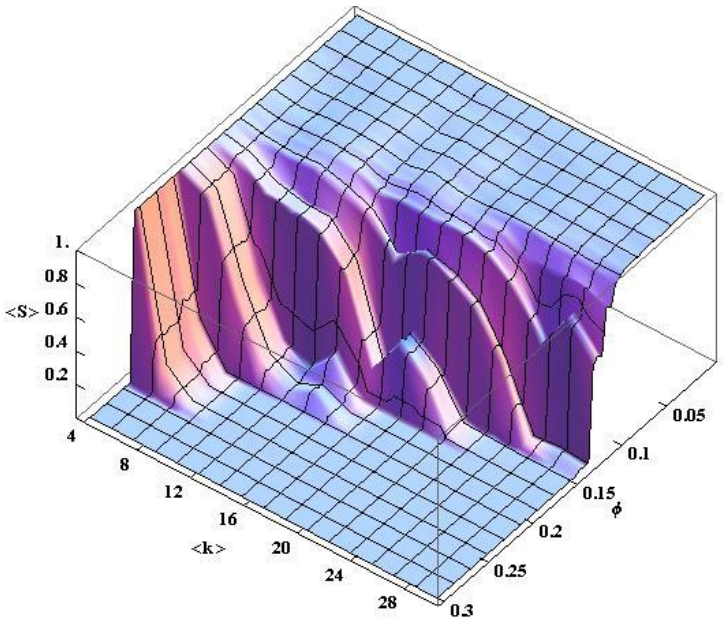

Figure 5.31 The average cascade size from reiterative simulation over 1000 times on GA networks. The only one node is selected randomly as initially accepted node for each simulation. The network has 500 nodes. The average degree $\langle k \rangle$ is changed from 4 to 30 and the threshold ϕ is changed from 0.00 to 0.30.

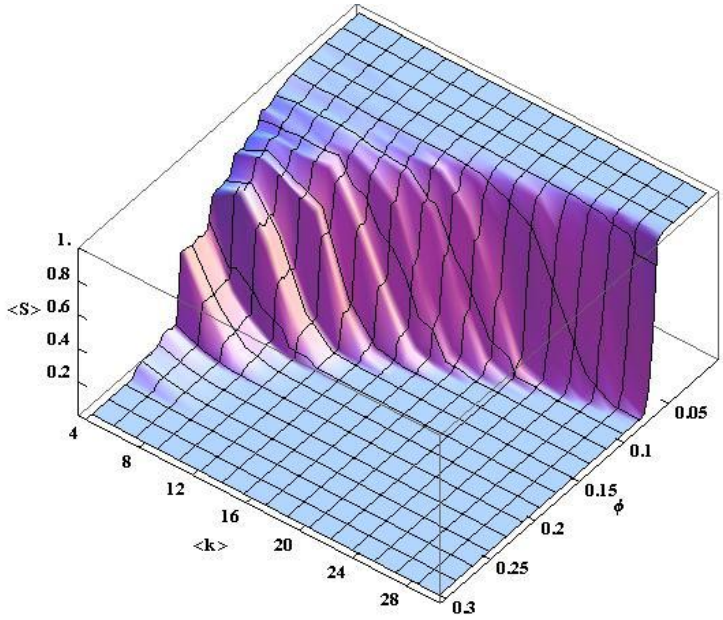

Figure 5.32 The average cascade size from reiterative simulation over 1000 times on SF(BA) networks. The only one node is selected randomly as initially accepted node for each simulation. The network has 500 nodes. The average degree $\langle k \rangle$ is changed from 4 to 30 and the threshold ϕ is changed from 0.00 to 0.30.

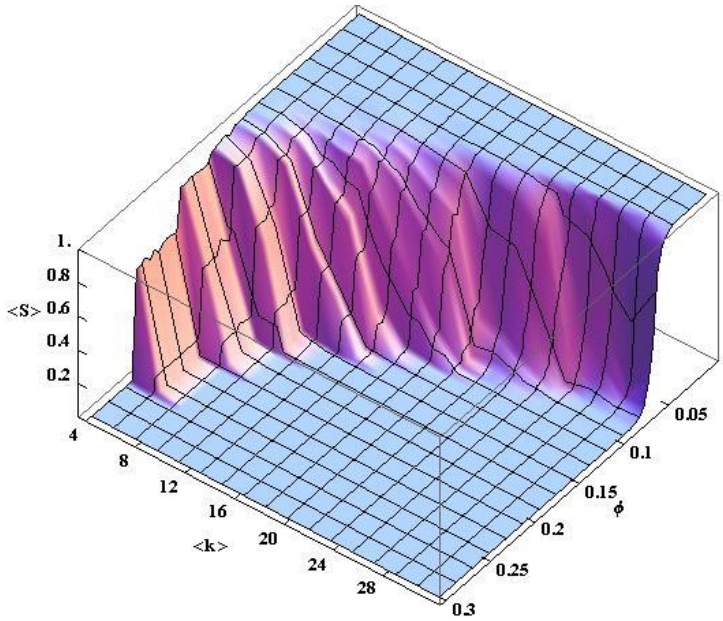

Figure 5.33 The average cascade size from reiterative simulation over 1000 times on EXP networks. The only one node is selected randomly as initially accepted node for each simulation. The network has 500 nodes. The average degree $\langle k \rangle$ is changed from 4 to 30 and the threshold ϕ is changed from 0.00 to 0.30.

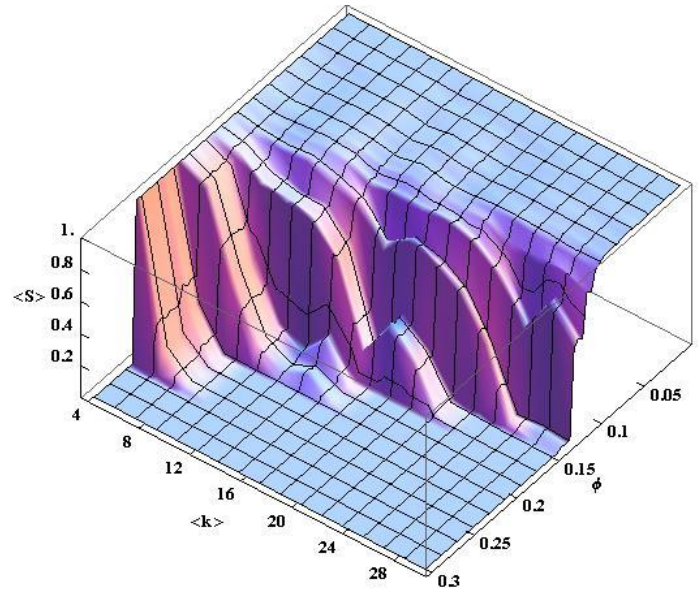

Figure 5.34 The average cascade size from reiterative simulation over 1000 times on random networks. The only one node is selected randomly as initially accepted node for each simulation. The network has 500 nodes. The average degree $\langle k \rangle$ is changed from 4 to 30 and the threshold ϕ is changed from 0.00 to 0.30.

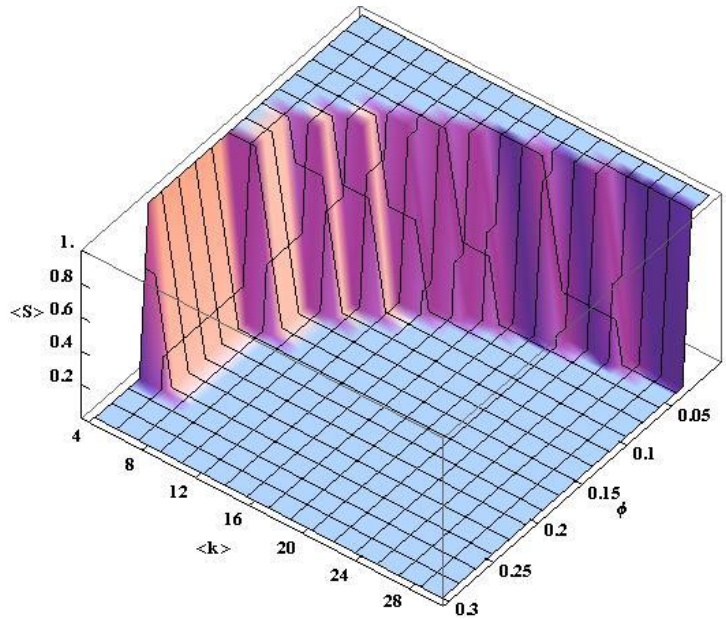

Figure 5.35 The average cascade size from reiterative simulation over 1000 times on homogeneous networks. The only one node is selected randomly as initially accepted node for each simulation. The network has 500 nodes. The average degree $\langle k \rangle$ is changed from 4 to 30 and the threshold ϕ is changed from 0.00 to 0.30.

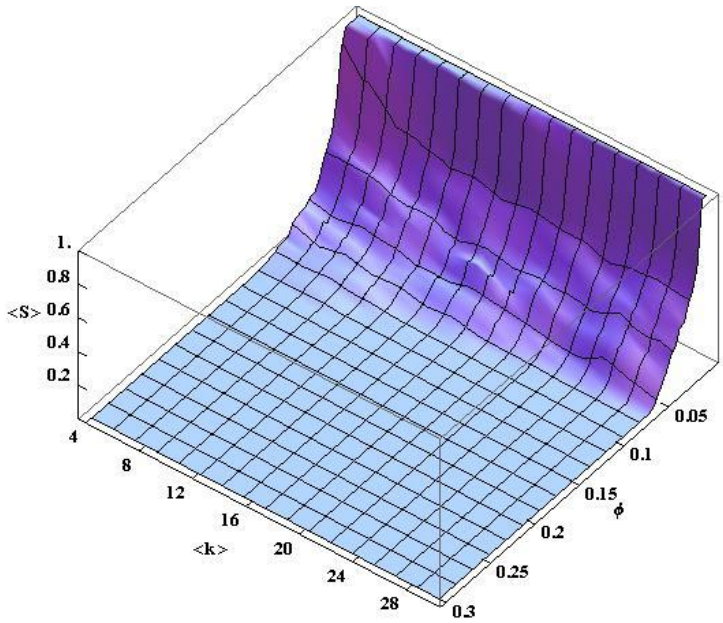

Figure 5.36 The average cascade size from reiterative simulation over 1000 times on KN networks. The only one node is selected randomly as initially accepted node for each simulation. The network has 500 nodes. The average degree $\langle k \rangle$ is changed from 4 to 30 and the threshold ϕ is changed from 0.00 to 0.30.

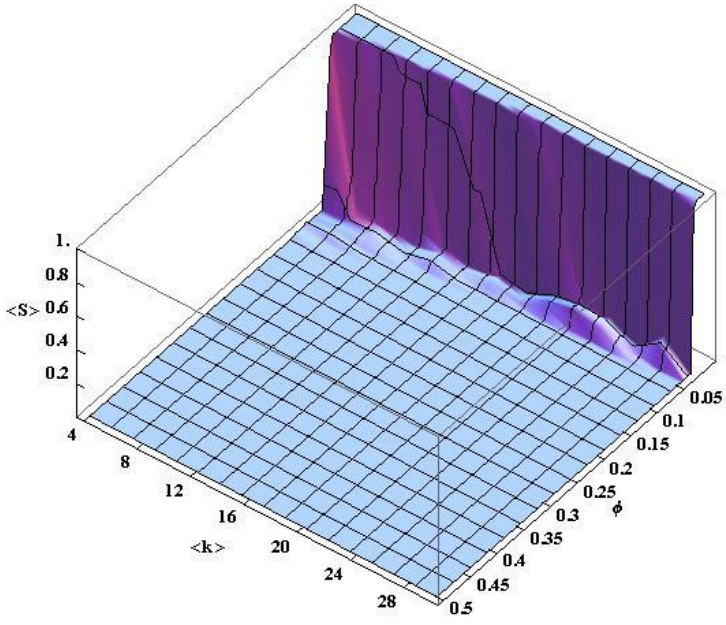

Figure 5.37 The average cascade size from reiterative simulation over 1000 times on CPA networks. The only one node is selected randomly as initially accepted node for each simulation. The network has 500 nodes. The average degree $\langle k \rangle$ is changed from 4 to 30 and the threshold ϕ is changed from 0.00 to 0.30.

Chapter 6

Consensus Dynamics

This chapter shows optimal networks for fast consensus by evolutionary optimization. Consensus dynamics on optimized networks is faster than Ramanujan graphs that are classical networks for fast consensus. Especially, when networks are very sparse where the average degree is 2, the optimized networks form a very fast consensus compared to the Ramanujan graphs. Heuristic network model for fast consensus when network is sparse is proposed. Furthermore, the optimal network for slow consensus is also considered.

6.1 A consensus model

In the networked system, "consensus", which is also called "synchronization", means to accomplish coordination between elements in the system as results of their interactions [22, 62, 108, 109]. The concept of the consensus is applied in the coordination of multi-agent networks including synchronization of coupled oscillators, flocking behaviors, data fusion in large sensor networks, and rendezvous of moving agents. From the symmetry of mathematical expression, consensus dynamics can be seen as the dynamics of markov chain [110, 111]. The state of each node is represented by $x_i(t)$, and nodes interact with other nodes connected by links simultaneously. The interaction between adjacent agents is defined as,

$$\dot{x}_i(t) = \sum_{j \in N_i} a_{ij} \left(x_j(t) - x_i(t) \right), \tag{6.1}$$

where $\dot{x}_i(t)$ represents the amount of change in the state of agent (node) i at time t and N_i represents the set of adjacent nodes of node i. Using the adjacency matrix $\mathbf{A}$ and the degree matrix $\mathbf{D}$, of which the diagonal elements equals the degree of node i ($\mathbf{D}_{ii} = d_i$), this interaction can be formulated using matrix expressions as,

$$\dot{\boldsymbol{x}}(t) = -(\mathbf{D} - \mathbf{A})\boldsymbol{x}(t), \tag{6.2}$$

where $\boldsymbol{x}(t)$ represents a column vector consisting of $x_i(t), (1 \leq i \leq N)$, N denotes the number of agents (nodes) in a network.

This model is formed as a continuous function, and the solution can be obtained analytically as shown in equation (6.3).

$$\boldsymbol{x}(t) = \exp(-\mathbf{L}t)\,\boldsymbol{x}(0), \tag{6.3}$$

where the matrix $\mathbf{L} = \mathbf{D} - \mathbf{A}$, which is called the Laplacian matrix. The equation (6.3) can be rewritten using the set of eigenvalues of the Laplacian matrix $\mathbf{L}$ as shown in equation (6.4).

$$\boldsymbol{x}(t) = \mathbf{z}\begin{pmatrix} \mathrm{e}^{-\lambda_1(\mathbf{L})\mathrm{t}} & & & \\ & \mathrm{e}^{-\lambda_2(\mathbf{L})\mathrm{t}} & & \\ & & \ddots & \\ & & & \mathrm{e}^{-\lambda_N(\mathbf{L})\mathrm{t}} \end{pmatrix}\mathbf{z}^{\mathrm{T}}\boldsymbol{x}(0), \tag{6.4}$$

where $\lambda_i(\mathbf{L})$ represents the i-th minimum eigenvalue of the Laplacian matrix $\mathbf{L}$ and $\mathbf{z}$ is the set of corresponding eigenvector. 0 is one of eigenvalues of the matrix $\mathbf{L}$ and the column vector $\mathbf{1} = (1,1,\cdots,1)^{\mathrm{T}}$ is corresponding eigenvector, because $\mathbf{L1} = 0 \cdot \mathbf{1}$. Then, the element (1,1) of $\exp(-\mathbf{L}t)$ should be 1 at any time t and other diagonal elements decrease exponentially. When the time t becomes sufficiently large, the equation (6.4) converges to

$$\begin{aligned} \boldsymbol{x}(\infty) &= \mathbf{z}\begin{pmatrix} 1 & & & \\ & 0 & & \\ & & \ddots & \\ & & & 0 \end{pmatrix}\mathbf{z}^{\mathrm{T}}\boldsymbol{x}(0), \\ &= \left(\frac{1}{N}\right)\mathbf{1}\mathbf{1}^{\mathrm{T}}\,\boldsymbol{x}(0). \end{aligned} \tag{6.5}$$

Note that the corresponding eigenvector to eigenvalue 0 of the matrix $\mathbf{L}$ is normalized as $1/\sqrt{N}(1,1,\cdots,1)^{\mathrm{T}}$. Therefore, the size of the second minimum eigenvalue $\lambda_2(\mathbf{L})$ decides the consensus speed and the network that has large $\lambda_2(\mathbf{L})$ is optimal to achieve fast consensus.

The consensus process in networked agents proceeds with the discrete time step and it can be modeled by the same manner of continuous consensus model above mentioned with introducing the coefficient of changing rate ϵ as shown in (6.6).

$$\begin{aligned} \boldsymbol{x}(t+1) &= (\mathbf{I} - \epsilon\mathbf{L})\boldsymbol{x}(t), \\ &= \mathbf{W}\boldsymbol{x}(t), \\ &= \mathbf{W}^{\mathrm{t}}\boldsymbol{x}(0), \end{aligned} \tag{6.6}$$

where the matrix $\mathbf{W}$ is $(\mathbf{I} - \epsilon\mathbf{L})$. The iteration will converge and make average consensus when the following equation (6.7) is true.

$$\lim_{t\to\infty}\mathbf{W}^{\mathrm{t}} = \left(\frac{1}{N}\right)\mathbf{1}\mathbf{1}^{\mathrm{T}}. \tag{6.7}$$

The necessary and sufficient condition of the equation (6.7) is obtained as

$$\rho(\mathbf{W} - (1/N)\mathbf{1}\mathbf{1}^{\mathrm{T}}) < 1, \tag{6.8}$$

where the function $\rho(\mathbf{W} - (1/N)\mathbf{1}\mathbf{1}^{\mathrm{T}})$ represents the spectrum radius of the matrix $\mathbf{W} - (1/N)\mathbf{1}\mathbf{1}^{\mathrm{T}}$ and $\rho(\mathbf{W} - (1/N)\mathbf{1}\mathbf{1}^{\mathrm{T}})$ is given as,

$$\rho(\mathbf{W} - (1/n)\mathbf{1}\mathbf{1}^{\mathrm{T}}) = \max\{1 - \epsilon\lambda_2(\mathbf{L}), \epsilon\lambda_{\mathrm{N}}(\mathbf{L}) - 1\}. \tag{6.9}$$

For the fast consensus, the spectrum radius ρ should be small, and it is minimized at $\epsilon = \epsilon^*$, which is defined by equation (6.10) [74].

$$\epsilon^* = \frac{2}{\lambda_2(\mathbf{L}) + \lambda_N(\mathbf{L})}. \tag{6.10}$$

The ρ^* at $\epsilon = \epsilon^*$ is given,

$$\begin{aligned} \rho^*(\epsilon^*) &= \frac{\lambda_N(\mathbf{L}) - \lambda_2(\mathbf{L})}{\lambda_2(\mathbf{L}) + \lambda_N(\mathbf{L})}, \\ &= \frac{1 - R}{1 + R}. \end{aligned} \tag{6.11}$$

It is clear that the eigenvalue ratio $R = \lambda_2(\mathbf{L})/\lambda_N(\mathbf{L})$ defines the spectrum radius ρ^* and in the consensus with discrete time the network having large eigenvalue ratio R is optimal to form fast consensus.

In this dissertation, the consensus with discrete time step, which is valid in networked systems by agents, is considered, and the network topology, which maximize or minimize the eigenvalue ratio R, is studied by using evolutionary network optimization and the analysis of the distribution of eigenvalue of the Laplacian matrix.

6.2 Laplacian spectrum of networks

Define the network is formed by the adjacency matrix **A**, and the degree matrix **D** that is diagonal matrix having degree of nodes in diagonal elements. As mentioned at equation (6.3), the Laplacian matrix is defined as,

$$\mathbf{L} = \mathbf{D} - \mathbf{A}\,. \tag{6.12}$$

The eigenvalues of the Laplacian matrix includes important information about the network topology. One of well-known properties is that the number of $\lambda(\mathbf{L}) = 0$ represents the number of isolated networks. Then, if the network has no disconnected nodes, the network has $N - 1$ eigenvalues including multiple ones where N is the number of nodes in the network. The relationship between the eigenvalues of the Laplacian matrix and the index of network topology is also found as,

$$\lambda_2(\mathbf{L}) \le \frac{N}{N-1} d_{min} \le \frac{N}{N-1} d_{max} \le \lambda_N(\mathbf{L}) \le 2d_{max}, \tag{6.13}$$

where λ_i represents *i*-th minimum eigenvalue of the Laplacian matrix, and d_{min} and d_{max} are minimum or maximum degree of nodes in the network.

Then, the eigenvalue ratio $R = \lambda_2(\mathbf{L})/\lambda_N(\mathbf{L})$, which is related to the fast consensus, can be bounded as,

$$\frac{\lambda_2(\mathbf{L})}{\lambda_N(\mathbf{L})} \leq \frac{Nd_{min}}{(N-1)2d_{max}} \leq \frac{d_{min}}{d_{max}} \leq 1, \tag{6.14}$$

and the relationship as shown in equation (6.15) is known.

$$\begin{aligned} &2e(G)(1-\cos(\pi/N) \leq \lambda_2(\mathbf{L}), \\ &d_{max}+1 \leq \lambda_N(\mathbf{L}), \end{aligned} \tag{6.15}$$

where the function $e(G)$ is edge connectivity, which is defined as the minimal number of edges whose removal result in loosing connectivity of the network G.

The lower bound of $\lambda_2(\mathbf{L})$ by equation (6.15) implies the edge connectivity affects the spectrum gap $\lambda_2(\mathbf{L})$, however, it is meaningless when the network is large-scale network. From the equation (6.14) and (6.15), the homogeneous network, such as regular network, seems to be optimal for the fast consensus, and the heterogeneous network, such as scale free network, seems to be optimal for slow consensus. Figure 6.1 shows the spectrum, which is set of eigenvalues of the Laplacian matrix of the networks. The circle lattice networks is one of k-regular networks, in which nodes are connected to $k/2$ left and right adjacent nodes that form circle type network as shown in Figure 6.2, is very homogeneous network, and the edge connectivity equals average degree ($= 4$). However, the $\lambda_2(\mathbf{L_c})$ of circle lattice is smaller than scale free networks $\lambda_2(\mathbf{L}_{\mathrm{SF}})$ that has nodes with 2 degree, and the eigenvalue ratio is $0.0008/6.25 = 0.000128$, which is smaller than the eigenvalue ratio of scale free network $0.5736/63.1551 = 0.00908$. On the other hand, the random regular network, which is also one of k-regular network and links are wired randomly, has large $\lambda_2(\mathbf{L}_{\mathrm{RR}}) = 0.562$ and relatively small $\lambda_N(\mathbf{L}_{\mathrm{RR}}) = 7.45$. From only this example, it is clear that the estimation of performance of network for consensus dynamics from the degree distribution is difficult.

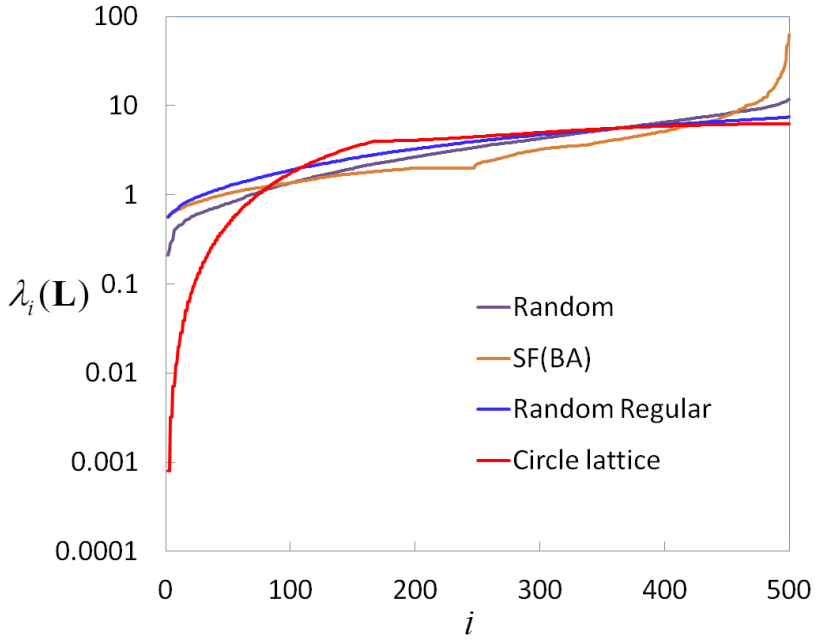

Figure 6.1 The spectrum, which is the set of eigenvalues of the Laplacian matrix, of networks with 500 nodes and 1000 links is plotted.

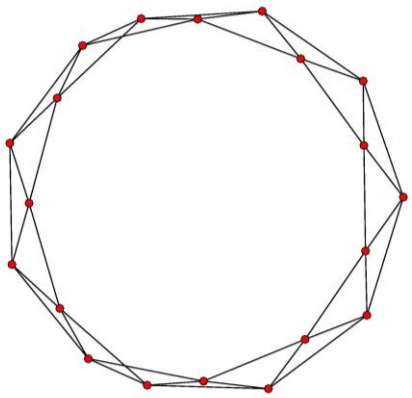

Figure 6.2 A circle-lattice network with degree $k = 4$.

It is needed to understand the properties of Laplacian spectra, which is the index of consensus dynamics as shown in previous section, to optimize network topology for consensus dynamics. Therefore, it begins with the overview of the Laplacian spectra of typical network topologies and the difficulties of the network optimization for consensus dynamics by global statistical data is shown, which are ordinary used to study complex network.

Ramanujan graph is a *k*-random regular graph, and it is known that the classical network for fast consensus having the largest value of $\lambda_2(\mathbf{L})$ [75, 112, 113]:

$$\lambda_2(\mathbf{L}) \geq k - 2\sqrt{k-1}. \tag{6.16}$$

Figure 6.3 shows $\lambda_2(\mathbf{L})$ of several networks. It validates that the Ramanujan graphs have the largest $\lambda_2(\mathbf{L})$ compared to typical network topologies including random networks, scale-free networks, and KN networks. Under the continuous-time consensus model, of which the speed is defined by $\lambda_2(\mathbf{L})$ as shown in equation (6.5), the fastest consensus will achieve on the Ramanujan graphs.

The discrete-time consensus is modeled by equation (6.6), such as a system consisting of networked agents, where the eigenvalue ratio $R = \lambda_2(\mathbf{L})/\lambda_N(\mathbf{L})$ defines the consensus speed. According to the study by Kar et al. the eigenvalue ratio is more sensitive to the variations in the second minimum eigenvalue $\lambda_2(\mathbf{L})$ than the variations in the maximum eigenvalue $\lambda_N(\mathbf{L})$ [109]. Figure 6.4 shows the eigenvalue ratio R of networks. The Ramanujan graphs also have the largest value of *R*, and the Ramanujan graphs can drive the fastest consensus dynamics.

The comparison of Figure 6.3 and Figure 6.4 shows that the consensus speed depends on whether the protocol is continuous time step or discrete time step: the scale free network is the second fastest network under continuous time consensus model, but the random network is the second under discrete time consensus model. It is also clear that the existence of a power law of the degree distribution does not directly imply the performance for consensus dynamics from the results of scale free networks SF(BA) and KN networks (KN): The consensus speed is different drastically between scale free networks and KN network, even they share similar property of the degree distribution that is power law.

One of the reasons that the global statistical properties such as power law of the degree distribution cannot predict the second minimum eigenvalue $\lambda_2(\mathbf{L})$, which is the dominant index of consensus dynamics, is that it will be affected by the local topological properties of the network. According to [114], the upper bound of $\lambda_2(\mathrm{L})$ is given as

$$\lambda_2(\mathbf{L}) \leq 2\frac{|E(S,S^c)|}{|S|}, \tag{6.17}$$

where $|S|$ is total number of nods in any subset of nodes S satisfying $0 < |S| \leq N/2$, and $|E(S,S^c)|$ is the number of edges between S in the complement of $|S|$. Consider there are two sub graphs: a large Ramanujan graphs with 500 nodes and a small Ramanujan graphs with 100 nodes that are connected by only one link (Figure 6.5).

Although each graph is optimal for consensus dynamics: $\lambda_2\ (\mathbf{L}_{\text{Left}}) = 0.617$ $\lambda_2\ (\mathbf{L}_{\text{Right}}) = 0.938$, $\lambda_2(\mathbf{L})$ of the entire network is close to 0 ($\lambda_2(\mathbf{L}) = 0.00698$) due to small $|E(S, S^c)|$ that is 1 in this case. Therefore, the globally statistical properties of network is sometimes useless to estimate the performance of the network for consensus dynamics.

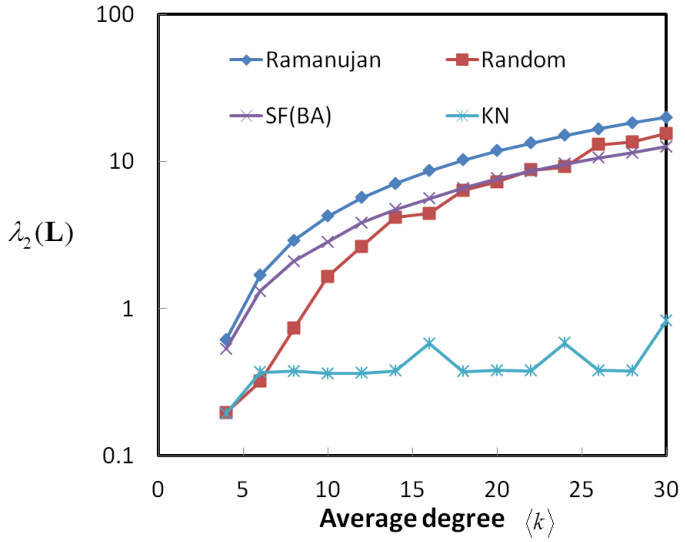

Figure 6.3 The comparison of $\lambda_2(\mathbf{L})$ second minimum eigenvalue of the Laplacian matrix $\mathbf{L}$ of several networks: Each network consists of 500 nodes.

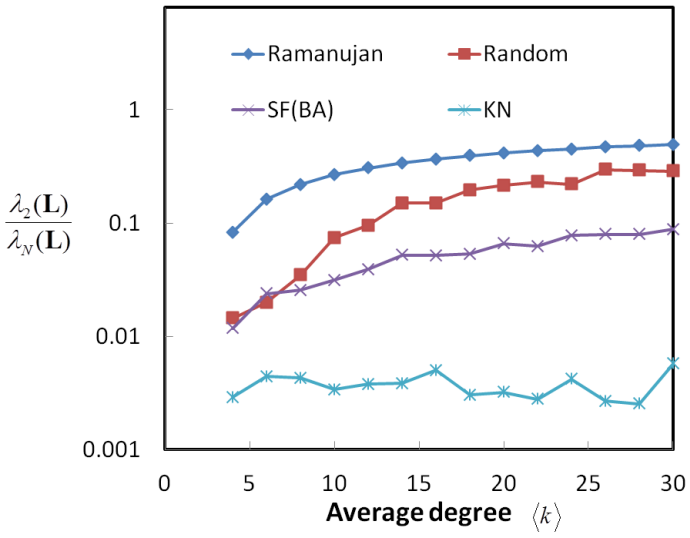

Figure 6.4 The comparison of $\lambda_2(\mathbf{L})/\lambda_n(\mathbf{L})$ the eigenvalue ratio of the Laplacian matrix $\mathbf{L}$ of several networks: Each network consists of 500 nodes.

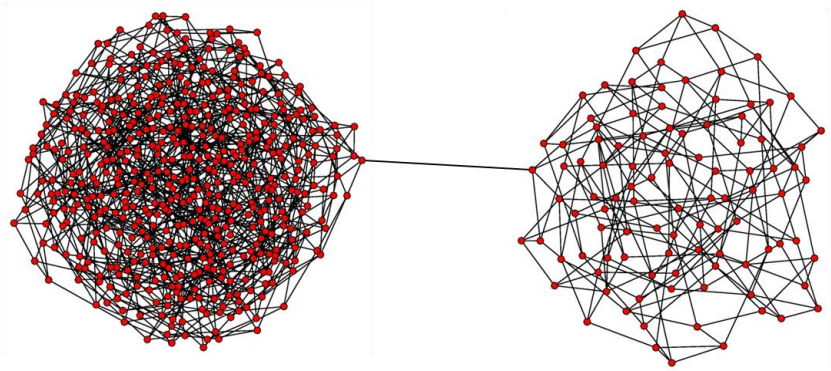

Figure 6.5 The network consisting of two Ramanujan graphs connected by a link. The Ramanujan graph in left side has 500 nodes and $\langle k \rangle = 4$, and $\lambda_2(\mathbf{L}_{\text{Left}}) = 0.617$. The Ramanujan graph in right side has 100 nodes and $\langle k \rangle = 4$, and $\lambda_2(\mathbf{L}_{\text{Right}}) = 0.938$. The whole network has $\lambda_2(\mathbf{L}) = 0.00698$, which is smaller than $\lambda_2(\mathbf{L})$ of each network.

6.3 Evolutionary optimization for fast or slow consensus

In this section, the evolutionary optimization is applied to design networks that maximize or minimize the consensus process using eigenvalue ratio $R = \lambda_2(\mathbf{L})/\lambda_n(\mathbf{L})$ as objective function.

6.3.1 Fast consensus: minimizing convergence time for consensus

The evolutionary optimization can create networks that has larger eigenvalue ratio $R = \lambda_2(\mathbf{L})/\lambda_N(\mathbf{L})$ by up to 5 % than Ramanujan graphs, which is considered as most optimal networks for consensus dynamics in previous studies [75, 113] (Figure 6.6). Note that each Ramanujan graph used in this comparison is created to have the largest R by over 1000 iteration of the creation of Ramanujan graph. Figure 6.7, in which Figure 6.6 is plotted on semi-logarithmic scale, features the performance of optimized network when average degree $\langle k \rangle = 2$, which has very large R compared to the Ramanujan graphs ($R_{\text{optimized}}/R_{\text{Ramanujan}} = 17.8$).

Figure 6.8 and Figure 6.9 show $\lambda_2(\mathbf{L})$ and $\lambda_N(\mathbf{L})$ of evolutionary optimized networks and Ramanujan graphs respectively. It is shown that the large R of the optimized network with $\langle k \rangle = 2$ comes from very large $\lambda_2(\mathbf{L})$ compared to Ramanujan graph. It is also shown that $\lambda_N(\mathbf{L})$ of the optimized network is larger than that of Ramanujan graph when average degree is small, but it is relatively smaller than the ratio of $\lambda_2(\mathbf{L})$ between those networks.

The degree distribution of evolutionary optimized networks is shown in Figure 6.10. It is very clear that evolutionary optimized network is not k-regular graphs. This result combined with results from Figure 6.6 to Figure 6.8 implies the regular network is not necessary condition to achieve the fastest consensus including continuous time consensus and discrete time consensus, of which the consensus speed is defined by $\lambda_2(\mathbf{L})$ and $\lambda_2(\mathbf{L})/\lambda_N(\mathbf{L})$ respectively.

Finally, the topology of optimized network with $\langle k \rangle = 2$ is visualized in Figure 6.11. The network has a characteristic topology (ring-trees structure) having a ring-network at the center of the network and several modularized tree networks interconnected via the ring network.

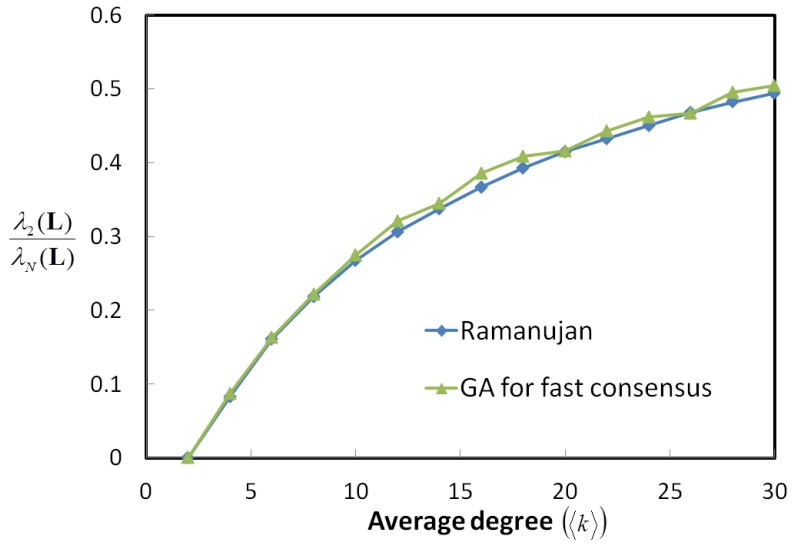

Figure 6.6 The eigenvalue ratio $R = \lambda_2(\mathbf{L})/\lambda_n(\mathbf{L})$ of Laplacian matrix $\mathbf{L}$ of evolutionary optimized network (GA) and Ramanujan network (Ramanujan) is plotted as a function of the average degree. Each network has 500 nodes.

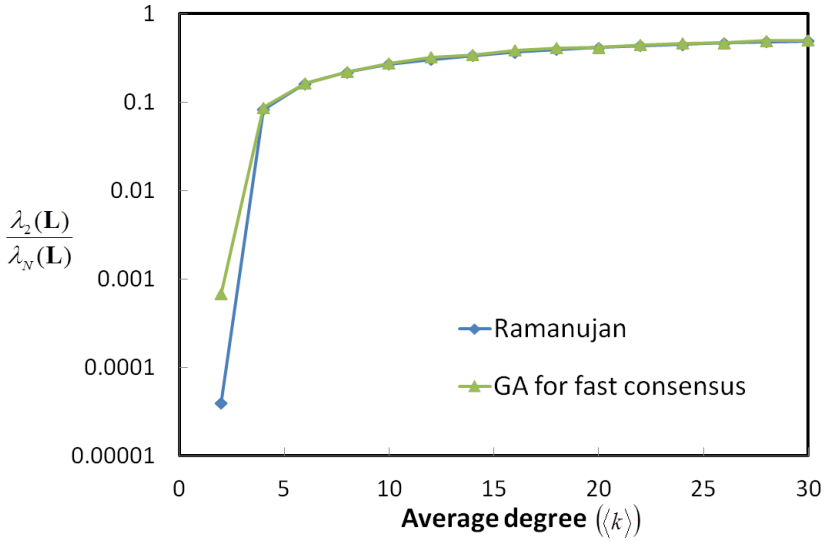

Figure 6.7 The eigenvalue ratio $R = \lambda_2(\mathbf{L})/\lambda_n(\mathbf{L})$ of Laplacian matrix $\mathbf{L}$ of evolutionary optimized network (GA) and Ramanujan network (Ramanujan) is plotted as a function of the average degree on semi-logarithmic scale. Each network has 500 nodes.

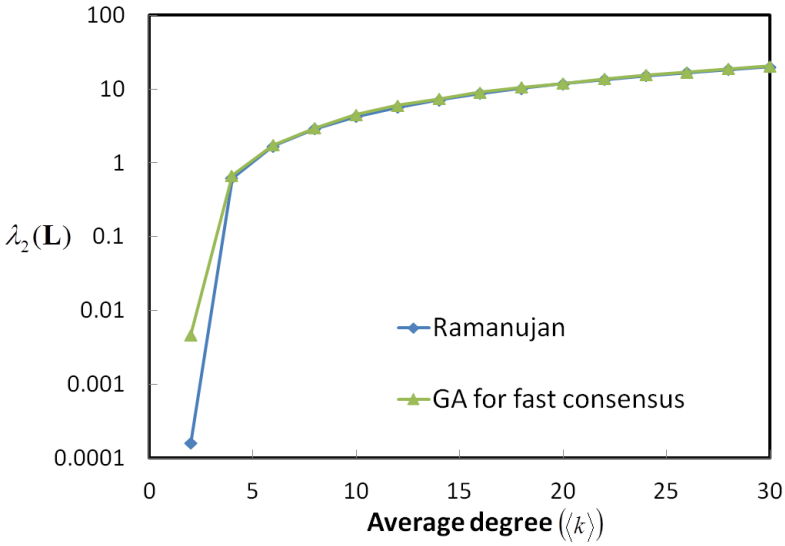

Figure 6.8 The second minimum eigenvalue $\lambda_2(\mathbf{L})$ of Laplacian matrix $\mathbf{L}$ of evolutionary optimized network (GA) and Ramanujan network (Ramanujan) is plotted as a function of the average degree. Each network has 500 nodes.

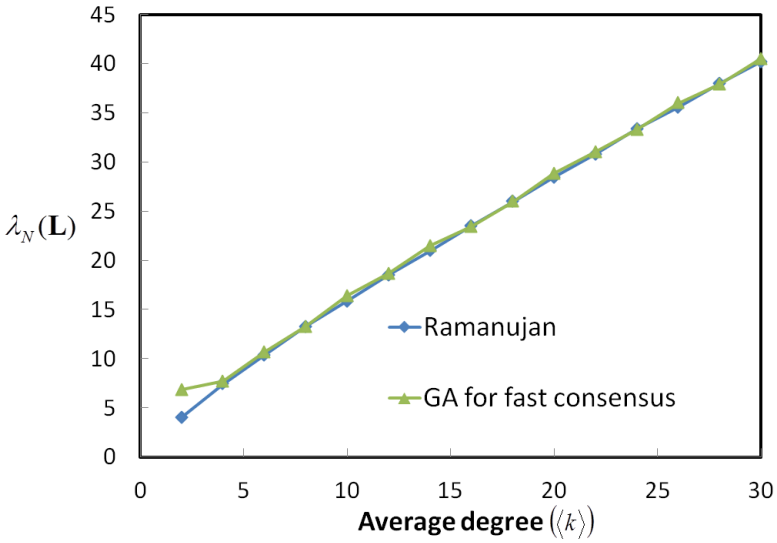

Figure 6.9 The maximum eigenvalue $\lambda_N(\mathbf{L})$ of Laplacian matrix $\mathbf{L}$ of evolutionary optimized network (GA) and Ramanujan network (Ramanujan) is plotted as a function of the average degree. Each network has 500 nodes.

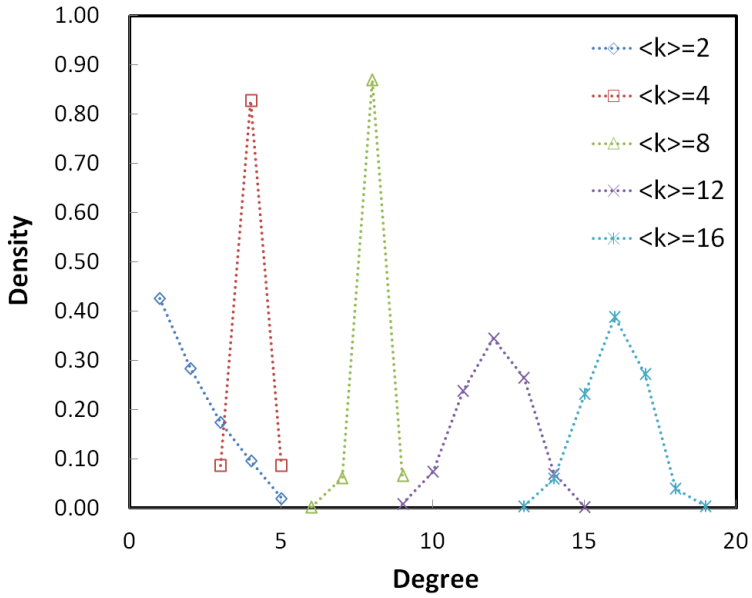

Figure 6.10 The degree distribution of evolutionary optimized networks for the maximization of consensus-dynamics. Every networks have 500 nodes and each legend represents the average degree $\langle k \rangle$.

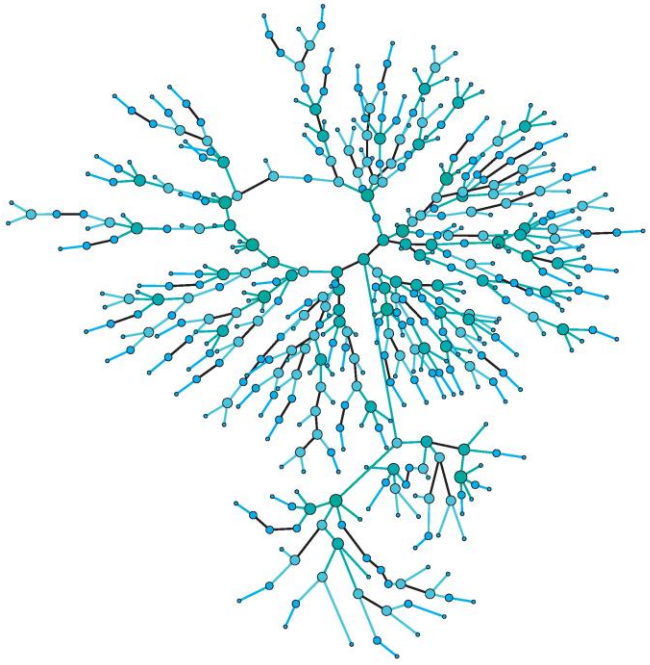

Figure 6.11 The evolutionary optimized networks with 500 nodes and 500 links to maximize the eigenvalue ratio $\lambda_2(\mathbf{L})/\lambda_n(\mathbf{L})$.

6.3.2 Slow consensus: maximizing convergence time for consensus

In this subsection, the evolutionary optimization is applied to minimize the eigenvalue ratio $R = \lambda_2(\mathbf{L})/\lambda_n(\mathbf{L})$. Figure 6.12 shows the results of the optimization. It is clear that the evolutionary optimization can create networks that have very small eigenvalue ratio R compared to CPA networks and KN networks, which also have small R. The crated networks have small $\lambda_2(\mathbf{L})$ and large $\lambda_n(\mathbf{L})$ to minimize R as shown in Figure 6.13 and Figure 6.14.

The evolutionary optimized networks have characteristic topology as shown in Figure 6.15: consisting of a dense core network and line shaped network. The dense core has many pathways to communicate with others in the core, but the line network does not have redundant path for consensus dynamics.

The difference of R between evolutionary optimized network and CPA or KN networks becomes small along with the increase of the average degree of networks. This seems to come from the failure to make long line shaped network by evolutionary optimization, because the optimized network at average degree $\langle k \rangle = 30$ has much shorter line shaped network, which is shown in Figure 6.16, compared to the network when the average degree is relatively small (Figure 6.15).

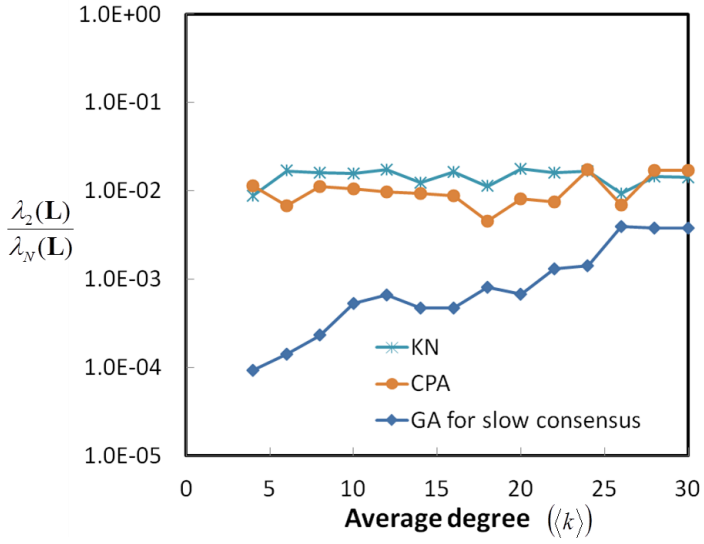

Figure 6.12 The eigenvalue ratio $R = \lambda_2(\mathbf{L})/\lambda_n(\mathbf{L})$ of Laplacian matrix $\mathbf{L}$ of evolutionary optimized network (GA), the partial complete graph (CPA) and KN network (KN) is plotted as a function of the average degree.

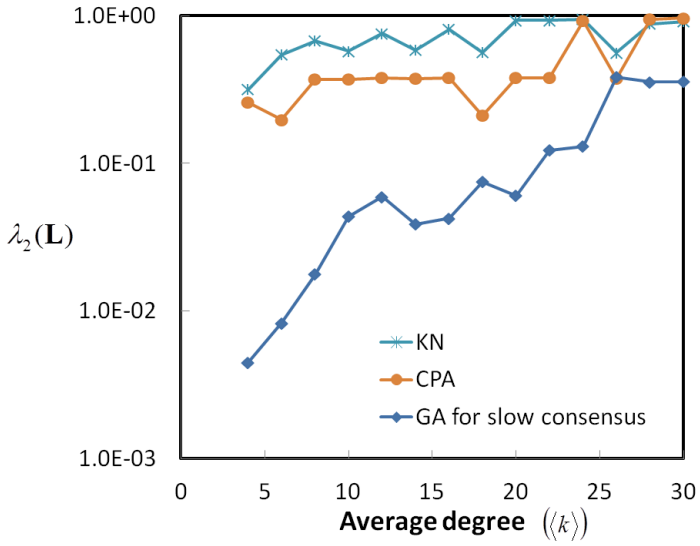

Figure 6.13 The second minimum eigenvalue $\lambda_2(\mathbf{L})$ of Laplacian matrix $\mathbf{L}$ of evolutionary optimized network (GA), the partial complete graph (CPA) and KN network (KN) is plotted as a function of the average degree.

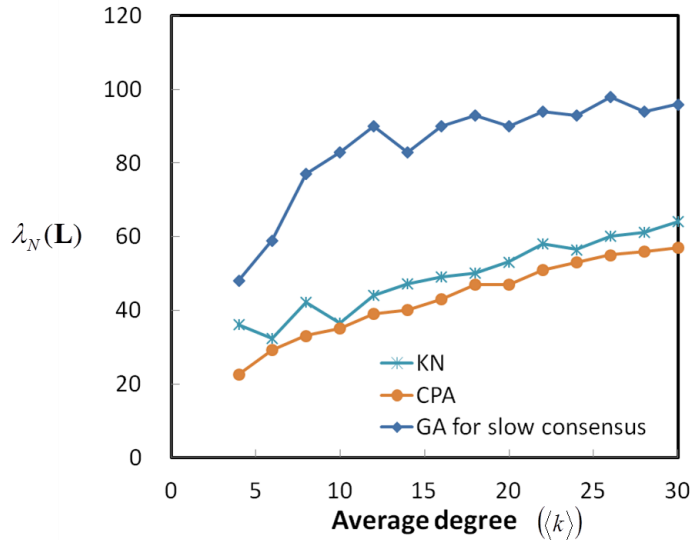

Figure 6.14 The maximum eigenvalue $\lambda_N(\mathbf{L})$ of Laplacian matrix $\mathbf{L}$ of evolutionary optimized network (GA), the partial complete graph (CPA) and KN network (KN) is plotted as a function of the average degree.

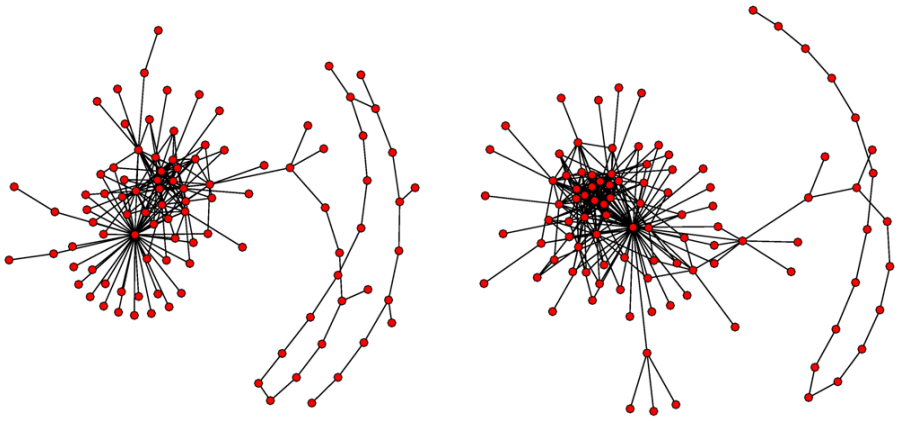

Figure 6.15 The evolutionary optimized networks with 100 nodes, which minimize the eigenvalue ratio $\lambda_2(\mathbf{L})/\lambda_n(\mathbf{L})$. The left network has 200 links and right network has 300 links.

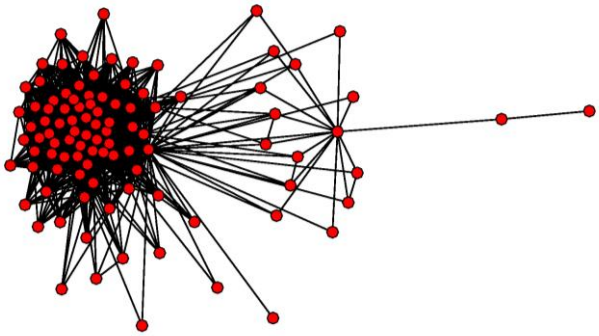

Figure 6.16 The evolutionary optimized networks with 100 nodes and 1500 links to minimize the eigenvalue ratio $\lambda_2(\mathbf{L})/\lambda_n(\mathbf{L})$.

6.4 Heuristic models for optimizing consensus dynamics

In this section, heuristic models to minimize or maximize the convergence time of consensus dynamics is proposed.

6.4.1 Fast consensus (Ring-Trees model)

This subsection proposes ring-trees network model as heuristic model to design optimal networks for fast consensus when the network is sufficiently sparse, in precise $\langle k \rangle = 2$.

The ring-trees network has a ring network with n_r nodes at the center and n_r tree networks with n_t nodes Figure 6.17. Therefore, total number of nodes in the network is $N = n_t * n_r$. This network model has same topological properties of the evolutionary optimized network with the average degree $\langle k \rangle = 2$. Figure 6.18 shows example of ring-trees network with 100 nodes. The topology of ring-trees network is controlled by the parameter α that is the ratio of n_t to n_r (=n_t/n_r). Figure 6.19 shows the topology of ring-trees network having different parameter α. By changing α, the network topology is changed from ring network to tree network, and the network with intermediate value of α has largest eigenvalue ratio R (Figure 6.20). The optimal network has modularized tree networks and a ring network at the center. This result shows the certain size modularized networks that divide agents to groups are necessary for the fast consensus when the network is sparse. Figure 6.21 shows the performance of ring-trees network for fast consensus compared to the evolutionary optimized networks and Ramanujan networks with changing the number of nodes from 50 nodes to 500 nodes.

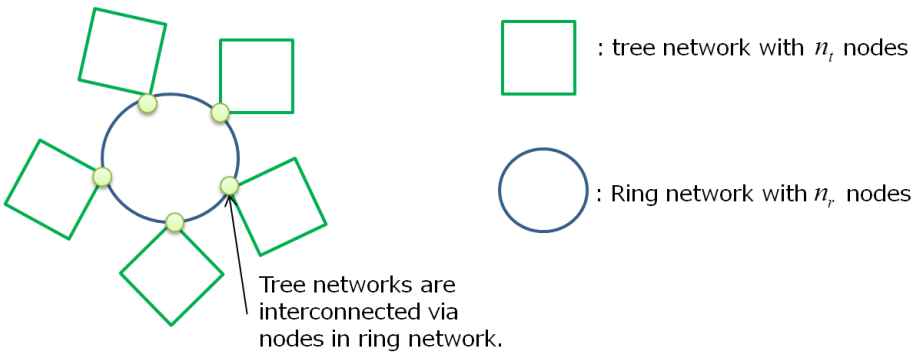

Figure 6.17 Model of ring-trees network.

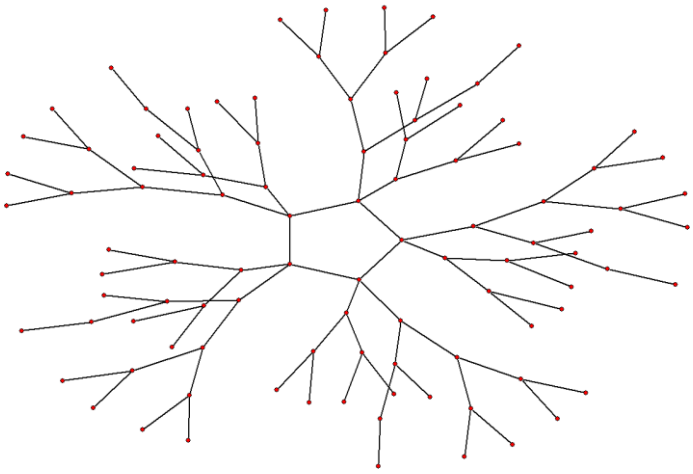

Figure 6.18 Example of ring-trees network: Total number of nodes *N*: 100, Number of nodes in each tree n_t: 20, Number of nodes in each tree n_r: 5.

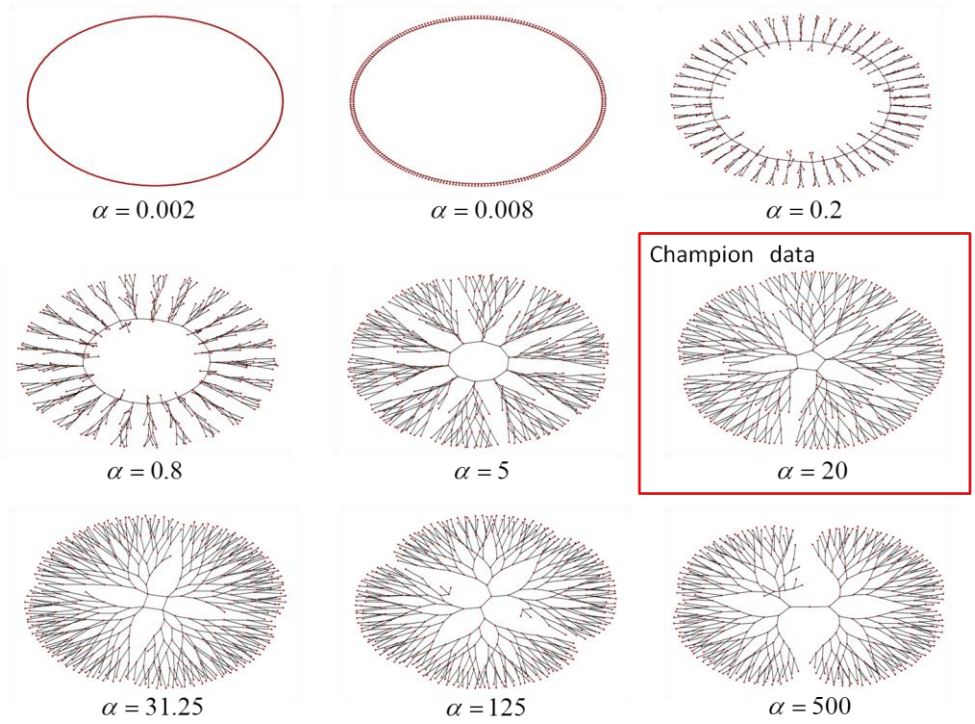

Figure 6.19 The sequence of ring-trees networks having different α is visualized. The total number of nodes in all cases is 500. The ring-trees network with $\alpha = 20$ has the largest R (Champion data).

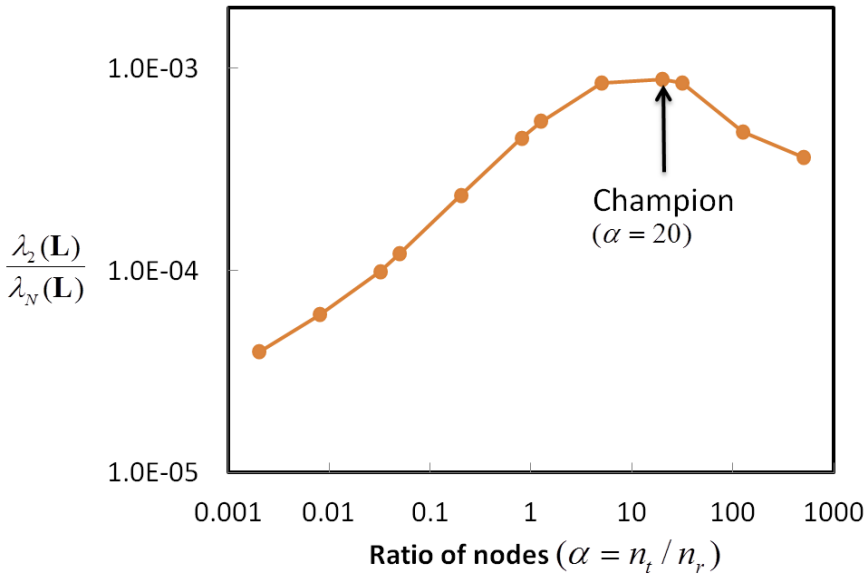

Figure 6.20 The eigenvalue ratio $\lambda_2(\mathbf{L})/\lambda_n(\mathbf{L})$ of Laplacian matrix $\mathbf{L}$ of ring-trees network is plotted as a function of the ratio of nodes n_t/n_r. The total number of nodes in all cases is 500.

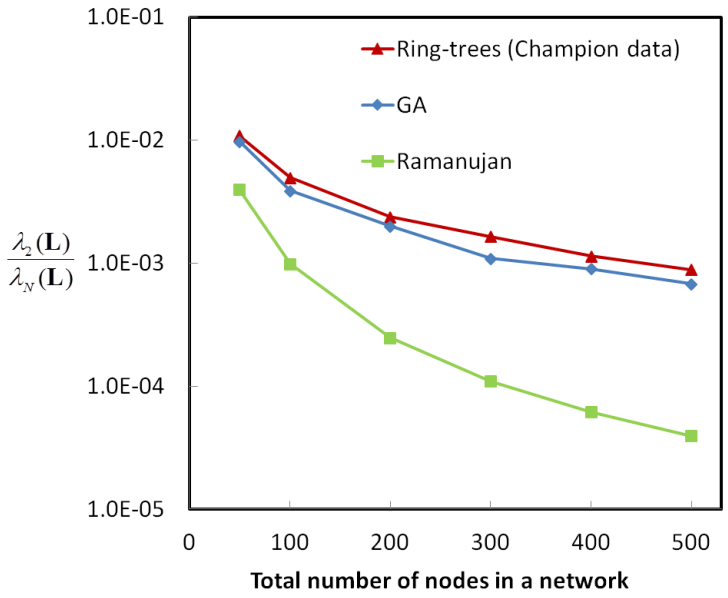

Figure 6.21 The eigenvalue ratio $\lambda_2(\mathbf{L})/\lambda_n(\mathbf{L})$ of Laplacian matrix $\mathbf{L}$ of networks is plotted as a function of the total number of nodes in network: Ring-trees networks with best parameter α (Ring-trees (Champion data)), Evolutionary optimized networks for fast consensus (GA), and Ramanujan networks (Ramanujan). All networks have average degree $\langle k \rangle = 2$.

6.4.2 Slow consensus (Core with Line model)

This subsection proposes a core with line network as heuristic model for slow consensus.

The line network with a single core has N_M nodes in the dense core and N_{Line} nodes in the line network. There are L_M links in the core and L_{Line} links in the line network. If the total resource of building network is limited by N nodes and L links, the following relationships between variants are obtained as,

$$\begin{aligned} N &= N_M + N_{\mathrm{Line}}, \\ L &= L_M + L_{\mathrm{Line}}, \\ L_{\mathrm{Line}} &= N_{\mathrm{Line}}. \end{aligned} \tag{6.18}$$

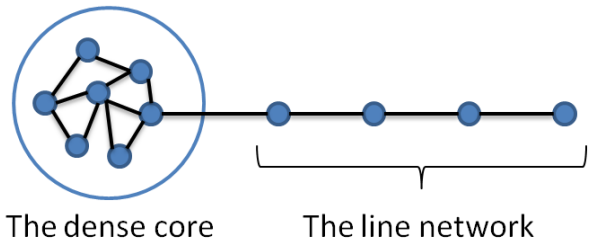

Figure 6.22 The diagram of network consisting of a dense core and a line network.

When the length of line network with N_{Line} nodes is given in addition to total nodes and total links (N and L), the N_{Line} should meets the following condition to avoid disconnected network and double links between same two nodes.

$$N - N_{Line} - 1 \leq L - N_{Line} \leq_{N-N_{Line}} C_2. \tag{6.19}$$

Figure 6.23 shows the comparison of the eigenvalue ratio $R = \lambda_2(\mathbf{L})/\lambda_N(\mathbf{L})$ of networks, in which the maximum number of nodes in line network is set. The line network with a dense core has small R, and it implies the speed of the consensus process is very slow.

It is straightforward question that what will happen when the number of core is increased. Figure 6.24 shows the eigenvalue ratio R of the networks, which consists of two cores connected by line network. It is shown that along with the increase of the number of nodes in line network, the eigenvalue ratio decrease linearly. The increase of number of core network affects efficiency to reduce the ratio. When the number of nodes in the line network is relatively small, two cores with the line network can have more small R than a core with line network. However, due to the topological upper bound, the maximum number of nodes in the line network is larger in the case of single core than the case of two cores. Then, when the maximum number of nodes in the line network is set, the core with line network can have the smallest ratio R.

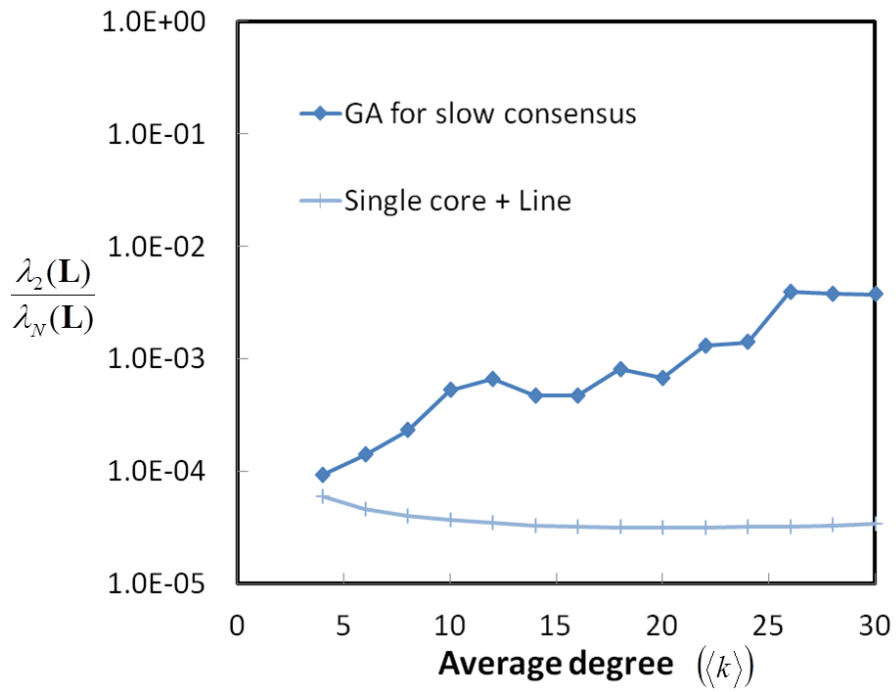

Figure 6.23 The eigenvalue ratio $\lambda_2(\mathbf{L})/\lambda_n(\mathbf{L})$ of networks is plotted as a function of average degree of networks with 100 nodes.

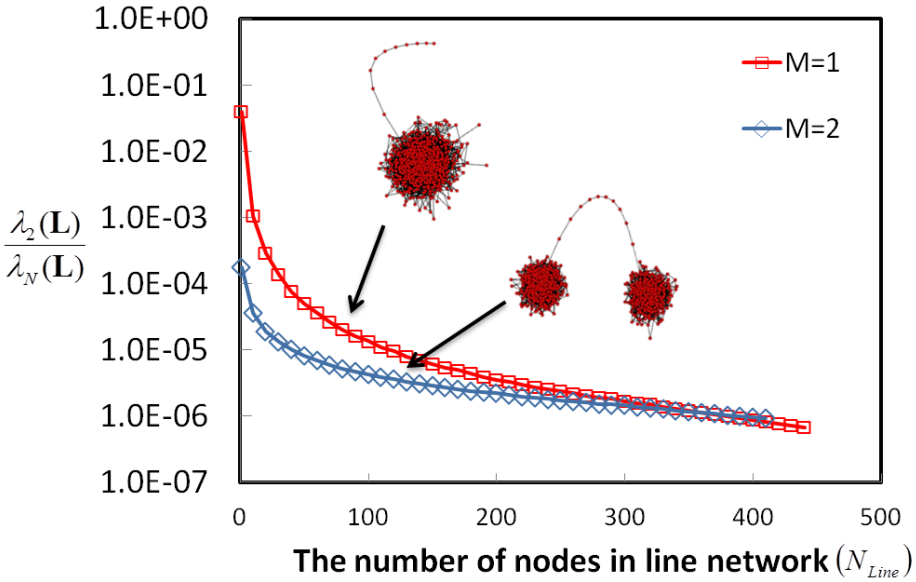

Figure 6.24 The eigenvalue ratio $\lambda_2(\mathbf{L})/\lambda_n(\mathbf{L})$ of a core with line network and two cores with line network is plotted as a function of the number of nodes in the line network, which is connected to core network. A total node is 500 and total link is 2000.

6.5 **Simulation on optimal networks**

In this section, consensus dynamics between networked agents is simulated. The number of agents is 100, and they have number that is given randomly from the space $S = [0, 100]$ as the initialization. The several types of network are used: the evolutionary optimized network for maximization or minimization of consensus dynamics, Ramanujan graph, Random network, Scale free network by Balabási-Albert model, exponential network, CPA network proposed in Chapter 4, KN network proposed in Chapter 4, and a core with line networks. All agents communicate with adjacent agents along the links simultaneously, of which protocol is defined by equation (6.1). Note that it is assumed that the formation of consensus between agents is achieved when the standard deviation of numbers of agents becomes less than 10^{-4} and each plot comes from over 100 iterations.

Figure 6.25 shows the eigenvalue ratio $R = \lambda_2(\mathbf{L})/\lambda_N(\mathbf{L})$ of each network. It is shown that the evolutionary optimization and network model can create networks that maximize or minimize *R* the index of consensus dynamics respectively. Figure 6.26 shows the average time step for the formation of consensus between agents. It is interesting that the network with same number of nodes and same number of links can have drastically different average time step for consensus, which depends on the network topology. The evolutionary optimized networks to maximize consensus dynamics have about same performance with Ramanujan graphs that belong to k-random regular graph. This implies the regularity of network is not necessary condition for the fast consensus, because the optimized networks are not k-regular network (Figure 6.10). On the other hand, the evolutionary optimized networks for minimization of consensus dynamics (GA (minimization)) and a core with line network (Single core + Line) need extremely longer time to achieve the consensus than average consensus time on other networks. Especially on a core with line network, the average consensus time does not decrease even if the average degree of the network increases.

In order to compare how the consensus process proceed on the two extreme cases (evolutionary optimized network for maximization of consensus speed and a single core network with line network for minimizing consensus speed), the state of each agents is plotted as a function of time step on Figure 6.27 and Figure 6.28 respectively. Note that in this case the number i is assigned to agent i initially for the visualization. On a core with line network (Figure 6.27), the consensus between agents in the core is achieved at first. After that they try to achieve the global consensus. The all agents in the core network have to communicate with agents in the line network via a single node, which connects the core and line network. The decrease of the chances of the global interaction between agents make the time of consensus dynamics very long. On the other hand, consensus dynamics between agents is achieved very smoothly on the evolutionary optimized networks (Figure 6.28).

As shown in Figure 6.21, when network has little redundancy to form connected network, which means average degree is $\langle k \rangle = 2$ in this case, evolutionary

optimization can design networks on which agents can make consensus much faster than Ramanujan graphs. Figure 6.29 compares the average convergence time of consensus dynamics on ring-trees network, evolutionary optimized networks for fast consensus (GA) and Ramanujan graphs. The number of nodes is changed from 50 to 500 nodes. In every cases, ring-trees network and evolutionary optimized networks form a fast consensus compared to Ramanujan graphs. Especially, ring-trees network can make faster consensus than the evolutionary optimized networks.

Figure 6.30 compares consensus dynamics on ring-trees network and Ramanujan network when they have 100 nodes and 100 links. Consensus dynamics on ring-trees network is achieved much faster than Ramanujan network where the time of consensus is 1201 steps on ring-trees network and over 5000 steps on Ramanujan network. On the ring-trees network where agents are divided into each tree network, local consensus is promoted in each tree network at first. After that, the global consensus is formed via the ring network. It is very interesting that this simple mechanism makes big difference between these networks on the convergence time of consensus dynamics.

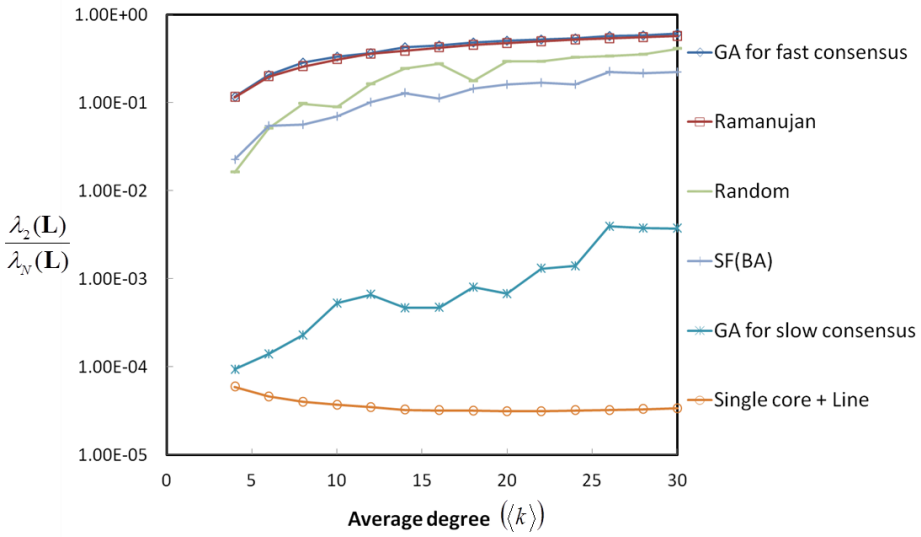

Figure 6.25 The eigenvalue ratio $\lambda_2(\mathbf{L})/\lambda_n(\mathbf{L})$ of Laplacian matrix of each network is plotted as a function of the average degree. Each legend represents the type of network of agents.

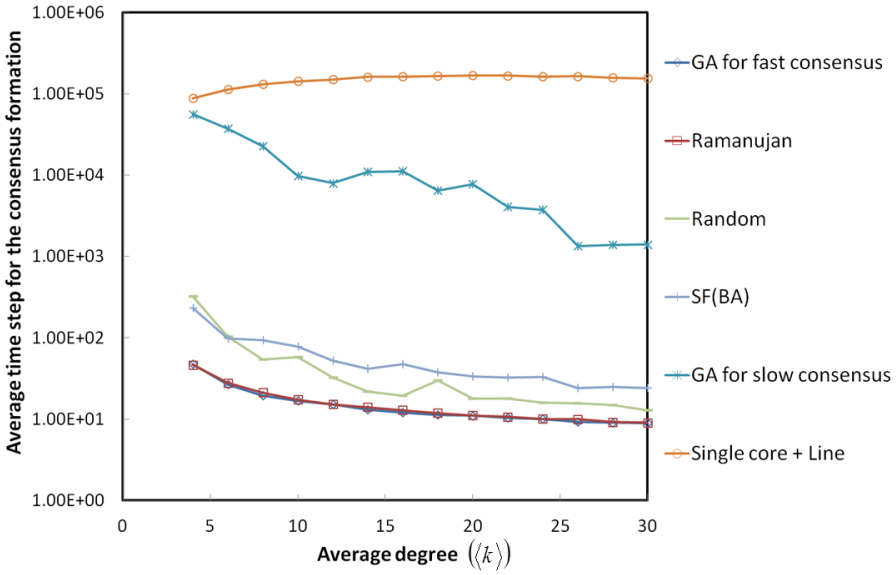

Figure 6.26 The average time step for the formation of consensus between $N = 100$ networked agents is plotted as function of the size of the average degree. Each legend represents the type of network of agents.

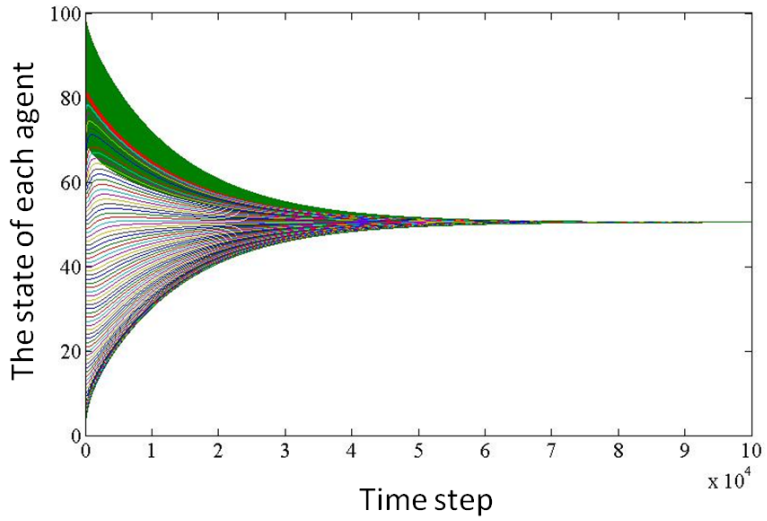

(a) The plot range of time step is [0, 10^5]

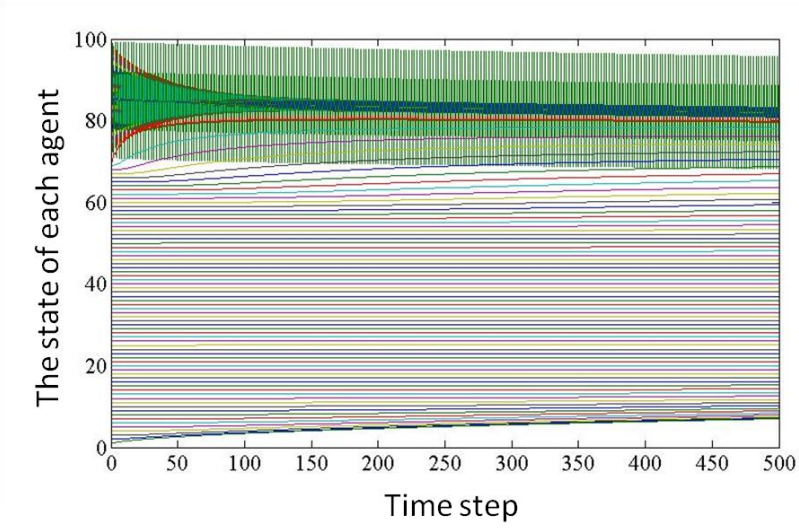

(b) The plot range of time step is [0, 500]

Figure 6.27 The diagram of consensus dynamics between agents on a single core + line network with $N = 100$ nodes and $L = 500$ links. The number of agents in a single core is 34. In this case the number i is assigned to agent i initially.

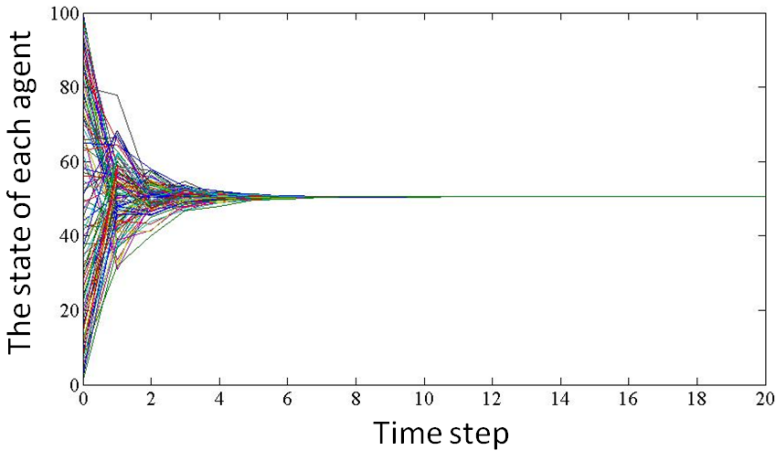

Figure 6.28 Consensus dynamics on evolutionary optimized network for fast consensus with $N = 100$ nodes and 500 links. In this case the number i is assigned to agent i initially.

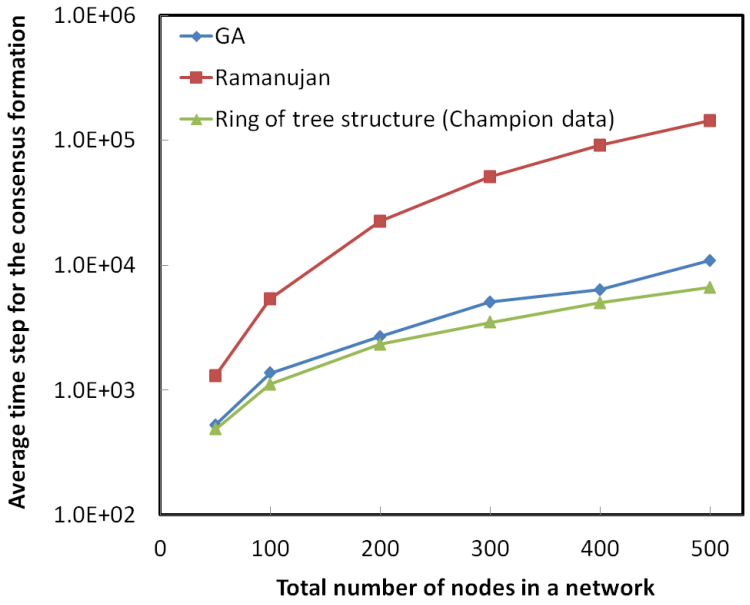

Figure 6.29 The average time step for the formation of consensus on several networks with average degree $\langle k \rangle = 2$ is plotted as function of the number of nodes in a network. Each legend represents the type of network: Evolutionary optimized networks for fast consensus (GA), Ramanujan graph (Ramanujan), networks by heuristic network design model for fast consensus (Ring-trees structure (Champion data)), which are selected as having largest eigenvalue ratio $\lambda_2(\mathbf{L})/\lambda_n(\mathbf{L})$.

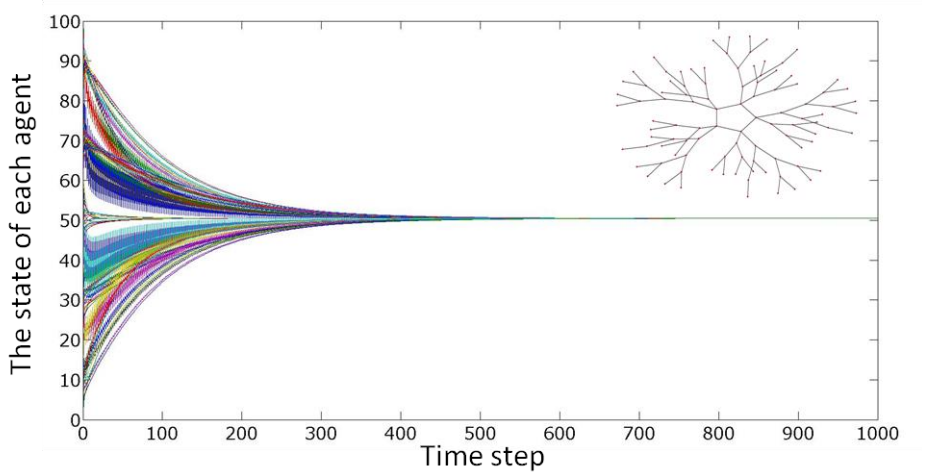

(a) Ring of tree structures

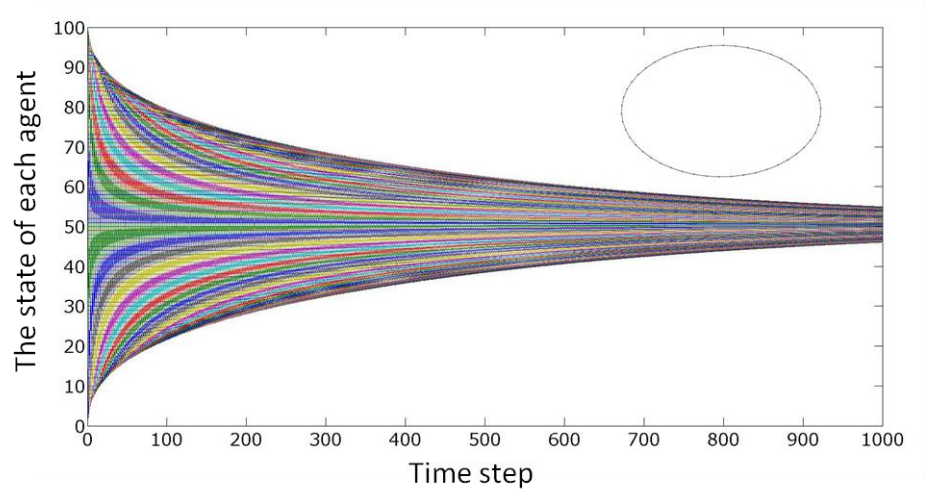

(b) Ramanujan networks

Figure 6.30 Consensus dynamics on (a) ring-trees network ($n_t = 20, n_r = 5$) and (b) Ramanujan network. They have 100 nodes and 100 links. The network topologies are drawn for understanding of network settings. The exact convergence time of each network is 1201 steps on ring-trees network and over 5000 steps on Ramanujan networks.

Chapter 7

Dynamical Processes on Modular Networks

A network composed of interconnected sub-networks is called “modular networks”, where there are a lot of interactions in each module but a few interactions of inter-modules. This chapter studies dynamical processes on the modular networks and also proposes recursive design method to design very large-scale modular networks, which interconnect optimized networks as modules recursively.

7.1 **Motivation**

In our life, the interconnection of networks, which are relatively small or medium size, is usually used to form a very large-scale network efficiently. For example, in the case of an airline network, each domestic airline is interconnected by international airlines, which form literally world-wide network. In the financial network, city bank, local bank and public-sector financial institutions each has their own network, and they form a huge financial network by their interconnections such as transactional relationship. Furthermore there are other examples in road networks, power transmission networks and social communities. These types of network are called “modular networks”, “network of networks” or “community network” and they attract the interest of researchers [52, 67, 70, 93, 95, 115-119].

Modularity is an important concept for understanding the structure and the functions of networked systems. Recently, Gao et al. [67] studied the relationship between the number of modular networks and the performance of modular networks connected randomly by using percolation dynamics, which are actually called “interdependent networks”. They introduced interdependent links to connect a pair of nodes in different modular networks, which represents the relationship that a function of a node depends on the state of a node connected. The interdependent network is very destructible compared to a single network having only connecting links and the threshold fraction of removed nodes for breaking network connectivity becomes much

smaller. The interdependency of modular networks works as an amplifier of the failure of nodes.

The modularization of a network is also used to protect complex networked systems by reducing contact with the external modular-networks [120]. The sparse connectivity of inter-modules prevents the spreading of risk contagion. In those systems, the links between modular networks do not represent a strong tie such as interdependent links, but they are pathways of the interaction of agents. The difference of links connecting inter-modules changes the influence of modularization.

Barabási et al. used modular networks to replicate complex networks in real life [93]. The proposed modular networks can form a network where the scale-free property in the degree distribution and high clustering coefficient coexist, which are common properties in biological, sociological and technological systems. All above mentioned results point to the importance of understanding dynamical processes on modular networks.

In previous studies about dynamical processes on modular networks [67, 70], simple networks, including random network, tree network or star network, are considered as a topology of inter-modules. In addition the number of modules is relatively small, for example modular networks comprising 4 modularized networks are studied in [70].

In the past, many papers have studied modular networks to discover something new which is not observed on non-modular networks. However, this dissertation studies modular networks in terms of network design method.

This chapter proposes a network design method by recursive structure of a unit modular network, where modular networks have a topology of inter-modules, which is the same as a modular network. It is based on an intuitive idea that the optimal topology defining the interaction between nodes in a network should be optimal to define the interaction between modular networks. The proposed design model can deal with modular networks comprising many modules, and it enables the consideration of the influence of the topology of inter-modules toward dynamical processes. This chapter also demonstrates the performance of the network design model under several scenarios by numerical simulations. Note that the interdependency between a pair of nodes is not considered in this dissertation as in Barabási et al [93].

7.2 **A recursive design model of modular networks**

The one of key properties on modular networks is how modularized networks are interconnected. The recursive design model is a network model that interconnects modular networks recursively and we can design a very large-scale network.

The formation of the recursive network starts by the creation of a relatively small optimized network as a unit network (modular network) (Figure 7.1(a)). Next n replicas of the unit network are generated, where n represents the number of nodes in the original unit network. Each replicated network is deployed at the position of each node in the unit network (Figure 7.1(b)), and they are interconnected by links (Figure 7.1(c)).

The most important property of the network design model is that the topology between modular networks is the same with the topology of the unit network. The number of links between modular networks is the same number of links in a unit network l. Then, the total number of links interconnected network is $l(n+1)$. The average degree is $2l(n+1)/n^2 = 2l/n + 2l/n^2 = \langle k_{unit} \rangle + \epsilon$, which is almost same size compared to the average degree of a single unit network $\langle k_{unit} \rangle$.

The second point of the network design model is the method interconnecting a pair of nodes, which belong to different unit networks. Let's assume D_K represents the number of adjacent modular networks of intended modular network K, and $d_{i,K}$ represents the degree of node i in modular network K. When the modular network K is connected to one of adjacent modular networks by a link, the probability that node i in the modular network K will be selected as one of edge of the connecting link is defined by the following equation (7.1),

$$p(d_{i,K}|D_K) = \frac{1}{1+\alpha|D_K - d_{i,K}|} / \sum_i \frac{1}{1+\alpha|D_K - d_{i,K}|}, \tag{7.1}$$

where α is non-negative parameter to control which nodes will be selected. If α is large, the probability that a node i with degree $d_{i,K} \neq D_K$ to be selected becomes small. On the other hand, if $\alpha = 0$, topology of inter-modules is still recursive, but a pair of nodes used for connecting modules is selected randomly (Figure 7.1(d)). For comparison, modular networks, which are connected randomly, are also shown in (Figure 7.1(e))

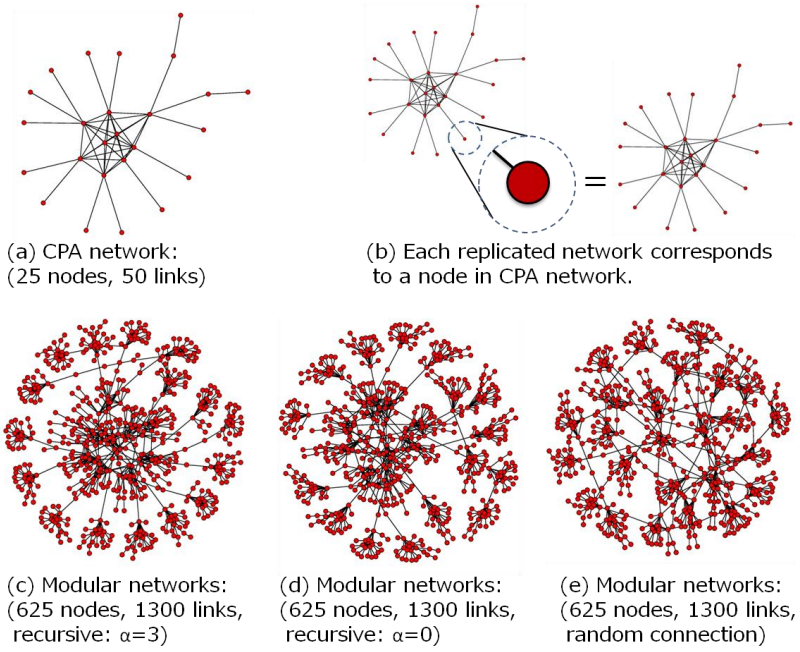

Figure 7.1 The recursive design of a large-scale network with modular networks: The topology of each modular network is also CPA which is a network proposed in Chapter 4. Each modular network has 25 nodes and 50 links, and the formed modular networks have 25 modularized networks: totally 625 links and 1300 links. (c), (d): The topology between modular networks is CPA. Each modular network is interconnected by equation (7.1). (e): Modularized networks are interconnected randomly.

7.3 **Simulation on modular networks**

In this section, a set of simulation results is shown regarding probabilistic diffusion, cascade dynamics and consensus dynamics on recursively designed networks with modular networks. In each case of simulation, the performance of modular networks with recursive architecture and modular networks connected randomly is compared. The simulation results support the recursively designed modular networks have better performance than modular networks connected randomly. In order to understand the influence of the modularization of a network, the optimal modular networks is also compared to a single globally optimized network. Note that the size of modular network is set to relatively small size (ex. 25 nodes or 26 nodes) for the comparison. However, the recursive network design model can be applied directly to design a very large-scale modular networks, for example, if network with 500 nodes is used as modular network, we can design networks with 250,000 nodes easily. The simulations on those very large-scale networks are discussed in next section 7.4.

7.3.1 Probabilistic diffusion

(1) Modular networks with CPA as a module (maximizing probabilistic diffusion)

Maximizing probabilistic diffusion by SIS model on modular networks is demonstrated. From the results of Chapter 4, the single globally optimized network for maximizing probabilistic diffusion is a CPA network, which has largest maximum eigenvalue of the adjacency matrix. The analysis by simulation begins with the comparison of the maximum eigenvalue of the adjacency matrix between modular networks by the proposed recursive network design and modular networks connected randomly, in which each module network is formed using CPA model (Figure 7.2). It is shown that modular networks with recursive structure have larger maximum eigenvalue compared to modular networks connected randomly. This implies modular networks with recursive structure are more diffusive and it is more suitable for maximizing probabilistic diffusion.

The maximum eigenvalue of the modular networks with recursive structure is also compared to a single globally optimized CPA network (Figure 7.3). It is shown that the modularization of network make a network less diffusive and the influence is increased with the size of average degree $\langle k \rangle$.

The numerical simulation is also done with the average degree $\langle k \rangle = 4$ (Figure 7.4). At each simulation, one node with largest degree in a single CPA network or one node with largest degree in modular network with most adjacent modular networks in modular networks is selected as a trigger of probabilistic diffusion. The fraction of infected nodes at a steady state is observed and the average value of 100 same experiments is plotted on vertical axis. The score on horizontal axis is relative infection rate ($=\beta/\delta$) normalized by the mathematical threshold of a single CPA network (the inverse of maximum eigenvalue of the adjacency matrix $\lambda_1(\mathbf{A}_{\mathrm{CPA}})$). The modular networks with recursive topology takes off more early than modular networks connected randomly.

The modularization of a network makes a network less diffusive even if each modular network has optimal topology (CPA), but the modular networks with recursive topology can be most diffusive under such a condition.

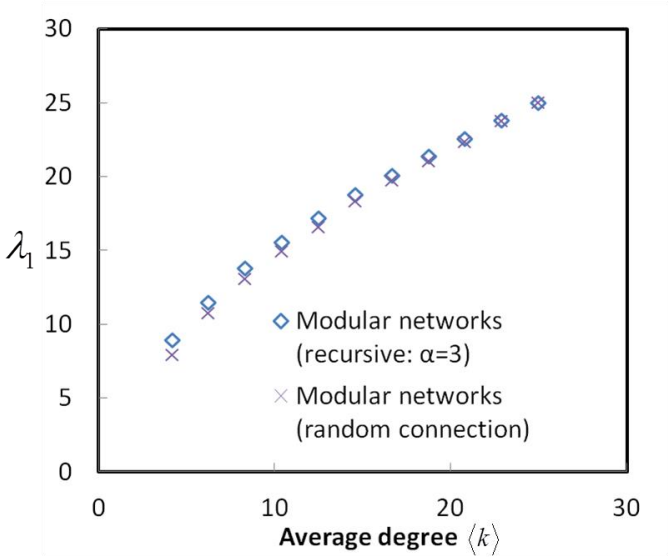

Figure 7.2 The maximum eigenvalue $\lambda_1$of adjacency matrix of modular networks are plotted as a function of average degree $\langle k \rangle$. Modular networks (recursive: $\alpha = 3$): the modular networks by proposed recursive network design ($\alpha = 3$ in equation (7.1)). Modular networks (random connection): modular networks connected randomly. Both of modular networks consist of 25 CPA networks with 25 nodes, and then they have 625 nodes totally. Note that the variable α is a parameter of equation (7.1).

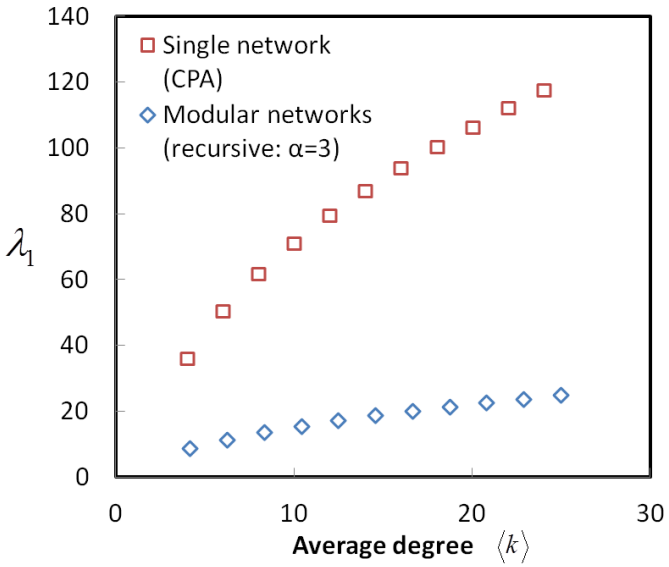

Figure 7.3 The maximum eigenvalue λ_1 of adjacency matrix is plotted as a function of average degree. Single network (CPA): single CPA network with 625 nodes. Modular networks (recursive: $\alpha = 3$): same with Figure 7.2.

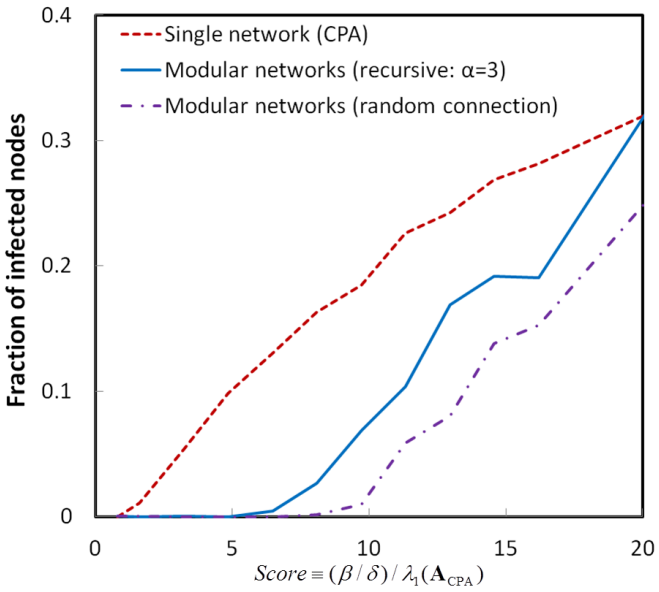

Figure 7.4 The fraction of infected nodes at a steady state on networks is plotted as a function of Score, which is the relative infection rate β/δ divided by the tipping point of the diffusion $1/\lambda_1 = 1/32.4$ of single CPA network that has $\langle k \rangle = 4$ (score $= \beta/\delta * 32.4$). The curing rate δ is always 0.1. The legend represents same network in Figure 7.2 and Figure 7.3.

(2) Modular networks with random regular network as a module (Minimizing probabilistic diffusion)

Minimizing probabilistic diffusion by SIS model on modular networks is demonstrated. From the results of Chapter 4, the globally optimized single network for minimizing probabilistic diffusion is random regular network, which has smallest maximum eigenvalue of the adjacency matrix. The analysis begins with the comparison of maximum eigenvalue of the adjacency matrix. Figure 7.5 shows the maximum eigenvalue of modular networks by the proposed recursive network design model and modular networks connected randomly, where each modular network is random regular network. It is shown that modular networks with recursive topology has almost same maximum eigenvalue compared to modular networks connected randomly. This implies both of modular networks have same threshold for probabilistic diffusion.

The maximum eigenvalue of the modular networks by recursive network design model is also compared to single random regular network, which is globally optimized (Figure 7.6). The maximum eigenvalue of those two types of networks is plotted on the same line. This means both modular networks with recursive structure and single network optimized globally has same small threshold.

The numerical simulation is also done to demonstrate the performance of those networks including the single random regular network with 625 nodes and modular

networks consisting of 25 random regular networks with 25 nodes, which have same average degree $\langle k \rangle = 4$ (Figure 7.7). At each simulation, the state of one randomly selected node is changed to be infected as a trigger of probabilistic diffusion. The fraction of infected nodes at a steady state is observed and the average value of 100 same experiments is plotted. From results, it is clear that the topology of inter-modules have little influence on the threshold of modular networks, which is the same value with single random regular network optimized globally.

The modularization of a network does not change the threshold of a network into small one if single network has already been optimized for minimizing probabilistic diffusion.

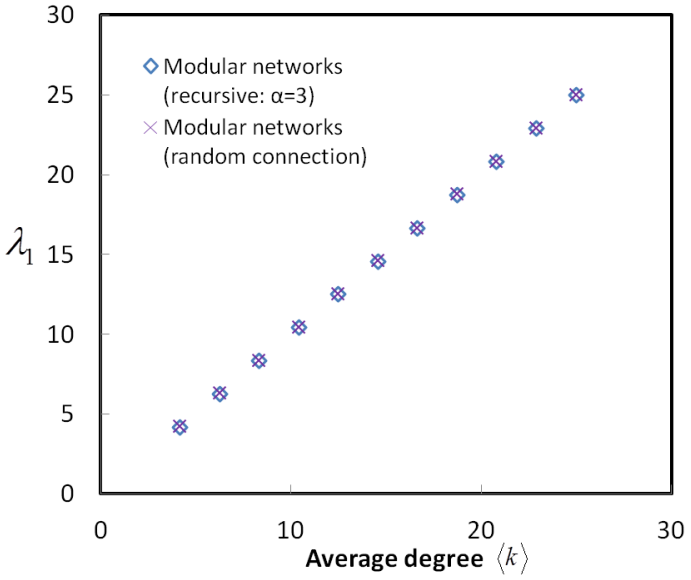

Figure 7.5 The maximum eigenvalue λ_1 of adjacency matrix of modular networks are plotted as a function of average degree of network. Modular networks (recursive: $\alpha = 3$): the modular networks by proposed recursive network design ($\alpha = 3$ in equation (7.1)). Modular networks (random connection): modular networks connected randomly. Both of modular networks consist of 25 random regular networks with 25 nodes, and then they have 625 nodes totally.

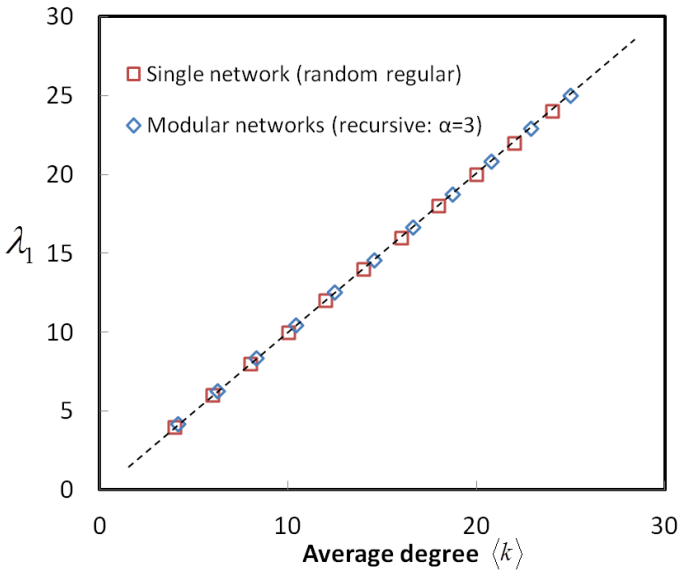

Figure 7.6 The maximum eigenvalue $\lambda_1$of adjacency matrix is plotted as a function of average degree of network. Single network (random regular): single random regular network with 625 nodes. Modular networks (recursive: $\alpha = 3$): same with Figure 7.5.

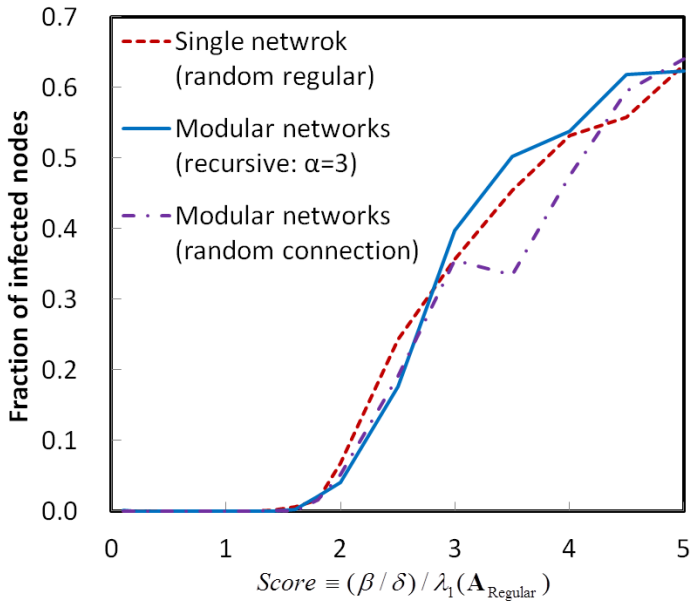

Figure 7.7 The fraction of infected nodes at a steady state on networks is plotted as a function of Score, which is the relative infection rate β/δ divided by the tipping point of the diffusion $1/\lambda_1 = 1/4$ of single random regular network that has $\langle k \rangle = 4$ (score $= \beta/\delta * 4$). The curing rate δ is always 0.1. The legend represents same network in Figure 7.5 and Figure 7.6.

7.3.2 Cascade dynamics

(1) Modular networks with GA network as a module (maximizing cascade window)

Maximizing cascade dynamics on modular networks is demonstrated. From the results of Chapter 5, the globally optimized network for maximizing cascade window is achieved using the proposed P model. The cascade window of the single network using P model is compared to modular networks with recursive structure of evolutionary optimized network for maximizing cascade window and modular networks connected randomly by numerical simulations (Figure 7.8). At each simulation, one node selected randomly becomes a trigger of cascade dynamics. It is shown that the modularization of a network makes the size of cascade window small. It is good results for protecting networked system from cascade failure, but it is bad results for diffusion of innovation by cascade dynamics on coordination game. It is also shown that the modular networks with recursive structure has large cascade window especially at small average degree compared to modular networks connected randomly.

The modularization of a network makes a network less diffusive like a probabilistic diffusion even if each modular network has optimal topology, but the modular networks with recursive topology can maximize the cascade window.

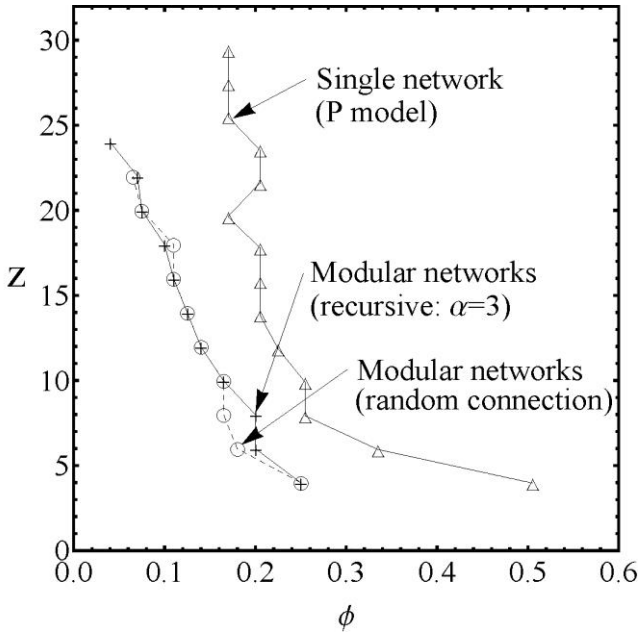

Figure 7.8 Cascade window of networks: Single network (P model): single network with 500 nodes by P model. Modular networks (recursive: $\alpha = 3$): modular networks by proposed recursive network design ($\alpha = 3$ in equation (7.1)). Modular networks (random connection): modular networks connected randomly. Both modular networks consist of 25 optimal networks by evolutionary optimization with 25 nodes, which have 625 nodes totally.

(2) Module networks with CPA network as a module (minimizing cascade)

Minimizing cascade dynamics on modular networks is demonstrated. From the results of Chapter 5, the globally optimized network for minimizing cascade window is achieved using the proposed CPA model. The cascade window of the single network using CPA model is compared to modular networks with recursive structure of CPA network and modular networks connected randomly by numerical simulation (Figure 7.9). At each simulation, one node is selected randomly as a trigger of cascade dynamics. The modular networks with recursive structure has narrow cascade window compared to modular networks connected randomly. This implies modular networks with recursive structure are more suitable to prevent cascade failure.

It is also shown the modularization of network makes a network more diffusive even if each modular network has optimal topology for minimizing cascade window (CPA). This result meets the study by Young [12, 105], which told the modular structure in the network is essential as a foothold for diffusion on cascade dynamics. The modularization limits the number of interconnected nodes, which relaxes the necessary number of adopting adjacent agents for an intended agent to adopt.

Considering the expansion of cascade window in this simulation along with the results of previous subsection, the effect of the modularization is not only to minimize cascade window, and it depends on the topology of modular networks.

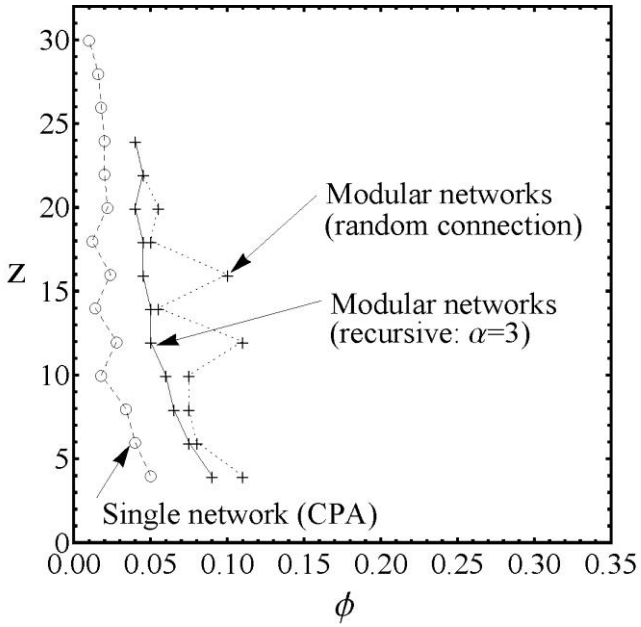

Figure 7.9 Cascade window of networks: Single network (CPA): single network with 500 nodes by CPA, Modular networks (recursive: $\alpha = 3$): the modular networks by proposed recursive network design ($\alpha = 3$ in equation (7.1)). Modular networks (non recursive): modular networks connected randomly. Both modular networks consist of 25 CPA networks with 25 nodes, which have 625 nodes totally.

7.3.3 Consensus dynamics

(1) Modular network with GA network as a module (fast consensus)

Fast consensus dynamics on modular networks is demonstrated. Eigenvalue ratio of the laplacian matrix of each module is compared in Figure 7.10. GA optimized network have a larger eigenvalue ratio compared to other networks. Especially there is a big difference between the optimized network (GA) and Ramanujan network when the average degree is $\langle k \rangle = 2$.

Modular networks are formed by interconnecting those modules recursively or randomly. The eigenvalue ratio of those modular networks using GA networks as a unit module is shown in Figure 7.11. They are also compared to single globally optimized GA network. It is shown that the modularization of a network makes small eigenvalue ratio and also prevents fast consensus.

On the other hand, the modular networks with recursive topology have larger eigenvalue ratio than modular networks connected randomly. It implies modular networks with recursive topology will make fast consensus. The difference of eigenvalue ratio increases along with the decrease of average degree. The importance of interaction patters of inter-modules becomes relatively large on sparse networks.

The consensus processes are simulated among 676 networked agents (Figure 7.12). Modular networks consist of 26 optimized networks (GA) with 26 nodes as modules. The initial value of each agent i is given randomly from the space $\mathrm{S} = [0, 676]$. All agents communicate with adjacent agents along the links simultaneously, of which protocol is defined by equation (6.1). Note that it is assumed that the formation of consensus between agents is achieved when the standard deviation of numbers of agents becomes less than 10^{-4} and each plot comes from over 100 iterations of same simulations.

It is confirmed that the convergence time becomes larger on modular networks than single globally optimized networks. In addition, consensus dynamics is still faster on the modular networks with recursive structure than modular networks connected randomly, especially when network is sparse ($\langle k \rangle \simeq 2$).

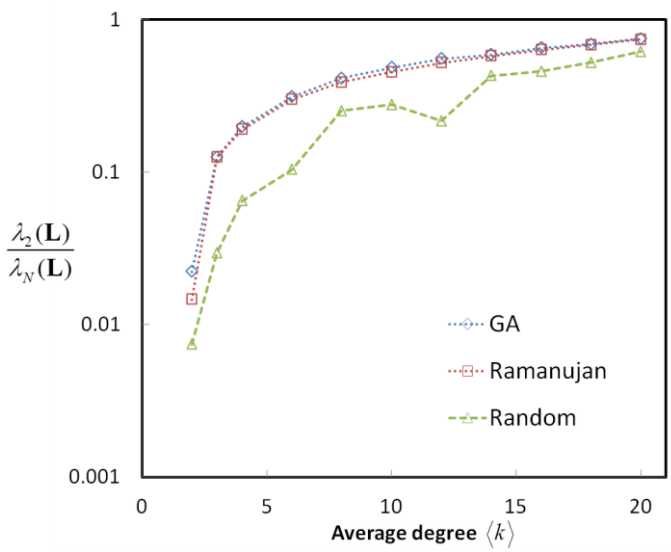

Figure 7.10 The eigenvalue ratio $\lambda_2(\mathrm{L})/\lambda_n(\mathrm{L})$ of Laplacian matrix of each network is plotted as a function of the average degree. GA: network optimized by evolutionary optimization method for maximizing eigenvalue ratio. Ramanujan: Ramanujan network. Random: random network. All networks have 26 nodes.

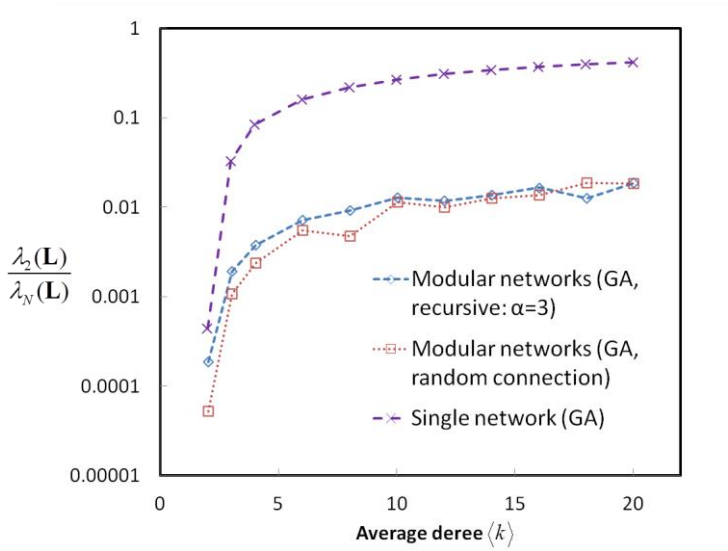

Figure 7.11 The eigenvalue ratio $\lambda_2(\mathrm{L})/\lambda_n(\mathrm{L})$ of Laplacian matrix of each network is plotted as a function of the average degree. Single network (GA): single optimal network with 676 nodes by GA optimized for fast consensus. Modular networks (GA, recursive: $\alpha = 3$): modular networks by proposed recursive network design ($\alpha = 3$ in equation (7.1)). Modular networks (GA, random connection): modular networks connected randomly. Both modular networks consist of 26 optimal networks by evolutionary optimization with 26 nodes, which have 676 nodes totally.

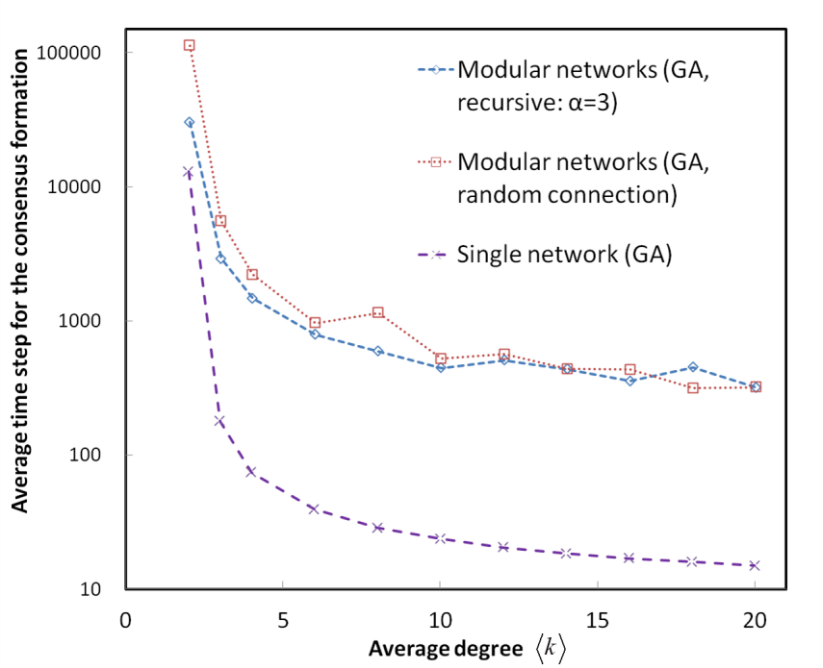

Figure 7.12 The average time step of consensus dynamics among $N = 676$ networked agents is plotted as function of the average degree. Each legend represents same in Figure 7.11.

7.4 **Design of very large-scale networks with recursive modular structure**

The very large-scale network with 250,000 nodes, which consists of 500 modular networks having 500 nodes, is designed by the recursive design method. With numerical simulations, the network performance is investigated regarding probabilistic diffusion, cascade dynamics, and consensus dynamics on modular networks with recursive topology and modular networks connected randomly.

7.4.1 Probabilistic diffusion

(1) Modular networks with CPA as a module (maximizing probabilistic diffusion)

Figure 7.13 shows the fraction of infected nodes under the SIS model. Modular networks consist of 500 optimal modular networks (CPA networks) having 500 nodes and average degree $\langle k \rangle = 4$. The average degree of inter-modules is also $\langle k \rangle = 4$. Therefore, the link density between inter-modules is sufficiently small compared to inside-module. Single network in the figure represents CPA network with 500 nodes and $\langle k \rangle = 4$. Initially, 0.2% nodes in the network are infected as trigger of the diffusion. To be precise, a node with largest degree in each modular network is infected initially in modular networks, and a node with largest degree is infected initially in single network (CPA).

The simulation results show the tipping point seems to be nearly not affected by connecting modular networks recursively. The tipping point is almost same value in the case of modular networks connected randomly and single network (CPA). The recursive structure has no additional effect to maximize probabilistic diffusion when the each modular network is optimized.

(2) Modular network with random regular network as a module (Minimizing probabilistic diffusion)

Figure 7.14 shows the fraction of infected nodes under the SIS model. Modular networks consist of 500 optimal modular networks (random regular networks) having 500 nodes and average degree $\langle k \rangle = 4$. The average degree of inter module is also $\langle k \rangle = 4$. Therefore, the link density between inter-modules is sufficiently small compared to inside-module. Single network in the figure represents random regular network with 500 nodes and $\langle k \rangle = 4$. Initially, 0.2% nodes in the network are infected as trigger of the diffusion. To be precise, a randomly selected node in each modular network is infected initially in modular networks, and a randomly selected node is infected initially in single network (random regular).

The simulation results show the tipping point seems to be nearly not affected by connecting modular networks recursively. The tipping point is almost same value in the case of modular networks connected randomly and single network (random regular).

Thus, the recursive structure has no additional effect to minimize probabilistic diffusion when the each modular network is optimized.

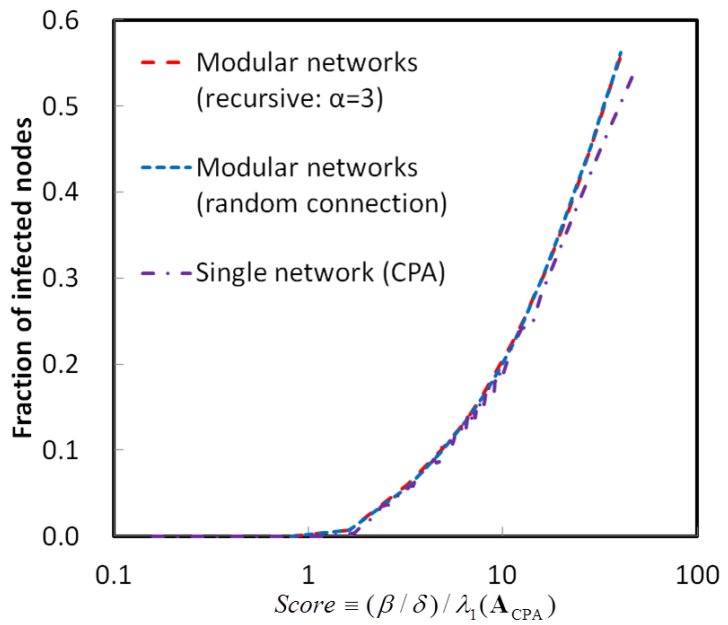

Figure 7.13 The fraction of infected nodes at a steady state on networks is plotted as a function of Score, which is the relative infection rate β/δ normalized by the tipping point of the diffusion $1/\lambda_1 = 1/32.4$ of CPA network that has 500 nodes and average degree $\langle k \rangle = 4$ (score $= \beta/\delta * 32.4$). The curing rate δ is always 0.1. Modular networks (recursive: $\alpha = 3$): modular networks consist of 500 modules (CPA network) with recursive structure. Modular networks (random connection): modular networks consist of 500 modules (CPA network) with random connection. Each module has 500 nodes and then the modular networks have totally 250,000 nodes. The average degree of inter-module is the same with inside module $\langle k \rangle = 4$. Single network (CPA): CPA network consisting of 500 nodes with $\langle k \rangle = 4$. Note that the variable α is a parameter of equation (7.1).

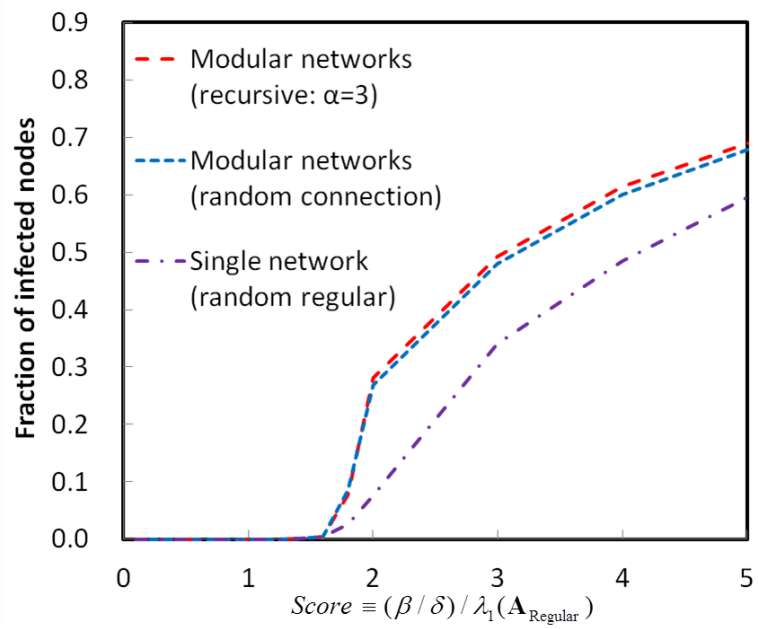

Figure 7.14 The fraction of infected nodes at a steady state on networks is plotted as a function of Score, which is the relative infection rate β/δ normalized by the tipping point of the diffusion $1/\lambda_1 = 1/4$ of random regular network that has 500 nodes and $\langle k \rangle = 4$ (score $= \beta/\delta * 4$). The curing rate δ is always 0.1. Modular networks (recursive: $\alpha = 3$): modular networks consist of 500 modules (random regular network) with recursive structure. Modular networks (random connection): modular networks consist of 500 modules (random regular network) with random connection. Each module has 500 nodes and then the modular networks have totally 250,000 nodes. The average degree of inter-module is the same with inside module $\langle k \rangle = 4$. Single network (random regular): random regular network consisting of 500 nodes with $\langle k \rangle = 4$. Note that the variable α is a parameter of equation (7.1).

7.4.2 Cascade dynamics

(1) Module networks with P model as a module (maximizing cascade window)

Figure 7.15 compares cascade window of networks. Modular networks consist of 500 networks. Each module is designed using P model with 500 nodes as an optimal network for maximizing cascade window. Single network in the figure represents network designed using P model with 500 nodes.

At each simulation, one randomly selected node in each modular network or single network is activated initially as trigger of cascade. The interconnected modular networks have narrower cascade window than cascade window of a module (Single network). The result comes from the property of modular networks that have few links between inter-modules. The sparse connectivity between modules prevents the influence of activated nodes from spreading into nodes in other modules, even if all nodes in one module become activated. Furthermore modular networks that are randomly connected have wider cascade window than modular networks with recursive topology.

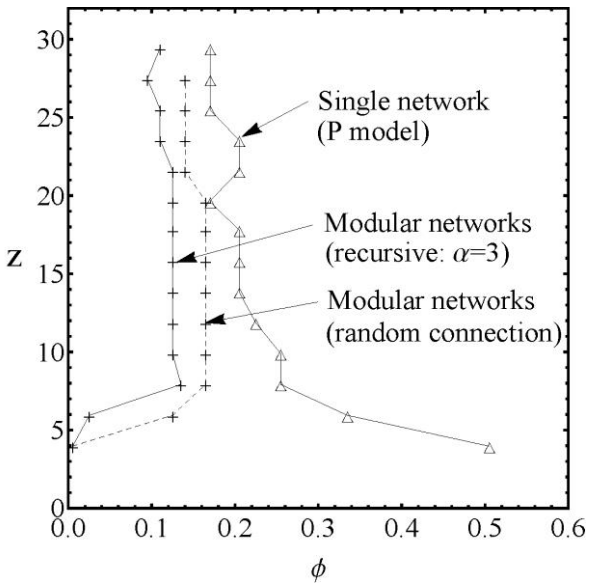

Figure 7.15 Cascade window of networks. Single network (P model): single network by P model with 500 nodes and average degree $\langle k \rangle = 4$. Modular networks (recursive: $\alpha = 3$): modular networks consist of 500 modules (P model) with recursive structure. Modular networks (random connection): modular networks consist of 500 modules (P model) with random connection. Each module has 500 nodes and then the modular networks have totally 250,000 nodes. The average degree of inter-module is the same with inside module. Note that the variable α is a parameter of equation (7.1).

(2) Module networks with CPA network as a module (minimizing cascade window)

Figure 7.16 compares cascade window of networks. Modular networks consist of 500 networks. Each module is designed using CPA with 500 nodes as an optimal network for minimizing cascade window. Single network in the figure represents network designed using CPA with 500 nodes.

At each simulation, one randomly selected node in each modular network or single network is activated initially as trigger of cascade. The interconnected modular networks have narrower cascade window than cascade window of a module (single network). The result comes from the discontinuous structure of modular networks mentioned in previous simulations. Modular networks with recursive topology have same or narrower cascade window than modular networks that are randomly connected.

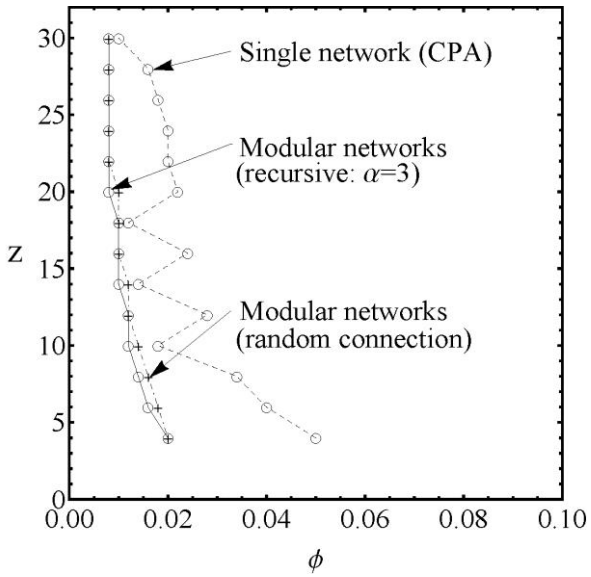

Figure 7.16 Cascade window of networks. Single network (CPA): single CPA network with 500 nodes and average degree $\langle k \rangle = 4$. Modular networks (recursive: $\alpha = 3$): modular networks consist of 500 modules (CPA network) with recursive structure. Modular networks (random connection): modular networks consist of 500 modules (CPA network) with random connection. Each module has 500 nodes and then the modular networks have totally 250,000 nodes. The average degree of inter-module is the same with inside module. The variable α is a parameter of equation (7.1).

7.4.3 Consensus dynamics

Modular network with GA network as a module (fast consensus)

Figure 7.17 compares the average time steps of consensus dynamics between modular networks with recursive topology and modular networks connected randomly, where optimized network by GA is used as a modular network. On modular networks, consensus is achieved among nodes in the same module at first. After that the consensus of inter-modules is achieved. The results show that the optimal connectivity for fast consensus in a module is also optimal for fast consensus of inter-modules.

The modular networks by a recursive network design method are effective to minimize the average time for fast consensus.

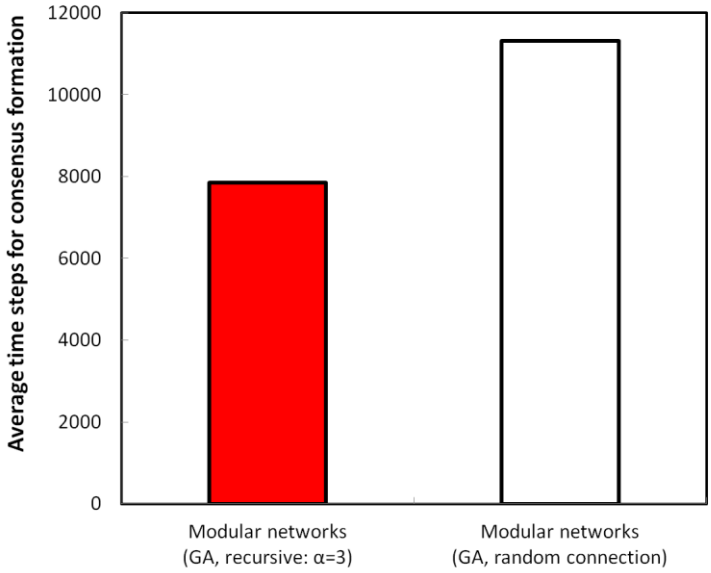

Figure 7.17 Average time steps of consensus dynamics: Modular networks (GA, recursive $\alpha = 3$): modular networks consist of 500 optimized networks with recursive topology. Modular networks (GA, random connection): modular networks consist of 500 optimized networks with random connection. Each module has 500 nodes, and the average degree of inter-module is the same with inside module $\langle k \rangle = 4$. At each simulation, each node has random number initially. Simulation is terminated when the standard deviation of values among nodes become less than 10^{-4}.

7.5 **The effect of modularization for consensus dynamics**

In previous sections, the properties of dynamical processes on optimized modular networks are discussed. This section studies the effect of the modularization of a network on consensus dynamics in greater details from eigenvalue view points. Note that the similar analyses on other dynamics are left for future work. However, the analytical approach and viewpoints will become basement for further study on modular networks for other dynamical processes.

A network consists of N nodes and L links. There are M modules in the network and each node belongs to only one module. For the simplicity all modules have same number of nodes N_m. There are two type links in the network: internal links L_M connecting nodes inside a module and external links L_{IM} connecting nodes in different modules. The link density in each module is p and the link density between modules is q. Then, the relationships between above variables are formulated as,

$$\begin{aligned} &N = mM, \\ &L = L_M + L_{IM}, \\ &L_M =_m C_2 \times pM, \\ &L_{IM} =_M C_2 \times_m C_1 \times_m C_1 \times q, \\ &p = \frac{1}{{}_mC_2 \times M} f_{L_M} L, \\ &q = \frac{1}{{}_MC_2 \times_m C_1 \times_m C_1} f_{L_{IM}} L, \\ &f_{L_M} + f_{L_{IM}} = 1, \end{aligned} \tag{6.20}$$

where f_{L_M} is the fraction of links that are deployed inside modules and $f_{L_{IM}}$ is the fraction of links that are deployed between modules.

The formation of modular network begins with the initialization process: N nodes are deployed on the space, and the total number of links L and the fraction f_{L_M} is given. The L_M/M internal links are introduced to connect nodes randomly inside each module. After that, the L_{IM} external links are introduced to connect nodes randomly in different modules. Figure 7.18 shows examples of modular network created by the procedures, and it is clear that the network becomes modularized along with the increase of f_{L_M}. If $f_{L_M} = 1$, the network consists of isolated modular networks, on the other hand if $f_{L_M} = 0$, nodes in each modular network are only connected to nodes in other module.

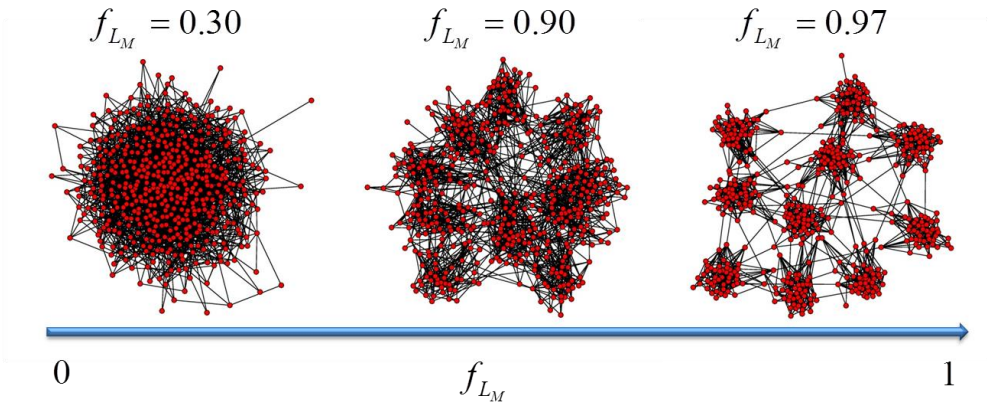

Figure 7.18 The formation of modular network. The network consists of 10 modular networks and each node belongs to one of them. f_{L_M} is the fraction of internal links that are deployed in the inside module. A total node is 500 and total link is 2000.

Figure 7.19 shows the index for consensus dynamics (the eigenvalue ratio $\lambda_2(\mathbf{L})/\lambda_N(\mathbf{L})$ of the Laplacian matrix of the modular networks) is plotted as a function of f_{L_M} the fraction of links that are deployed in the inside modules with changing the number of modules under fixed total number of nodes and links, which are 500 nodes and 2000 links. It is shown that there are four points, which are relationships between the index and the number of modules from the figure.

First one is that the modular networks with certain number of modules and intermediate f_{L_M} have larger size of index than single random network (non-modularized network). It is very interesting because the modularization of a network adds new constraint on the communication between agents. However, this result implies the modularity of a network can work to enhance consensus dynamics.

Second one is that the network with large number of modules (ex. $\mathrm{M} = 50$) has large size of index compared to the network with small number of modules (ex. $\mathrm{M} = 10$) when the links are used as internal links and external links equally ($f_{L_M} = 0.5$).

Third one is that the difference of the index becomes small along with the increase of f_{L_M}, which implies the network becomes modularized, and the difference is zero at certain fraction ($f_{L_M} = 0.7$).

Finally fourth one is that the difference of the index between networks with different number of modules increase again when the network is modularized sufficiently ($f_{L_M} \geq 0.7$). However, in that case, the network with small number of modules (ex. $M = 10$) has large size of index compared to the network with large number of modules (ex. $M = 50$). The influence of the number of module becomes very large when the network is almost isolated to each module, which is compared to the difference at $f_{L_M} = 0.5$.

The difference of the index of modular network, which depends on the fraction of internal link f_{L_M}, comes from the change of $\lambda_2(\mathbf{L})$ mainly (see Figure 7.20 and

Figure 7.21). The change of $\lambda_2(\mathbf{L})$ in Figure 7.20 is as same as the change of the index $\lambda_2(\mathbf{L})/\lambda_N(\mathbf{L})$ in Figure 7.19. The $\lambda_N(\mathbf{L})$ of modular network with large number of modules is usually smaller than that of the network with small number of modules. The difference expands with the increase with f_{L_M}. Therefore, it is clear that the variation of $\lambda_2(\mathbf{L})$ has dominant effect to decide the index $\lambda_2(\mathbf{L})/\lambda_N(\mathbf{L})$.

The modularization of network changes the value of eigenvalues drastically, which belongs to a part of smallest eigenvalues including second smallest eigenvalue $\lambda_2(\mathbf{L})$. In Figure 7.22, the smallest 30 eigenvalues of the Laplacian matrix of the modular network consisting of 10 modular networks is plotted with changing the fraction of internal links $f_{L_M}(= 0.3, 0.6, 0.9, 0.97)$. It is shown that when the network is not sufficiently modularized ($f_{L_M} = 0.3$), the network has only one 0 eigenvalue. However, when the network is sufficiently modularized ($f_{L_M} = 0.97$), the network has 10 almost 0 eigenvalues, which is the same number of modules. On the other hand, other eigenvalues of the Laplacian matrix are not influenced by the modularization of the network (Figure 7.23). This result can be inducted mathematically by considering consensus dynamics as markov chain [121].

The modular networks have effects not only to prevent consensus dynamics, which can be understood intuitively, but also to enhance it. The modularization of a network means adding new constraint on communications among agents, but the loose constraint by the modularization of a network with intermediate f_{L_M} can enhance consensus dynamics.

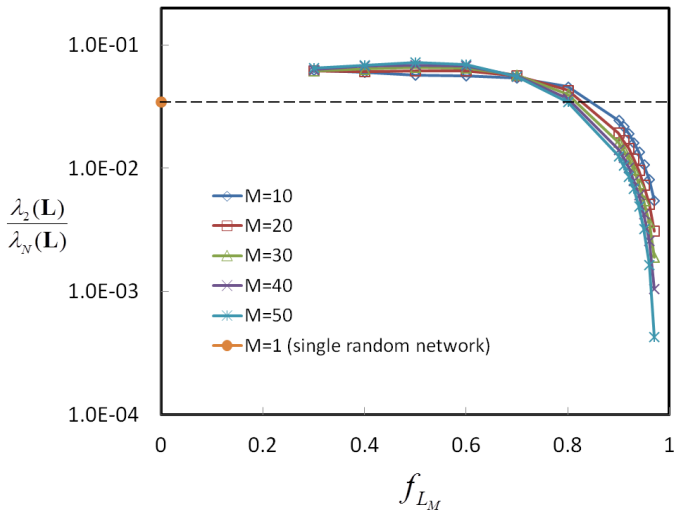

Figure 7.19 The eigenvalue ratio $\lambda_2(\mathbf{L})/\lambda_n(\mathbf{L})$ of Laplacian matrix of modular network consisting of M modules is plotted as a function of f_{L_M} the fraction of internal links that are deployed to connect nodes in the same modules. Note that for the comparison the eigenvalue ratio $\lambda_2(\mathbf{L})/\lambda_n(\mathbf{L})$ of single random network is also plotted at $f_{L_M} = 0$ (M=1 (single random network)). All networks have $N = 500$ nodes and $L = 2000$ links respectively.

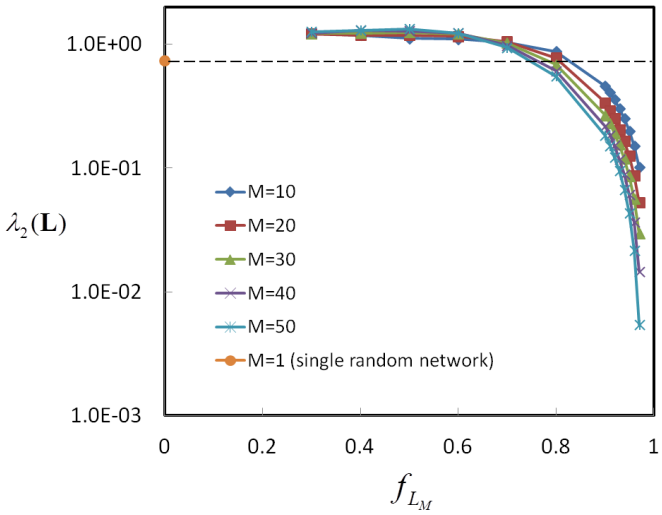

Figure 7.20 The $\lambda_2(\mathbf{L})$ second minimum eigenvalue of Laplacian matrix of modular network consisting of M modules is plotted as a function of f_{L_M} the fraction of internal links that are deployed to connect nodes in the same modules. Note that for the comparison the second minimum eigenvalue $\lambda_2(\mathbf{L})$ of single random network is also plotted at $f_{L_M} = 0$ (M=1 (single random network)). All networks have $N = 500$ nodes and $L = 2000$ links respectively.

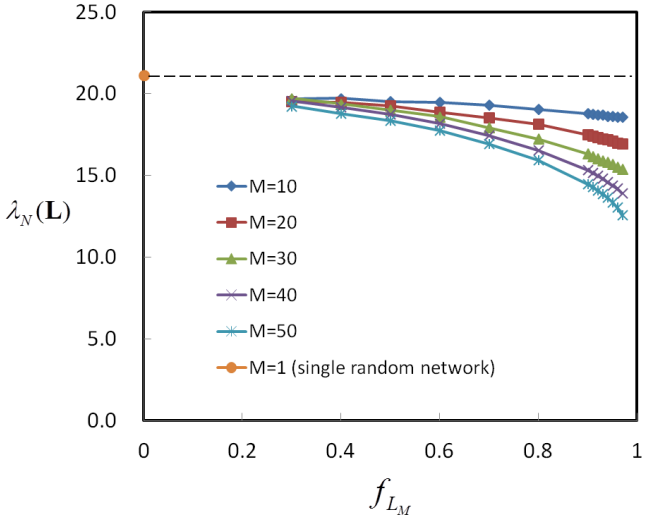

Figure 7.21 The $\lambda_N(\mathbf{L})$ maximum eigenvalue of Laplacian matrix of modular network consisting of M modules is plotted as a function of f_{L_M} the fraction of internal links that are deployed to connect nodes in the same modules. Note that for the comparison the maximum eigenvalue $\lambda_N(\mathbf{L})$ of single random network is also plotted at $f_{L_M} = 0$ (M=1 (single random network)). All networks have $N = 500$ nodes and $L = 2000$ links respectively.

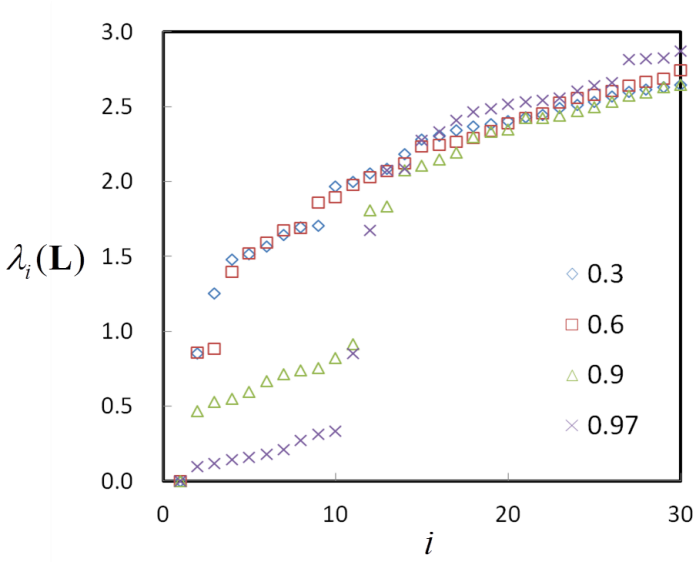

Figure 7.22 The small 30 eigenvalues of the Laplacian matrix of the modular network consisting of 10 modular networks are plotted. A total nodes and links of the modular network are $N = 500$ nodes and $L = 2000$ links respectively. The legend in the figure such as $0.3, 0.6, 0.9\ 0.97$ represents the fraction of internal links f_{L_M} that are deployed to connect nodes in the same modules. When $f_{L_M} = 1$, the network is separated completely to 10 modules.

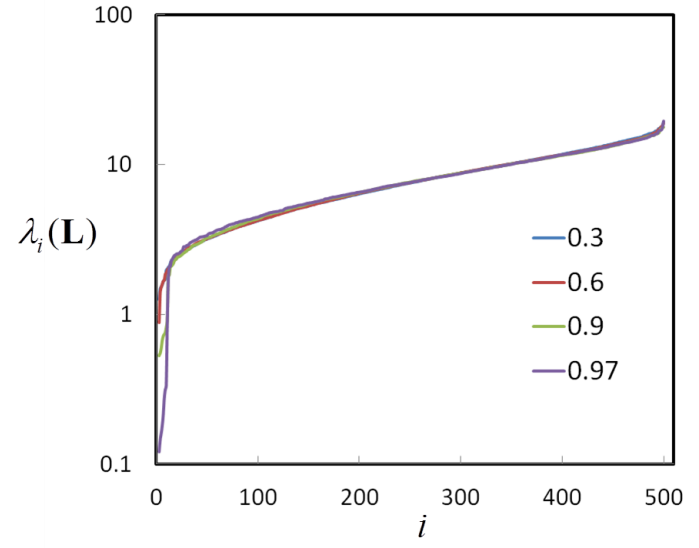

Figure 7.23 The spectrum of Laplacian matrix of the modular network consisting of 10 modular networks is plotted. A total nodes and links of the modular network are 500 nodes and 2000 links respectively. The legend in the figure such as $0.3, 0.6, 0.9\ 0.97$ represents the fraction of internal links f_{L_M} that are deployed to connect nodes in the same modules. When $f_{L_M} = 1$, the network is separated completely to 10 modules.

Chapter 8

Conclusion and Future Work

8.1 Conclusion

The discovery of principles between dynamical processes and underlying network is the ultimate goal of the study on the topology of networks [29]. This dissertation elucidated optimal network topologies that make specific patterns of the interactions and the coordinated pathways to maximize or minimize dynamical processes on networks, which include diffusion dynamics, cascade dynamics, and consensus dynamics. They are well studied topics and have wide range of applications in engineering. In order to design those optimal networks efficiently under fixed network resources such as nodes and links, three types of network design methods are proposed. They are evolutionary optimization by genetic algorithm, network models by heuristic method, and recursive interconnection of modularized networks. Their combination brings new framework to create optimal networks, which has enough scalability from small-scale to very large-scale. The optimal networks can be explained in terms of the role of the cluster of nodes, homogeneity and symmetry. The details of contributions are summarized in following paragraphs.

A network designing framework by evolutionary optimization: Because the complexity of network designing problem increases exponentially along with the network size, an alternative method for network design is required instead of designing it manually. However, the efficient and versatile method for designing optimal networks has not been defined yet, due to the complexity of the problem. On the other hand nature is a typical example of complex and unpredictable environment. Natural life forms have been able to survive by finding better or best solutions even if they are not optimal. Therefore, this dissertation also accepts the concept called “survival of the fittest”. It was applied to the proposed framework of the network design, and mathematical analysis and numerical simulations validated the effectiveness. Especially, the proposed evolutionary optimization method has sufficient flexibility toward many network designing problems by giving a proper objective function.

An analysis from eigenvalue view points: This dissertation used a maximum eigenvalue of an adjacency matrix of a network to characterize its network topology, which is maximized in a complete graph and minimized in a completely homogeneous network. Although the degree distribution, which is usually used to classify networks, could not catch topological properties that affect dynamical processes, the eigenvalue index can show the existence of hub nodes and how those hub nodes are interconnected, which usually have dominant effect on dynamical processes such as diffusion dynamics and cascade dynamics. The ratio of the average degree to maximum eigenvalue $\langle k \rangle / \lambda_{max}(\mathbf{A})$ can be used to explain the relationship between topological properties of a network and its influence on dynamical processes simply and directly.

Networks minimizing or maximizing the tipping point on diffusion dynamics: By using the evolutionary optimization, it was shown that the cluster of hub nodes is essential to minimize the tipping point. In order to replicate the topology, KN network model is proposed as a heuristic method. The KN model can make networks with the same topological properties of the optimized networks, which are power-law in the degree distribution and Rich-club phenomena (the formation of a cluster of hub nodes). In addition, the CPA and CRA networks are also proposed as extreme cases of the cluster of hub nodes, in which there is a complete graph at the center of a network and the rest of nodes (peripheral nodes) are connected to the complete graph or to other peripheral nodes. The formed networks by the models have dense connection in the core and sparse connection between peripheral nodes. The networks by CPA and CRA model can have almost theoretical upper limit of maximum eigenvalue of the adjacency matrix, which minimize the tipping point for diffusion dynamics. On the other hand, the k-regular graph where all nodes have k neighbors is shown to be optimal to maximize the tipping point.

Networks maximizing or minimizing the cascade window on cascade dynamics: By using the evolutionary optimization, it was shown that the combination of the cluster of hub nodes and the cluster of vulnerable nodes is essential to maximize the cascade window. The global cascades are easily driven using the cluster of vulnerable nodes as a foothold, which can be formed by the cluster of hub nodes. The proposed P model can replicate the topology, and networks by the P model have the largest cascade window compared to even the evolutionary optimized networks. On the other hand, the CPA, CRA and KN networks having only the cluster of hub nodes are optimal to minimize cascade window. The large cluster of hub nodes, which are very stable, prevents cascade dynamics from spreading to the whole network.

Networks minimizing or maximizing the convergence time of consensus dynamics: By using the evolutionary optimization, it was shown that the complete homogeneity in terms of a node degree is not a necessary condition to design networks for fast consensus. Previous studies found the Ramanujan graph is optimal to minimize the

convergence time of consensus dynamics, which belongs to k-regular graph. However, our mathematical analysis of evolutionary optimized networks and numerical simulations results show the network with small fluctuation in degrees can also make fast consensus. Especially, when the network is sufficiently sparse (average degree is $\langle k \rangle = 2$), the 50 % of the time of consensus dynamics on Ramanujan graph is reduced on evolutionary optimized networks. Furthermore, the Ring-Trees model can replicate the optimized network topology and minimize the convergence time of consensus dynamics compared to even the evolutionary optimized networks. On the optimal network the local consensus achieved between each grouped agents (nodes) by trees at first, and the global consensus is formed via a ring network after that. On the other hand, the convergence time of consensus dynamics is maximized on a core with line network. The agents in the dense core make fast consensus locally, and the consensus state is very stable because they have few paths to communicate with external agents in a line network. The interaction gap forms slow consensus globally.

Modular networks: Modularity is an important concept for understanding the structure and the functions of complex systems. There are usually many interactions between nodes in the same module but little interaction between the different modules. In this dissertation, a modular network is used as one component of a very large-scale network, and the modular networks with recursive structure is proposed as a method to connect many modules efficiently. The topology between modules is the same with the topology between nodes in a modular network.

The common property of diffusion dynamics and cascade dynamics is that the new state occurred at part of the nodes in a network spreads into the rest of a network. In addition, the local environment around the trigger nodes decides whether the new state will survive at a steady state or disappear. Therefore, the topology of each modular network is more important to decide the spreading process than the topology of inter-modules. As a result, modular networks with recursive topology have almost the same performance as modular networks connected randomly. Optimizing each modular network is necessary to design optimal modular networks for diffusion dynamics and cascade dynamics.

In the case of consensus dynamics on modular networks, the topology of inter-module is very important, because there are no redundant links connecting different modules. The optimal network for fast consensus between nodes in the same modular network is also optimal for fast consensus of inter-module. Therefore, the recursive structure of modular networks is necessary to design optimal modular networks for consensus dynamics.

Modularization of a network: Modularization of a network means a single network split up into several networks (modular networks), where the link density of inter-module is sparse. This dissertation studied what kind of influence the modularization of a single network has on dynamical processes.

In general, it is known that the modularization of a network prevents diffusion, cascade or fast consensus. Admittedly, simulation results confirmed that this is true in the case of diffusion dynamics, but this is not true in the case of cascade dynamics and consensus dynamics with specific conditions. For example, cascade occurs more easily on modular networks with CPA networks than on a single CPA network. The modularization of a network makes the cluster size of hub nodes smaller, which makes spreading of cascade more easily. In addition, the modularization of a network can coordinate sequence of consensus dynamics. When the average degree of a network is $\langle k \rangle = 2$, fast consensus between agents is achieved on modularized network with ring-trees structure compared to the consensus on a single tree network. A local consensus is achieved in each modular tree-network at first. After that the global consensus is achieved. Also, in the case for average degree is $\langle k \rangle > 2$, it is shown that a random network modularized to a certain extent is more optimal for fast consensus than on a non-modularized random network. Modularization of a network may lead to a wide cascade window and a fast consensus when the interaction region of nodes is confined to an appropriate size by it.

Interrelationship between optimal networks for different dynamical processes: Through this dissertation, optimal networks are created to maximize or to minimize diffusion dynamics, cascade dynamics, and consensus dynamics. Each dynamics has different optimal networks to maximize or minimize itself. They are CPA (CRA) network, regular network, P model network, Ring-Trees network and a core with line network. On the other hand, it is interesting that the optimal network maximizing one dynamics is also optimal to minimize another dynamics.

The keywords characterizing these complex and optimal networks are cluster of nodes, homogeneity and symmetry. The cluster of hub nodes characterizes a CPA (CRA) network. It maximizes the number of contact processes among nodes under diffusion dynamics, and it also works like a firewall to minimize cascade dynamics. Homogeneity in terms of node connectivity characterizes a regular network. It minimizes the number of contact processes and prevents diffusion dynamics. The coexistence of a cluster of hub nodes and a cluster of vulnerable nodes characterizes a P model network. It makes a foothold for the spreading of cascade dynamics and maximizes it. The sufficient homogeneity and symmetry in terms of network topology characterize a Ring-Trees network and an evolutionary optimized network for fast consensus. The topological patterns with no interaction gap promote consensus dynamics smoothly and form fast consensus. Finally, the breaking of homogeneity and symmetry characterizes a core with line network. It reduces the global redundant pathways for consensus dynamics and forms slow consensus.

Although the degree of each node and its fraction are conventional points of view in previous studies on complex network, the above-mentioned three keywords represent the interconnecting patterns among nodes, which is not the property of a single node. Especially, the three keywords consider both the degree of each node and

how nodes interconnect each other. This is due to the fact that an aggregation of nodes has utterly different effects compared to the effects of a single node. The three keywords should be the most important points of view to understand and to explain the dynamical processes on the complex networks.

8.2 **Future work**

When a network topology can be assumed to be static or unchanged during dynamical processes, the coordination of the interaction patterns between nodes is an effective way to design optimal networks for dynamical processes as shown through this dissertation. However, if the birth and death processes of nodes and links occur, which depend on the dynamical processes, how should optimal networks be designed?

On the dynamics-driven networked system, network topology and effects by dynamical processes are changed simultaneously, and initial network topology is not enough to explain the collective behavior as a result. The response rules or mechanisms to environments become important for the understanding of the complex dynamical systems. In a biological system, which is one example of a dynamics-driven networked system, it is said that the evolvability of the system incurs robustness that is its ability to maintain specific functions after changes in topology occur due to perturbation [120]. There are interesting studies on dynamical optimization of networks using biologically inspired adaptation mechanism such as intercellular information exchange by multi-agents [122-124]. Studying response rules with an evolving mechanism for designing complex dynamical systems, which can maintain its performance as much as possible, is one challenge for future research to advance the study of this dissertation.

Acknowledgments

Foremost, I would like to express my utmost gratitude to my advisor at National Defense Academy, Dr. Akira Namatame for his thoughtful directions and affectionate encouragements. This dissertation would not have been materialized without his careful guidance and continuous support. I would like to acknowledge my advisory committee members Drs. Yukio Hayashi of Japan Advanced Institute of Science and Technology (JAIST), Takakazu Kurokawa of National Defense Academy, and Hiroshi Sato of National Defense Academy for their enlightening comments and constructive suggestions of my work. I would also like to acknowledge Drs. Masao Kubo and Tomohiro Shirakawa at National Defense Academy for giving valuable inspirations to advance my study through open-minded discussions.

In addition, I would like to thank the staff members in the Dept. of Computer Science and also the support staff at National Defense Academy for supporting my study through grants and course planning. I also want to thank all the members of the Intelligent Information Systems Laboratory at National Defense Academy for helping my research through constructive discussions and fruitful collaborations. I miss those days when all the students got together every week to present the progress, discuss the problems, and share ideas.

Finally, I would also like to say a heartfelt “thanks” to everyone who has supported me during my graduate studies. Especially, I must single out my wife, Hiroko, to thank her for her dedicated help, allowing me to concentrate on my study. I would also like to thank my sons, Haruki and Yuto, for cheering me up with their lovely smile.

Bibliography

[1] M. Faloutsos, P. Faloutsos, and C. Faloutsos, "On power-law relationships of the internet topology," *In Proceedings of SIGCOMM'99*, pp. 251–262, 1999.

[2] A.-L. Barabasi, R. Albert, and H. Jeong, "Scale-free characteristics of random networks: the topology of the world-wide web," *Physica A*, vol. 281, pp. 69–77, 2000.

[3] V. Colizza, A. Barrat, M. Barthélemy, and A. Vespignani, "The role of the airline transportation network in the prediction and predictability of global epidemics." *Proceedings of the National Academy of Sciences of the United States of America*, vol. 103, no. 7, pp. 2015–2020, Feb 2006.

[4] D.Braess, "On a paradox of traffic planning," *Transportation Sceince*, vol. 39, no. 4, pp. 446–450, Nov 2005.

[5] D.J.Watts and S.H.Strogatz, "Collective dynamics of small-world networks," *Nature*, vol. 393, pp. 440–442, 1998.

[6] E. Bompard, R. Napoli, and F. Xue, "Analysis of structural vulnerabilities in power transmission grids," *International Journal of Critical Infrastructure Protection*, vol. 2, no. 1-2, pp. 5–12, 2009. [Online]. Available: http://-www.sciencedirect.com/science/article/pii/S1874548209000031

[7] B. Chakravorti, "The slow pace of fast change: Bringing innovations to market in a connected world." Jun 2003.

[8] S. A. Delre, W. Jager, T. H. A. Bijmolt, and M. A. Janssen, "Will it spread or not? the effects of social influences and network topology on innovation diffusion," *Journal of Product Innovation Management*, vol. 27, pp. 267–282, 2010.

[9] B. H. Hall, "Innovation and diffusion," *National Bureau of Economic Research*, Jan 2004.

[10] J. Hauser, G. Tellis, and A. Griffin, "Research on innovation: A review and agenda for marketing science," *Marketing Science*, vol. 25, no. 6, pp. 687–717, 2006.

[11] N. Meade and T. Islam, "Modelling and forecasting the diffusion of innovation - a 25-year review," *International Journal of Forecasting*, vol. 22, no. 3, pp. 519–545, 2006.

[12] H. P. Young, "Innovation diffusion in heterogeneous populations: Contagion,

social influence, and social learning," *American Economic Review*, vol. 99, no. 5, pp. 1899–1924, 2009.

[13] H. P. Young, "The dynamics of social innovation," *Proceedings of the National Academy of Sciences*, vol. 108, no. Supplement 4, pp. 21285–21291, 2011. [Online]. Available: http://www.pnas.org/content/108/suppl.4/21285.abstract

[14] M. J. B. II, D. M. Katz, J. L. Zelner, and J. H. Fowler, "Distance measures for dynamic citation networks," *Physica A: Statistical Mechanics and its Applications*, vol. 389, no. 19, pp. 4201–4208, 2010. [Online]. Available: http://-www.sciencedirect.com/science/article/pii/S0378437110004930

[15] S. Bilke and C. Peterson, "Topological properties of citation and metabolic networks," *Phys. Rev. E*, vol. 64, no. 036106, Aug 2001. [Online]. Available: http://link.aps.org/doi/10.1103/PhysRevE.64.036106

[16] A. K. Salas and S. R. Borrett, "Evidence for the dominance of indirect effects in 50 trophic ecosystem networks," *Ecological Modelling*, vol. 222, no. 5, pp. 1192–1204, 2011. [Online]. Available: http://www.sciencedirect.com/science/-article/pii/S0304380010006514

[17] R. M. May, *Stability and Complexity in Model Ecosystems*. Princeton: Princeton Univ. Press, 1973.

[18] J. L. Garcia-Domingo and J. Saldaña, "Food-web complexity emerging from ecological dynamics on adaptive networks," *Journal of Theoretical Biology*, vol. 247, no. 4, pp. 819–826, 2007. [Online]. Available: http://-www.sciencedirect.com/science/article/pii/S0022519307001932

[19] R. M. May, "Will a large complex system be stable?" *Nature*, vol. 238, pp. 413–414, 1972.

[20] Y. Wang, D. Chakrabarti, C. Wang, and C. Faloutsos, "Epidemic spreading in real networks: An eigenvalue viewpoint," *International Symposium on Reliable Distributed Systems (SRDS'03)*, pp. 25–34, 2003.

[21] D. J. Watts, "A simple model of global cascades on random networks," *Proceedings of the National Academy of Sciences*, vol. 99, no. 9, pp. 5766–5771, April 2002.

[22] R. Olfati-Saber and R. M. Murray, "Consensus problems in networks of agents with switching topology and time-delays," *IEEE Transactions on Automatic Control*, vol. 49, pp. 1520–1532, 2004.

[23] G. L. Alexanderson, "About the cover: Euler and k0nigsberg's bridges: a historical view," *Bulletin of the american mathematical society*, vol. 43, no. 4, pp. 567–573, 2006.

[24] L. Euler, "Solutio problematis ad geometriam situs pertinentis (the solution to a problem relating to the geometry of position)," *Commentarii Academiae Scientiarum Imperialis Petropolitanae*, vol. 8, pp. 128–140, 1741.

[25] G. Kirchhoff, "Ueber die auflösung der gleichungen, auf welche man bei der untersuchung der linearen vertheilung galvanischer ströme geführt wird," *Annalen der Physik*, vol. 148, no. 12, pp. 497 – 508, 1847. [Online]. Available:

http://dx.doi.org/10.1002/andp.18471481202

[26] D. Rouvray, "The pioneering contributions of cayley and sylvester to the mathematical description of chemical structure," *Journal of Molecular Structure: THEOCHEM*, vol. 185, pp. 1–14, 1989. [Online]. Available: http://-www.sciencedirect.com/science/article/pii/0166128089850031

[27] V. Colizza, R. Pastor-Satorras, and A. Vespignani, "Reaction-diffusion processes and metapopulation models in heterogeneous networks," *Nature Physics*, vol. 3, pp. 276–282, 2007.

[28] M. Newman, "Assortative mixing in networks," *Phys. Rev. Lett.*, vol. 89, no. 208701, Oct 2002.

[29] M. E. J. Newman, "The structure and function of complex networks," *SIAM*, vol. 45, pp. 167–256, 2003.

[30] M. E. J. Newman, S. H. Strogatz, and D. J. Watts, "Random graphs with arbitrary degree distributions and their applications," *Phys. Rev. E*, vol. 64, no. 026118, 2001.

[31] G. Bianconi and A.-L. Barabási, "Competition and multiscaling in evolving networks," *Europhys. Lett.*, vol. 54, no. 4, pp. 436–442, 2001. [Online]. Available: http://dx.doi.org/10.1209/epl/i2001-00260-6

[32] A.-L. Barabási, E. Ravasz, and T. Vicsek, "Deterministic scale-free networks," *Physica A: Statistical Mechanics and its Applications*, vol. 299, pp. 559–564, 2001. [Online]. Available: http://www.sciencedirect.com/science/article/pii/-S0378437101003697

[33] E. Estrada and E. Vargas-Estrada, "Distance-sum heterogeneity in graphs and complex networks," *Applied Mathematics and Computation*, vol. 218, no. 21, pp. 10393–10405, 2012. [Online]. Available: http://www.sciencedirect.com/-science/article/pii/S0096300312003542

[34] A. L. P. y Piontti, L. A. Braunstein, and P. A. Macri, "Jamming in complex networks with degree correlation," *Physics Letters A*, vol. 374, no. 46, pp. 4658–4663, 2010. [Online]. Available: http://www.sciencedirect.com/science/-article/pii/S0375960110012715

[35] A. E. Motter, M. A. Matías, J. Kurths, and E. Ott, "Dynamics on complex networks and applications," *Physica D: Nonlinear Phenomena*, vol. 224, pp. vii–viii, 2006. [Online]. Available: http://www.sciencedirect.com/science/-article/pii/S0167278906003721

[36] L. Isella, J. Stehlé, A. Barrat, C. Cattuto, J.-F. Pinton, and W. V. den Broeck, "What's in a crowd? analysis of face-to-face behavioral networks," *Journal of Theoretical Biology*, vol. 271, no. 1, pp. 166–180, 2011. [Online]. Available: http://www.sciencedirect.com/science/article/pii/S0022519310006284

[37] R. Zia, W. Liu, S. Jolad, and B. Schmittmann, "Studies of adaptive networks with preferred degree," *Physics Procedia*, vol. 15, pp. 102–105, 2011. [Online]. Available: http://www.sciencedirect.com/science/article/pii/-S1875389211003397

[38] L. G. Moyano, M. L. Mouronte, and M. L. Vargas, "Communities and dynamical processes in a complex software network," *Physica A: Statistical Mechanics and its Applications*, vol. 390, no. 4, pp. 741–748, 2011. [Online]. Available: http://www.sciencedirect.com/science/article/pii/-S0378437110008848

[39] R. Pastor-Satorras and A. Vespignani, *Epidemics and immunization in scale-free networks*. Wiley-VCH Verlag GmbH & Co. KGaA, 2005, pp. 111–130. [Online]. Available: http://dx.doi.org/10.1002/3527602755.ch5

[40] N. Madar, T. Kalisky, R. Cohen, D. ben Avraham, and S. Havlin, "EnglishImmunization and epidemic dynamics in complex networks," *EnglishThe European Physical Journal B - Condensed Matter and Complex Systems*, vol. 38, pp. 269–276, 2004. [Online]. Available: http://dx.doi.org/-10.1140/epjb/e2004-00119-8

[41] C. Peng, X. Jin, and M. Shi, "Epidemic threshold and immunization on generalized networks," *Physica A: Statistical Mechanics and its Applications*, vol. 389, no. 3, pp. 549–560, 2010. [Online]. Available: http://-www.sciencedirect.com/science/article/pii/S0378437109008243

[42] P. Gai and S. Kapadia, "Contagion in financial networks," *Proceedings of the Royal Society A: Mathematical, Physical and Engineering Science*, vol. 466, no. 2120, pp. 2401–2423, 2010. [Online]. Available: http://-rspa.royalsocietypublishing.org/content/466/2120/2401.abstract

[43] P. Gai, A. Haldane, and S. Kapadia, "Complexity, concentration and contagion," *Journal of Monetary Economics*, vol. 58, no. 5, pp. 453–470, 2011.

[44] E. Hyytia and P. Emstad, "A model for tcp congestion control capturing the correlations in times between the congestion events," *Next Generation Internet Design and Engineering, 2006.2nd Conference*, pp. 168–175, Apr 2006.

[45] S.Floyd, "Promoting the use of end-to-end congestion control," *IEEE/ACM Trans on Networking*, vol. 7, no. 4, pp. 458–472, Aug 1999.

[46] F. S. and J. V., "Random early-detection gateways for congestion avoidance," *IEEE/ACM Transantions on Networking*, vol. 1, no. 4, pp. 397–413, Apr 1993.

[47] T. Komatsu and A. Namatame, "On the effectiveness of rate-limiting methods to mitigate distributed dos (ddos) attacks," *IEICE TRANSACTIONS on Communications*, vol. E90-B, no. 10, pp. 2665–2672, Oct 2007.

[48] W. J. J., G. Z. Y., S. H. J., and H. H. J., "Congestion in different topologies of traffic networks," *Europhysics Letters*, vol. 74, no. 3, pp. 560–566, 2006.

[49] L. Zhao, Y.-C. Lai, K. Park, and N. Ye, "Onset of traffic congestion in complex networks," *Physical Review E*, 2005.

[50] R. Cohen, K. Erez, D. ben Avraham, and S. Havlin, "Breakdown of the internet under intentional attack," *Phys. Rev. Lett.*, vol. 86, pp. 3682–3685, Apr 2001. [Online]. Available: http://link.aps.org/doi/10.1103/PhysRevLett.86.3682

[51] C. Reuven, E. Keren, B.-A. Daniel, and H. Shlomo, "Resilience of the internet to random breakdowns," *Phys. Rev. Lett.*, vol. 85, pp. 4626–4628, Nov 2000.

[Online]. Available: http://link.aps.org/doi/10.1103/PhysRevLett.85.4626

[52] C. D. Brummitt, R. M. D'Souza, and E. A. Leicht, "Suppressing cascades of load in interdependent networks," *Proceedings of the National Academy of Sciences*, 2012. [Online]. Available: http://www.pnas.org/content/early/2012/-02/15/1110586109.abstract

[53] T. Tanizawa, G. Paul, S. Havlin, and H. E. Stanley, "Optimization of the robustness of multimodal networks," *Phys. Rev. E*, vol. 74, no. 016125, Jul 2006. [Online]. Available: http://link.aps.org/doi/10.1103/PhysRevE.74.016125

[54] T. Tanizawa, G. Paul, R. Cohen, S. Havlin, and H. E. Stanley, "Optimization of network robustness to waves of targeted and random attacks," *Phys. Rev. E*, vol. 71, no. 047101, Apr 2005. [Online]. Available: http://link.aps.org/doi/-10.1103/PhysRevE.71.047101

[55] R. Albert, H. Jeong, and A.-L. Barabasi, "Error and attack tolerance of complex networks," *Nature*, vol. 406, pp. 378–382, 2000.

[56] A. E. Motter and Y.-C. Lai, "Cascade-based attacks on complex networks," *Phys. Rev. E*, vol. 66, no. 065102, Dec 2002. [Online]. Available: http://link.aps.org/-doi/10.1103/PhysRevE.66.065102

[57] Z. Bao, Y. Cao, L. Ding, Z. Han, and G. Wang, "Dynamics of load entropy during cascading failure propagation in scale-free networks," *Physics Letters A*, vol. 372, no. 36, pp. 5778–5782, 2008. [Online]. Available: http://-www.sciencedirect.com/science/article/pii/S0375960108010621

[58] A. Namatame and T. Komatsu, "Management of systemic risks and cascade failures in a networked society," *INFORMATION ・ KNOWLEDGE ・ SYSTEMS Management*, vol. 10, pp. 111–133, 2012.

[59] D. Helbing, "Systemic risks in society and economics," in *Social Self-Organization*, ser. Understanding Complex Systems, D. Helbing, Ed. Springer Berlin / Heidelberg, 2012, vol. 80, pp. 261–284, 10.1007/978-3-642-24004-1_14. [Online]. Available: http://dx.doi.org/10.1007/-978-3-642-24004-1_14

[60] T. Komatsu and A. Namatame, "Dynamic diffusion process in evolutionary optimized networks," *International Journal of Bio-Inspired Computation*, vol. 3, no. 6, pp. 384–392, 2011.

[61] S. Zhou and R. J. Mondragón, "The rich-club phenomenon in the internet topology," *Communications Letters*, vol. 8, no. 3, pp. 180–182, March 2004.

[62] R. Olfati-saber, J. A. Fax, and R. M. Murray, "Consensus and cooperation in networked multi-agent systems," in *Proceedings of the IEEE*, vol. 95, no. 1, 2007, pp. 215–233.

[63] S. Kar, S. Aldosari, and J. M. F. Moura, "Topology for distributed inference ongraphs," *IEEE Transactions on signal processing*, vol. 56, no. 6, pp. 2609–2613, JUNE 2008.

[64] W. O. Kermack and A. G. McKendrick, "A contribution to the mathematical theory of epidemics." *Proceedings of the Royal Society of London*, vol. 115, no.

772, pp. 700–721, 1927.

[65] J. O. Kephart and S. R. White, “Directed-graph epidemiological models of computer viruses,” *Research in Security and Privacy, 1991. Proceedings.*, pp. 343–359, 1991.

[66] R. Pastor-Satorras and A. Vespignani, “Epidemic spreading in scale-free networks,” *Phys. Rev. Lett.*, vol. 86, pp. 3200–3203, Apr 2001. [Online]. Available: http://link.aps.org/doi/10.1103/PhysRevLett.86.3200

[67] J. Gao, S. V. Buldyrev, H. E. Stanley, and S. Havlin, “Networks formed from interdependent networks,” *Nature Physics*, vol. 8, no. 1, pp. 40–48, January 2012.

[68] M. L. Sachtjen, B. A. Carreras, and V. E. Lynch, “Disturbances in a power transmission system,” *Phys. Rev. E*, vol. 61, pp. 4877–4882, May 2000. [Online]. Available: http://link.aps.org/doi/10.1103/PhysRevE.61.4877

[69] Y. Moreno, R. Pastor-Satorras, A. Vázquez, and A. Vespignani, “Critical load and congestion instabilities in scale-free networks,” *EPL (Europhysics Letters)*, vol. 62, no. 2, no. 292, 2003. [Online]. Available: http://stacks.iop.org/-0295-5075/62/i=2/a=292

[70] J. P. Gleeson, “Cascades on correlated and modular random networks,” *Phys. Rev. E*, vol. 77, no. 046117, Apr 2008. [Online]. Available: http://link.aps.org/-doi/10.1103/PhysRevE.77.046117

[71] N. Lynch, *Distributed Algorithms*. Morgan Kaufmann, 1997.

[72] M. DeGroot, “Reaching a consensus,” *Journal of the American Statistical Association*, vol. 69, no. 345, pp. 118–121, 1974.

[73] D. P. Bertsekas and J. N. Tsitsiklis, *Parallel and distributed computation: numerical methods*. Upper Saddle River, NJ, USA: Prentice-Hall, Inc., 1989.

[74] L. Xiao and S. Boyd, “Fast linear iterations for distributed averaging,” *Systems & Control Letters*, vol. 53, no. 1, pp. 65–78, 2004. [Online]. Available: http://www.sciencedirect.com/science/article/pii/S0167691104000398

[75] A. Lubotzky, R. Phillips, and P. Sarnak, “Ramanujan graphs,” *Combinatorica*, vol. 8, no. 3, pp. 261–277, 1988.

[76] T. Nishikawa, A. E. Motter, Y.-C. Lai, and F. C. Hoppensteadt, “Heterogeneity in oscillator networks: Are smaller worlds easier to synchronize?” *Phys. Rev. Lett.*, vol. 91, no. 014101, Jul 2003. [Online]. Available: http://link.aps.org/doi/-10.1103/PhysRevLett.91.014101

[77] R. Pastor-Satorras and A. Vespignani, “Epidemic dynamics in finite size scale-free networks.” *Physical Review E*, vol. 65, no. 3, no. 035108, Mar 2002.

[78] C. R. Edling, L. A. N. Amaral, S. H. E., and Y. Aberg, “The web of human sexual contacts,” *Nature*, vol. 411, pp. 907–908, 2001.

[79] P. Holme and G. Ghoshal, “Dynamics of networking agents competing for high centrality and low degree,” *Phys. Rev. Lett.*, vol. 96(9), no. 098701, 2006.

[80] P. Holme and M. E. J. Newman, “Nonequilibrium phase transition in the coevolution of networks and opinions,” *Phys. Rev. E*, vol. 74(5), no. 056018,

2006.

[81] S. Iwanaga and A. Namatame, "The complexity of organizational decision with individual adaptation," in *The 26th Annual Conference on Industrial Electronics, Control and Instrumentation 2000 (IECON-2000)*, 2000, pp. 2762–2767.

[82] A. E. Motter, T. Nishikawa, and Y.-C. Lai, "Large-scale structural organization of social networks," *Phys. Rev. E*, vol. 68, no. 036105, Sep 2003. [Online]. Available: http://link.aps.org/doi/10.1103/PhysRevE.68.036105

[83] G. Palla, I. Derenyi, I. Farkas, and T. Vicsek, "Uncovering the overlapping community structure of complex networks in nature and society," *Nature*, vol. 435, no. 7043, pp. 814–818, June 2005.

[84] E. Oh, K. Rho, H. Hong, and B. Kahng, "Modular synchronization in complex networks," *Phys. Rev. E*, vol. 72, no. 047101, Oct 2005. [Online]. Available: http://link.aps.org/doi/10.1103/PhysRevE.72.047101

[85] A. E. Motter and Z. Toroczkai, "Introduction: Optimization in networks," *Chaos*, vol. 17, no. 026101, 2007, 3 pages.

[86] Y.-B. Xie, T. Zhou, W.-J. Bai, G. Chen, W.-K. Xiao, and B.-H. Wang, "Geographical networks evolving with an optimal policy," *Phys. Rev. E*, vol. 75, no. 036106, Mar 2007. [Online]. Available: http://link.aps.org/doi/10.1103/-PhysRevE.75.036106

[87] A. L. Barabasi and R. Albert, "Emergence of scaling in random networks," *Science*, vol. 286, pp. 509–512, 1999.

[88] M. Barthélemy and A. Flammini, "Optimal traffic networks," *Journal of Statistical Mechanics: Theory and Experiment*, vol. 2006, no. 07, no. L07002, 2006. [Online]. Available: http://stacks.iop.org/1742-5468/2006/i=07/a=L07002

[89] J.-H. Qian and D.-D. Han, "A spatial weighted network model based on optimal expected traffic," *Physica A: Statistical Mechanics and its Applications*, vol. 388, no. 19, pp. 4248–4258, 2009. [Online]. Available: http://-www.sciencedirect.com/science/article/pii/S0378437109004130

[90] L. Li, D. Alderson, W. Willinger, and J. Doyle, "A first-principles approach to understanding the internet's router-level topology," *SIGCOMM Comput. Commun. Rev.*, vol. 34, no. 4, pp. 3–14, 2004.

[91] S. Gil and D. H. Zanette, "Coevolution of agents and networks: Opinion spreading and community disconnection," *Physics Letters A*, vol. 356, no. 2, pp. 89–94, 2006. [Online]. Available: http://www.sciencedirect.com/science/article/-pii/S037596010600418X

[92] E. Anderson, Z. Bai, C. Bischof, S. Blackford, J. Demmel, J. Dongarra, J. D. Croz, A. Greenbaum, S. Hammarling, A. McKenney, and D. Sorensen, *LAPACK Users' Guide*, 3rd ed. Philadelphia, PA: Society for Industrial and Applied Mathematics, 1999.

[93] A.-L. Barabási, Z. Dezso, E. Ravasz, S.-H. Yook, and Z. Oltvai, "Scale-free and hierarchical structures in complex networks," in *MODELING OF COMPLEX SYSTEMS: Seventh Granada Lectures*, American, Ed., vol. 661. American

Institute of Physics, April 2003, pp. 1–16. [Online]. Available: http://dx.doi.org/-10.1063/1.1571285

[94] E. Ravasz, A. L. Somera, D. A. Mongru, Z. N. Oltvai, and A.-L. Barabasi, "Hierarchical organization of modularity in metabolic networks," *Science*, vol. 297, no. 5586, pp. 1551–1555, 2002. [Online]. Available: http://-www.sciencemag.org/content/297/5586/1551.abstract

[95] L. H. Hartwell, J. J. Hopfield, S. Leibler, and A. W. Murray, "From molecular to modular cell biology," *Nature*, vol. 402, pp. C47–C52, 1999.

[96] S. Lawrence and C. L. Giles, "Accessibility of information on the web," *Nature*, vol. 400, no. 107, 1999.

[97] M. S. Granovetter, "EnglishThe strength of weak ties," *EnglishAmerican Journal of Sociology*, vol. 78, no. 6, pp. 1360–1380, 1973. [Online]. Available: http://www.jstor.org/stable/2776392

[98] D. J. Watts, P. S. Dodds, and M. E. J. Newman, "Identity and search in social networks," *Science*, vol. 296, no. 5571, pp. 1302–1305, 2002. [Online]. Available: http://www.sciencemag.org/content/296/5571/1302.abstract

[99] P. S. Dodds and D. J. Watts, "Universal behavior in a generalized model of contagion." *Physical Review Letters*, vol. 92, no. 21, no. 218701, Mar 2004.

[100] R. Anderson and R. May, *Infectious diseases in humans. Dynamics and control*. Oxford University Press, 1992.

[101] F. Brauer and C. Castillo-Chavez, *Mathematical Models in Population Biology and Epidemiology*. Springer, 2000.

[102] P. Van Mieghem, J. Omic, and R. Kooij, "Virus spread in networks," *IEEE/ACM Trans. Netw.*, vol. 17, no. 1, pp. 1–14, feb 2009.

[103] H. Yuan, "A bound on the spectral radius of graphs," *Linear Algebra and its Applications*, vol. 108, pp. 135–139, September 1988.

[104] H.Sato, O.Isao, and K.Shigenobu, "A new generation alternation model of genetic algorithms and its assessment," *Journal of Japanese Society for Artificial Intellligence*, vol. 12, no. 5, pp. 734–744, 1997.

[105] H. P. Young, "The evolution of conventions," *Econometrica*, vol. 61, pp. 57–84, 1993.

[106] D. Watts and P. Dodds, "Influentials, networks, and public opinion formation," *Journal of Consumer Research*, vol. 34, pp. 441–458, December 2007.

[107] D. López-Pintado, "Contagion and coordination in random networks," *International Journal of Game Theory*, vol. 34, no. 3, pp. 371–381, 2006.

[108] M. Barahona and L. M. Pecora, "Synchronization in small-world systems," *Phys. Rev. Lett.*, vol. 89, no. 054101, Jul 2002. [Online]. Available: http://link.aps.org/-doi/10.1103/PhysRevLett.89.054101

[109] S. Kar, S. Aldosari, and J. Moura, "Topology for distributed interference on graphs," *IEEE Transactions on Signal Processing*, vol. 95, no. 1, pp. 215–233, January 2007.

[110] S. Boyd, P. Diaconis, P. Parrilo, and L. Xiao, "Fastest mixing markov chain on

graphs with symmetries," *SIAM Journal on Optimization*, vol. 20, no. 2, pp. 792–819, 2009. [Online]. Available: http://epubs.siam.org/doi/abs/10.1137/-070689413

[111] S. Boyd, P. Diaconis, and L. Xiao, "Fastest mixing markov chain on a graph," *SIAM Review*, vol. 46, no. 4, pp. 667–689, 2004. [Online]. Available: http://-epubs.siam.org/doi/abs/10.1137/S0036144503423264

[112] L. Donetti, F. Neri, and M. A. Munoz. (2006, May) Optimal network topologies: Expanders, Cages, Ramanujan graphs, Entangled networks and all that. [Online]. Available: http://arxiv.org/abs/cond-mat/0605565

[113] R. Olfati-Saber, "Algebraic connectivity ratio of ramanujan graphs," in *Proceeding of American Control Conference, 2007. ACC '07*, 2007.

[114] F. M. Atay, T. B|y|koglu, and J. Jost, "Network synchronization: Spectral versus statistical properties," *Physica D: Nonlinear Phenomena*, vol. 224, pp. 35–41, 2006. [Online]. Available: http://www.sciencedirect.com/science/article/pii/-S0167278906003794

[115] M. Ouyang and L. Dueñas-Osorio, "An approach to design interface topologies across interdependent urban infrastructure systems," *Reliability Engineering & System Safety*, vol. 96, no. 11, pp. 1462–1473, 2011. [Online]. Available: http://-www.sciencedirect.com/science/article/pii/S0951832011001219

[116] P. Bajardi, C. Poletto, J. J. Ramasco, M. Tizzoni, V. Colizza, and A. Vespignani, "Human mobility networks, travel restrictions, and the global spread of 2009 h1n1 pandemic," *PLoS ONE*, vol. 6, no. 1, no. e16591, 01 2011. [Online]. Available: http://dx.doi.org/10.1371%2Fjournal.pone.0016591

[117] J. Donges, H. Schultz, N. Marwan, Y. Zou, and J. Kurths, "EnglishInvestigating the topology of interacting networks," *EnglishThe European Physical Journal B*, vol. 84, pp. 635–651, 2011. [Online]. Available: http://dx.doi.org/10.1140/epjb/-e2011-10795-8

[118] M. E. J. Newman and M. Girvan, "Finding and evaluating community structure in networks," *Phys. Rev. E*, vol. 69, no. 026113, Feb 2004. [Online]. Available: http://link.aps.org/doi/10.1103/PhysRevE.69.026113

[119] S. Allesina and M. Pascual, "Food web models: a plea for groups," *Ecology Letters*, vol. 12, no. 7, pp. 652 – 662, 2009. [Online]. Available: http://-dx.doi.org/10.1111/j.1461-0248.2009.01321.x

[120] H. Kitano, "Biological robustness," *Nature Reviews Genetics*, vol. 5, no. 11, pp. 826–837, November 2004.

[121] D. Hartfiel and C. D. Meyer, "On the structure of stochastic matrices with a subdominant eigenvalue near 1," *Linear Algebra and its Applications*, vol. 272, no. 1-3, pp. 193–203, 1998. [Online]. Available: http://www.sciencedirect.com/-science/article/pii/S0024379597003339

[122] P. Boonma and J. Suzuki, "La nina: framework in self-adaptive publish/subscribe middleware for wireless sensor networks," *International Journal of Autonomous and Adaptive Communications Systems*, vol. 4, no. 2, pp.

180–201, 2011.

[123] N. Mazhar and M. Farooq, “Beeais: Artificial immune system security for nature inspired, manet routing protocol, beeadhoc,” in *Artificial Immune Systems*, ser. Lecture Notes in Computer Science, L. Castro, F. Zuben, and H. Knidel, Eds. Springer Berlin Heidelberg, 2007, vol. 4628, pp. 370–381. [Online]. Available: http://dx.doi.org/10.1007/978-3-540-73922-7_32

[124] P. Boonma and J. Suzuki, “Monsoon: A coevolutionary multiobjective adaptation framework for dynamic wireless sensor networks,” in *HICSS*, 2008, p. 497.

Publications

Journals and book chapters (In English)

1. **Komatsu T.**, Namatame A., "Dynamic diffusion in evolutionary optimized networks", *International Journal of Bio-Inspired Computation*, Vol. 3, No. 6 pp. 384-392, 2011.

2. **Komatsu T.**, Namatame A., "Diffusion and Cascade dynamics on growing networks", chapter in *Dynamic Analysis for Social Networks*, Carlos Andre Pinheiro and Markus Helfert (Eds.), Chapter 5, iConcept, 2012.

3. Namatame A., **Komatsu T.**, "Management of systemic risks and cascade failures in a networked society", Information Knowledge Systems Management 10, IOS press, pp. 111-133, 2012.

4. **Komatsu T.**, Namatame A., "Distributed Consensus and Mitigating Risk Propagation in Evolutionary Optimized Networks", J.-H. Kim et al. (Eds.): AsiaSim2011, PICT 4, Springer, pp. 200-209, 2012.

5. **Komatsu T.**, Hiroshi S., Namatame A., "Maximizing cascade of innovation on networks", *SICE Journal of Control, Measurement, and System Integration*, Vol. 6, No. 2, pp. 1-10, 2013.

6. **Komatsu T.**, Tran Q. H. Anh, Namatame A., "Resource allocation for a resilient network against risk contagion", *International Journal of Autonomous and Adaptive Communications Systems* (IJAACS), 2013. (to be published)

7. Tran Q. H. Anh, **Komatsu T.**, Namatame A., "Mitigating Cascading Failure with Adaptive Networking", *Journal of New Mathematics and Natural Computation (JNM&NC)*, 2013. (selected paper to be submitted to a special issue on (JNM&NC), which consists of several articles selected from papers presented at the sixteenth Asia-Pacific Symposium on Intelligent and Evolutionary System (IES2012) in Kyoto, Japan.)

Journals (In Japanese)

1. Yamamoto T., **Komatsu T.**, Namatame A. “Networks of Genetic Algorithm Optimization”, *Journal of Computer Software*, Vol. 28, No. 1, pp. 26-33, 2011.

2. **Komatsu T.**, Namatame A., “Relation between network structure and cascade phenomena”, *Transaction of the Japan Society for Simulation Technology*, Vol.4, No. 2, pp. 33-40, 2012.

3. **Komatsu T.**, Namatame A., “Cascade phenomena based on probabilistic threshold rule”, *Journal of Information Processing*, Vol. 53, No. 11, pp. 2360-2369, 2012.

International conferences (Refereed)

1. **Komatsu T.**, Namatame A., "Optimal Diffusion in Evolutionary Designed Networks", in *Proc. Econophysics Colloquium 2010*, November 2010.

2. **Komatsu T.**, Namatame A., "Dynamic Diffusion in Evolutionary Designed Networks", in *Proc. The 14th Asia Pacific Symposium on Intelligent and Evolutionary Systems IES2010*, pp. 263-274, November 2010.

3. **Komatsu T.**, Namatame A., "Risk Contagion in Evolutionary Optimized Networks", in *Proc. The Workshop on Biography inspired approaches to security & resilience*, Florida, U.S.A., March 2011.

4. **Komatsu T.**, Namatame A., "An evolutionary optimal network design to mitigate risk contagion", in *Proc. The 7th International Conference on Natural Computation*, pp. 1980-1985. IEEE, June 2011

5. **Komatsu T.**, Namatame A., "Distributed Consensus and Mitigating Risk Propagation in Evolutionary Optimized Networks", in *Proc. Asia Simulation Conference 2011*, November 2011.

6. **Komatsu T.**, Namatame A., "Cascade Simulation on Optimized Networks", in *Proc. European Conference of Modeling and Simulation 2012*, pp. 89-95, May, 2012.

7. Sato H., Kubo M., **Komatsu T.**, Namatame A., "Epidemic Behavior in Networks", in *Proc. Inter-Asia Roundtable 2012: Methodological and Conceptual Issues in Cyber Activism Research*, August 2012.

8. **Komatsu T.**, Namatame A., "Least Susceptible Networks to Cascade Failures", in *Proc. The 4th World Congress on Social Simulation* (WCCS) 2012, September. 2012.

9. **Komatsu T.**, Namatame A., "Cascade of Coordinated behaviours in Interdependent Security Games", in *Proc. The 6th International Conference on Soft Computing and Intelligent Systems, and the 13th International Symposium on Advanced Intelligent Systems, (SCIS-ISIS) 2012*, November. 2012.

Domestic conferences (Refereed)

1. **Komatsu T.**, Namatame A., "A network design method for early diffusion", in *Proc. 7th NetecoSymp*, March 2011.

2. **Komatsu T.**, Namatame A., "Relation between network structure and cascade phenomena", in *Proc. JWEIN2011*, September 2011.

3. **Komatsu T.**, Namatame A., "Cascade on probabilistic threshold model", in *Proc. Joint Agent Workshop and Symposium 2011 (JAWAS2011)*, October 2011.